

TECHNISCHE UNIVERSITÄT MÜNCHEN
Lehrstuhl für Entwicklungsgenetik

The role of the ERK/MAPK pathway in the adult mouse brain for fear potentiated startle learning: a model to study fear-based anxiety disorders

Barbara Di Benedetto

Vollständiger Abdruck der von der Fakultät Wissenschaftszentrum Weihenstephan für Ernährung, Landnutzung und Umwelt der Technischen Universität München zur Erlangung des akademischen Grades eines

Doktors der Naturwissenschaften

genehmigten Dissertation.

Vorsitzender: Univ.-Prof. Dr. S. Scherer

Prüfer der Dissertation: 1. Univ.-Prof. Dr. W. Wurst
2. Univ.-Prof. Dr. M. Götz (Ludwig-Maximilians-Universität München)

Die Dissertation wurde am 19.09.2007 bei der Technischen Universität München eingereicht und durch die Fakultät Wissenschaftszentrum Weihenstephan für Ernährung, Landnutzung und Umwelt am 10.12.2007 angenommen.

*Strength does not come
from physical capacity.
It comes from an
indomitable will.*

Mahatma Gandhi

*Indian political and spiritual
leader (1869 – 1948)*

<u>1</u>	<u>SCOPE OF THE WORK</u>	6
<u>2</u>	<u>INTRODUCTION</u>	8
2.1	Anxiety and fear: brain regions and neural circuits involved in normal and pathological behavioral responses – the amygdala and the Fear Potentiated Startle	8
2.2	The signalling pathways involved in fear learning.....	19
2.3	The mouse as a model to study fear-based anxiety disorders	22
2.4	RNA interference (RNAi) to study anxiety disorders: silencing of gene expression and application in downregulation of the ERK/MAPK signalling pathway	23
2.5	Conditional inactivation of Pink1 in the mouse: an application to study the role of amygdala in fear-based anxiety behaviors in other pathologies of the Central Nervous System – the Parkinson’s Disease case	28
<u>3</u>	<u>RESULTS</u>	30
3.1	Expression analysis of mRNAs coding for components of the MAPK signalling pathway in the adult mouse brain	30
3.1.1	<i>Mek1</i> expression.....	32
3.1.2	<i>Mek2</i> expression.....	34
3.1.3	<i>Erk1</i> expression	35
3.1.4	<i>Erk2</i> expression	36
3.2	Protein expression of ERK/MAPK signalling pathway components in the lateral amygdala of the adult mouse.....	38
3.3	Establishment of the Fear Potentiated Startle in mice.....	39

3.4	ERK/MAPK is transiently activated in the amygdala after Pavlovian fear conditioning	40
3.5	Characterization of the expression of activated ERK/MAPK in different cell types: neuronal or glial?	41
3.6	Evaluation of the acquisition of the Fear Potentiated Startle after surgery	42
3.7	Pharmacological blockade of ERK/MAPK activation in the amygdala impairs fear learning in the mouse	43
3.8	Generation of a tool to study the specific role of the MAPK ERK2 in amygdala of mice via viral-mediated RNA interference.....	45
3.8.1	Selection and testing of shRNAs for efficient downregulation of ERK1/2 <i>in vitro</i>	45
3.8.2	Testing for the tropism of the virus - the adeno-associated virus (AAV)	46
3.8.3	Testing of downregulation efficiency <i>in vivo</i> after viral-mediated infection with shRNA against <i>Erk2</i> mRNA	46
3.9	Targeted conditional deletion of the <i>Pink1</i> gene in the mouse as a model to study Parkinson's Disease	49
4	<u>DISCUSSION.....</u>	51
4.1	Expression analysis of mRNAs coding for components of the MAPK signalling pathway.....	51
4.1.1	MAPK and neurogenesis: expression in the olfactory bulb.....	51
4.1.2	MAPK and neurogenesis: expression in the hippocampal formation.....	53
4.1.3	MAPK and the limbic system: expression in forebrain areas	54
4.2	Activation of the ERK/MAPK in the lateral amygdala of the mouse is required for acquisition of a fear potentiated startle response	55
4.2.1	General consideration.....	55

4.2.2	Analysis of expression of MEK1/2 and ERK1/2 shows the presence of all these proteins in the lateral amygdala of the mouse.....	56
4.2.3	Time course of ERK/MAPK activation after fear conditioning in the lateral amygdala of the mouse.....	57
4.2.4	The activation of ERK/MAPK after fear conditioning is specifically neuronal.....	58
4.2.5	The activation of ERK/MAPK in the lateral amygdala is necessary for the acquisition of a fear potentiated startle response.....	58
4.2.6	Generation of a tool to study the specific role of the MAPK ERK2 in amygdala of mice via viral-mediated RNA interference	59
4.3	Targeted conditional deletion of the Pink1 gene in the mouse as a model to study Parkinson´s Disease.....	60
4.4	Summary and further plans.....	60
5	<u>MATERIALS AND METHODS</u>	63
5.1	Animals	63
5.2	Expression analysis of mRNAs coding for components of the MAPK signalling pathway.....	63
5.2.1	Tissue preparation for <i>in situ</i> hybridization	63
5.2.2	Cloning of the probes for <i>in situ</i> hybridization	64
5.2.3	Preparation of radiolabelled RNA probes and <i>in situ</i> hybridization	64
5.2.4	Figure preparation	65
5.3	Analysis of the ERK/MAPK signalling pathway components expressed in the lateral amygdala of the adult mouse	65
5.3.1	Tissue preparation for Western blot analysis.....	65
5.3.2	Western blot procedure	66
5.4	Behavioral procedure: the Fear Potentiated Startle.....	66

5.4.1	Fear Potentiated Startle apparatus.....	66
5.4.2	Behavioral procedure.....	67
5.5	Analysis of the time course of activation of the ERK/MAPK in the amygdala of mice after fear conditioning	70
5.5.1	Behavioral procedure and tissue preparation for immunohistochemistry to quantify phospho-MAPK labelled cells	70
5.5.2	Immunohistochemistry (IHC)	71
5.5.3	Microscopy data analysis.....	72
5.6	Characterization of the expression of activated ERK/MAPK in different cell types: neuronal or glial?	72
5.6.1	Behavioral procedure and tissue preparation for immunohistochemistry	72
5.6.2	Immunofluorescent-immunohistochemistry (IF-IHC).....	72
5.6.3	Microscopy data analysis.....	73
5.7	Surgical procedure: the stereotactic surgery in mice to target the amygdala	73
5.7.1	Stereotactic apparatus.....	73
5.7.2	Surgical procedure.....	74
5.7.3	Histological analysis	75
5.8	Pharmacological analysis of the role of the ERK/MAPK during acquisition of fear conditioning in amygdala of mice.....	76
5.8.1	Surgery	76
5.8.2	Drugs	76
5.8.3	Behavioral procedure.....	77
5.9	Injections into the amygdala	78
5.9.1	Pharmacological inhibitor.....	78
5.9.2	Viral injections.....	79

5.10 Analysis of the differential role of the ERK/MAPK ERK1 and ERK2 during acquisition of fear conditioning in amygdala of mice using RNAi.....	80
5.10.1 Selection and <i>in vitro</i> testing of shRNAs for efficient downregulation of Erk1/2 mRNAs.....	80
5.10.2 Cloning of the viral construct and viral preparation.....	80
5.10.3 Surgery.....	80
5.10.4 Testing for the tropism of the virus - the adeno-associated virus (AAV).....	81
5.10.5 Preparation of DIG-labelled RNA probes and <i>in situ</i> hybridization.....	81
5.10.6 Testing for the efficiency of downregulation of the short hairpin against Erk2.....	82
5.11 Targeted conditional deletion of the Pink1 gene in the mouse as a model for Parkinson’s Disease.....	83
5.11.1 Construction of the targeting vector.....	83
5.11.2 Cloning of the probe for the Southern blot analysis of ES cells positive for homologous integration of the targeting vector.....	84
5.11.3 Southern blot procedure.....	86
5.11.4 Preparation of the radiolabelled probe and membrane hybridization.....	86
<u>6 REFERENCES.....</u>	<u>88</u>
<u>7 ACKNOWLEDGMENTS.....</u>	<u>101</u>
<u>8 ERKLÄRUNG/DECLARATION.....</u>	<u>103</u>

1 SCOPE OF THE WORK

The scope of this work was to characterize the mouse as a model for studying fear-based anxiety disorders and establish new methods to analyze the molecular mechanisms of fear-based anxiety in the mouse. Although several studies have been already performed in rats, so far only the mouse can be genetically manipulated to further characterize the role of specific genes in complex behaviours; creating the need for a careful characterization of this species for its specific molecular characteristics and behavioural responses.

Anxiety disorders are serious medical illnesses which affect a high percentage of the population at some point in their lives. To cast light on the aetiopathogenesis of these diseases, several approaches were used (from lesion studies to mutagenesis in mice) to identify the brain regions affected and the molecules involved in the regulation of anxiety responses. But the molecular factors which could be affected in these disorders are still largely unknown. Among the six major types of anxiety disorders classified in the clinic, at least three can be ascribed to defects in fear memory processes; namely, the Panic Disorder, the Post-Traumatic Stress Disorder and the Phobias. Thus, there is a need for a better understanding of the neural basis of fear memory formation. Studies done in rats could show that the mechanisms of long-term memory (LTM) formation during Pavlovian fear conditioning are based on the association between a conditioned stimulus and an unconditioned stimulus, when these are presented in pairings. The model for fear conditioning described by Blair et al (2001) sees the NMDA receptors as responsible for LTM, consequent to the activation of a cascade of events which leads to synaptic modifications, that are considered the physiological response to environmental stimuli. In particular, the activation of the MAPK signalling cascade downstream of the NMDA receptors in the lateral amygdala (LA) is one of the mostly studied signalling pathways for its involvement in fear responses. Activated by their upstream factors in a cascade of phosphorylation events, the ERK/MAPKs are translocated into the nucleus to promote the transcription/translation of specific target genes, leading to synaptic plasticity processes.

As the mouse can be genetically manipulated, it is the model of choice to specifically characterize the role of molecular determinants in complex behaviours. So, first I

decided to characterize the endogenous expression pattern of the mRNAs coding for components of the ERK/MAPK signalling pathway in the adult mouse brain. However, transgenic mice show limits in the generation of local genetic manipulations (e.g. tissue-/region-specific promoters to use the Cre/LoxP conditional mutagenesis are not always available). To compensate this, I established stereotactic injections for the local manipulation of candidate genes in anxiety behaviours. In parallel, I also decided to develop a reliable behavioural protocol for the Fear Potentiated Startle (FPS) in mice, to use this as a model for anticipatory anxiety in humans. To characterize the role of ERK/MAPK in the acquisition of FPS, I blocked the activation of this signalling pathway in the LA of the mouse with U0126, a pharmacological inhibitor of MEK1/2, the upstream activators of ERK1/2. Moreover, to compensate for the absence of specific pharmacological inhibitors to target single genes, I took the advantage of RNA interference (RNAi) technology to further investigate the role of ERK1 and ERK2 in anxiety behaviours. I developed molecular tools to inhibit the function of ERK/MAPK via injection of viral vectors transducing shRNAs for the downregulation of ERK1/2. The use of RNAi to inhibit the function of genes *in vivo* via local injections in specific areas of the brain could add a lot to our knowledge about their area-specific function in fear/anxiety behaviours.

Moreover, I generated a mouse for the conditional mutation of Pink1, a gene recently found to be associated with Parkinson's Disease (PD). As PD patients show a certain degree of defects in amygdala-related processing of fear stimuli, I thought that the analysis of this mouse could add precious information to our knowledge about the comorbidity between neuropathologies of the CNS and neuropsychiatric diseases like anxiety disorders.

2 INTRODUCTION

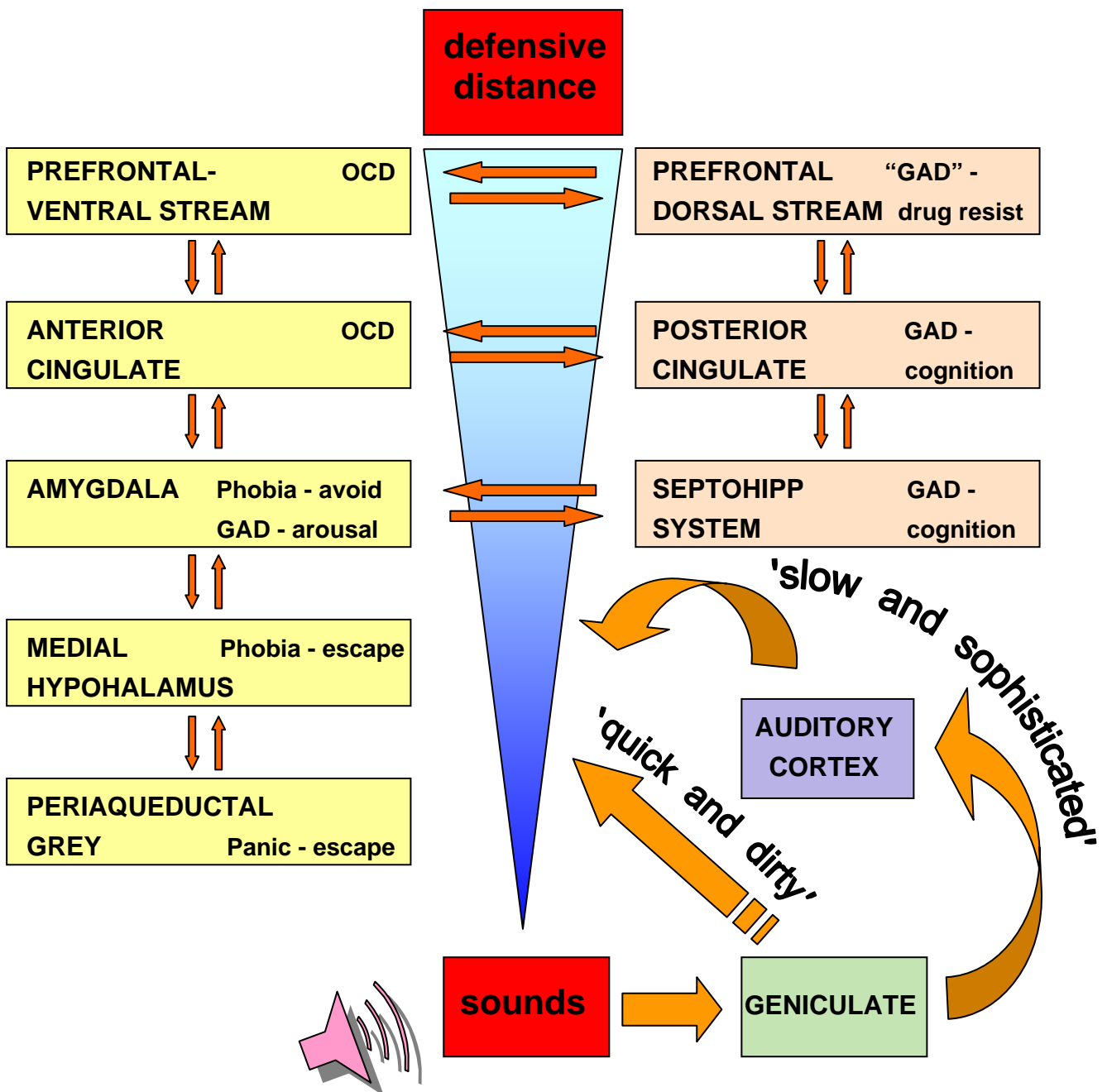
2.1 Anxiety and fear: brain regions and neural circuits involved in normal and pathological behavioral responses – the amygdala and the Fear Potentiated Startle

As defined in Pratt (1992) “Anxiety is an emotional state which is subjectively experienced as unpleasant or threatening”. Anxiety is, in fact, not a pathological response *per se*, but the natural response of a subject to threatening or stressful stimuli, expressed with an increase in arousal to the perceived stimuli. It becomes pathological when this response to the stimuli becomes disruptive, and hence interferes with a person’s capabilities during the everyday life. Anxiety disorders are serious medical illnesses which affect up to 10% of the adult population (Kaufman and Charney, 2000), with a high financial burden on the world’s health systems. As an example, this was estimated to be, only for the USA, US\$80 billion per year. Thus, a better understanding of the pathophysiology of these disorders and the development of novel therapeutic treatments are highly desirable. In humans two different types of anxiety can be distinguished: a “state” and a “trait” anxiety (Pratt, 1992). The first can be strictly associated to a specific stimulus, it is induced by the stimulus, and remits once this is removed. The latter (“trait”) is part of the individual’s personality, which is more subjective and more difficult to “remove”. But a main question remains: where do emotions “reside”?

In 1937 James Papez stated “emotion is such an important function that its mechanism, whatever it is, should be placed on a structural basis”. He suggested that sensory information from the environment, after arrival to the thalamus, can be divided into three pathways: “the stream of thought”, mediated by the cortex; “the stream of movement”, mediated by the basal ganglia; “the stream of feeling”, mediated by the hypothalamus. In 1949 Mclean and others extended Papez’ theory to include the amygdala. So the concept of the limbic system has evolved from Papez’ theory, to the one that we know now: a complex structure, including amygdala as part of the limbic lobe, important in the evaluation of stimuli and in the resulting experience and expression of emotions such as anxiety (Pratt, 1992).

For better understanding of neuroanatomical structures involved in normal and pathological anxiety, brain imaging studies have given a major contribution to cast light on the areas activated during the subjective experience of anxious states in the living human brains; and animal models have strongly helped in discovering the neuroanatomical basis and some molecular pathways involved in anxiety. But it is always under debate the definition of the areas where anxiety is developed. In a view from “The neuropsychology of anxiety” (Gray, 2000), the amygdala is recognized for its importance in the expression of the emotional aspects of anxiety, but it is mainly considered in its role through interactions with the septo-hippocampal system. This “neuropsychological” view also seems to be corroborated by studies with anxiolytic drugs, mainly reproduced by lesions in the septo-hippocampal system, again supporting the central role of this system in mediating the cognitive components of anxiety. But, as the brain is a complex structure, of course the septo-hippocampal system cannot be considered alone to work in response to the environmental sensory stimuli. It works as one part of a network of different brain regions (defined as the “defense system”), every one mainly mediating a specific response (behavior) to a threatening stimulus (represented by “sound” in Fig 1) depending on the distance (“defensive distance”) from it, as depicted in Fig 1. Thus, it becomes evident how one main difficulty in the clinical diagnosis of anxiety disorders is that the symptoms observed are difficult to interpret: they can be a perfectly normal activity in a specific site in the defense system, as an appropriate (even if extreme) response to environmental stimuli; or they can result from pathological activity in the same site; or from pathology elsewhere in the system, since this has multiple reciprocal connections. In the Blanchards’s analysis on anxiety, anxiety can be viewed as a set of responses to threat; but there must be considered at least two quite separated types of threat: on the one hand, there is a “definite, localizable, actual threat such as a predator, which must be avoided”; on the other hand, there is a “diffuse, indefinite, potential threat, which must be approached” (Blanchard, 1990). In the first case (an “actual threat”) the response elicited is avoidance or, in other terms, a moving *out of* a dangerous situation. In the second case (a “potential threat”) the response elicited is also mediated by the evaluation of the possible risk (“risk assessment”): when the perceived risk is high, behavioral inhibition is predominant; but it is accompanied by risk assessment when the perceived risk is moderate. In this second case both behavioral inhibition and risk assessment are part of a program which controls the animal while it is moving *into* a dangerous situation. The Blanchards’ analysis link

“actual threat” with “fear” and “potential threat” with “anxiety”. For Graeff (2004), part of the control on best-fitting behaviors elicited is related on opposite effects of serotonin release on periaqueductal grey and amygdala, respectively: in a sense, treatments that promote release of serotonin inform the system that a problem is soluble. This is the example of an “internal cross-talk” in response to a stimulus which does not induce any conflicts between goals; but instead it induces the activation of different levels of the hierarchy in the defense system; and some must be inhibited to avoid “internal” conflicts, while others must be activated to ensure the best-fitting response.



(redrawn with modification from Gray and McNaughton, “The neuropsychology of anxiety”, 2000)

Fig 1 The defense system viewed as a hierarchy of structures and in relation to anxiety disorders. The higher levels are engaged by increasing defensive distance and there are two parallel streams which control behavior when danger is to be avoided or approached, respectively. All parts of the system receive both fast poorly-digested (“dirty”) and slow well-digested (“sophisticated”) sensory informations. GAD, generalized anxiety disorder; OCD, obsessive-compulsive disorder.

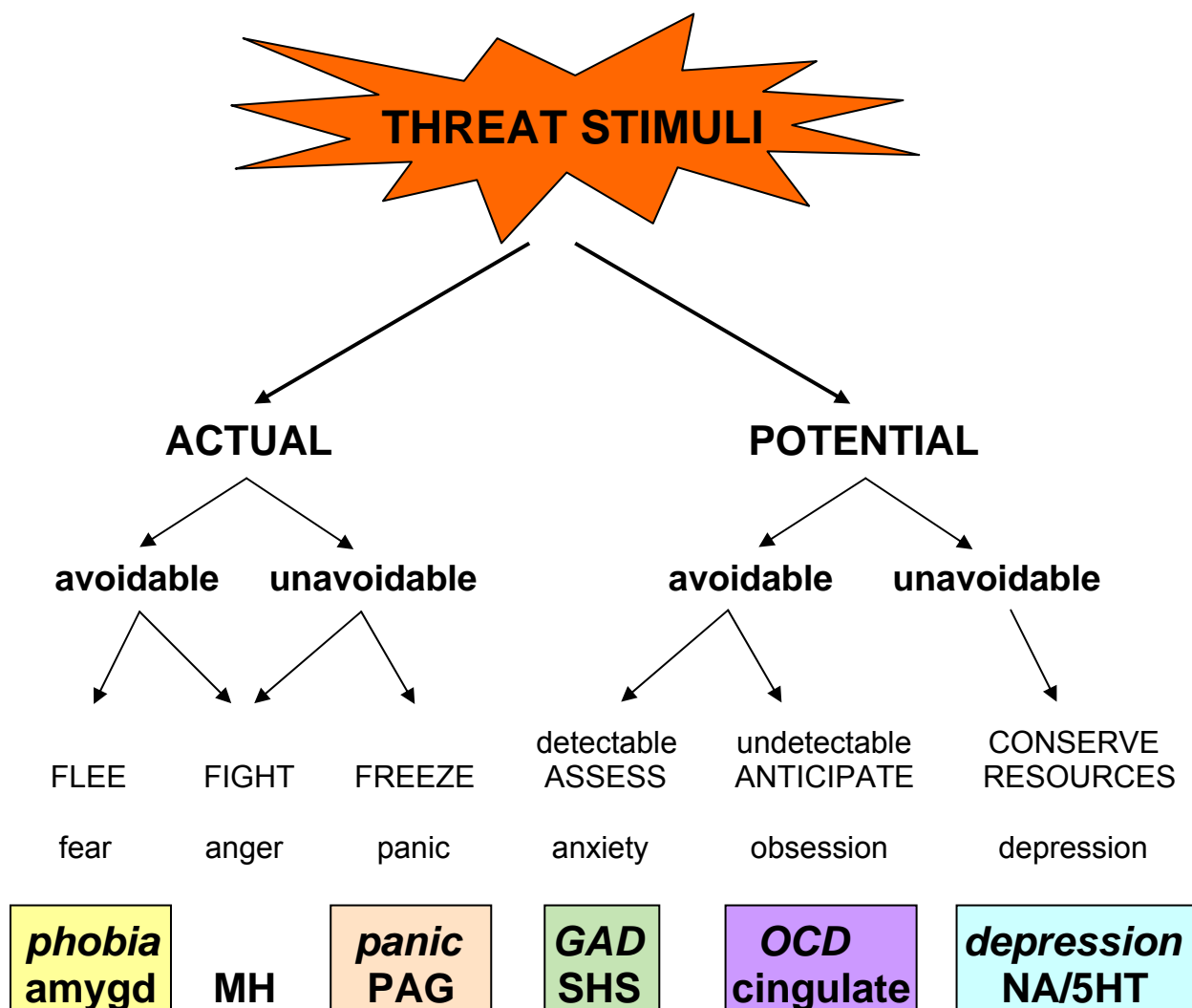
Also in this case, the septo-hippocampal system has the function of “organizing” the different regions, increasing (or decreasing) the negative associations to the stimuli. The major consequences of the activation of the inhibition system are produced, once more, by outputs from the septo-hippocampal system mainly to the amygdala.

Anxiolytic drugs, as a class, impair the function of the septo-hippocampal system (for a review, see Pratt, 1992). And the precise nature of this effect is critical for the clinical application of these theories. But they also act on amygdala, even if with a limited action. Thus, infusions of benzodiazepines (GABAA receptor agonists, enhancing GABA activity as an inhibitor of neuronal activity) directly into amygdala impair behavior in some tests of anxiety, such as passive avoidance; but the same effects are not blocked by amygdala lesions alone (for a review, see Davis, 1992). On the other hand, amygdala lesions impair behavior in tests such as active avoidance, effects not produced by benzodiazepine intra-amygdala infusions (Kopchia et al., 1992). This could be interpreted as the action of this class of anxiolytics on amygdala blocks an input that controls its activity towards production of passive rather than active avoidance. This input is the one coming from the septo-hippocampal system, with the role of regulating outputs from amygdala after detection of conflicts (Gray, 2000).

In this view, an hyperactivity of the septo-hippocampal system can produce cognitive dysfunction after perception of stimuli; and this hyperactivity can account for the excessive negative bias towards them, and, as a consequence, excessive anxiety. It is this hyperactivity on the basis of generalized anxiety disorder (GAD), and on which anxiolytics exert their clinically most important effects. In contrast with this, it is possible to attribute phobia to the amygdala and medial hypothalamus; and panic to the periaqueductal grey. But there are effects of anxiolytic drugs which impair behavior in other tests like fear potentiated startle, through their action directly on the amygdala; and they cannot be reproduced by lesions in the septo-hippocampal system (McNish et al., 1997).

Generally, amygdala is viewed as activated by emotions, like fear (“threat”), without any contaminating conflicting approach tendency; resolution of goal conflict would

arise from output from the septo-hippocampal system. But all these observations must be taken with caution, anyway, as they do not mean that anxiety has a “seat” only in the hippocampo-amygdalar circuit. As mentioned before, threat in general can be divided into two main types: “actual threat”, which must be avoided, and “potential threat”, which must be approached (Fig 2). And each of these can be subdivided into two subtypes: avoidable threat and unavoidable threat. Each of the resultant categories can be related to different types of required behavior (Gray, 2000).



(from Gray and McNaughton, “The neuropsychology of anxiety”, 2000)

Fig 2 Nature of stimuli and their relation to function, emotion, psychological disorder and principal neural systems involved. GAD, generalized anxiety disorder; OCD, obsessive-compulsive disorder; amygd, amygdala; MH, medial hypothalamus; PAG, periaqueductal grey; SHS, septo-hippocampal system; NA, noradrenaline; 5HT, 5-hydroxytryptamine.

On the basis of this discrimination, also different types of disorders can be described. The main difficulty in the diagnosis remains anyway in the complexity of responses elicited by stimuli, which normally do not activate only one and specific area. So in the end one symptom can arise either because of pathology in its specific controlling center, or because of changed activity in that center secondary to pathology in some other parts of the distributed defense control network. Six major types of anxiety disorders are described in the clinic (DSM-IV, 1994) and they are:

1. PANIC DISORDER: it is viewed as the inappropriate production of a response normally generated by proximity to an unavoidable major threat or stimulus, such as suffocation, which normally produces undirected escape responses. In spontaneous panic, freezing can occur instead of active escape attempts. The primary control center for panic as a symptom and the primary location of dysfunction in 'pure' panic disorder is the periaqueductal grey. The intensity of the syndrome may, in some cases, depend on the lack of control from hippocampal inhibitory system, reflecting a loss of function in it.

2. SPECIFIC PHOBIA: it is viewed as a reaction normally elicited by proximity to an avoidable major threat, or a stimulus which predicts its presence, and which normally produces a direct escape or active avoidance. The primary control centers for this are likely to lie in amygdala and medial hypothalamus. The specific phobia as a disorder can be caused by a greater than average negative association between innate threat stimuli and their innate response production system. Or it can result from conditioned avoidance. The occurrence of the phobic avoidance (recurrent presentation of the phobic stimulus) prevents its extinction; while the exposure to an innate or conditioned stimulus which predicts, but it is not followed by threat, facilitates extinction.

3. POST-TRAUMATIC STRESS DISORDER: this is most simply related to an extreme situation facing the individual. The symptoms appear to reflect a long-lasting conditioned response producing high activity in all regions of the defense system, the periaqueductal grey, hypothalamus, amygdala and anterior cingulate; combined in some case with a loss of hippocampal inhibitory control, as a consequence of structural damage in hippocampus itself, most probably due to the prolonged exposition to adrenocortical hormones (released after stress increase in response to fear-trauma).

4a. AGORAPHOBIA ('agora-anxiety'): this is viewed as a reaction from the conditioning of anxiety by spontaneous panic. But it can also derive from excessive

responsiveness to a diffuse set of poorly localizable, innately aversive spatial or social cues. The primary sites of activity are likely to be in the septo-hippocampal system and amygdala; and the behavioral pathology seems more the result of conditioning, and secondary to the panic attacks or phobic stimuli, which only provided a reinforcement of this conditioning, but they are not the main source to elicit the disorder.

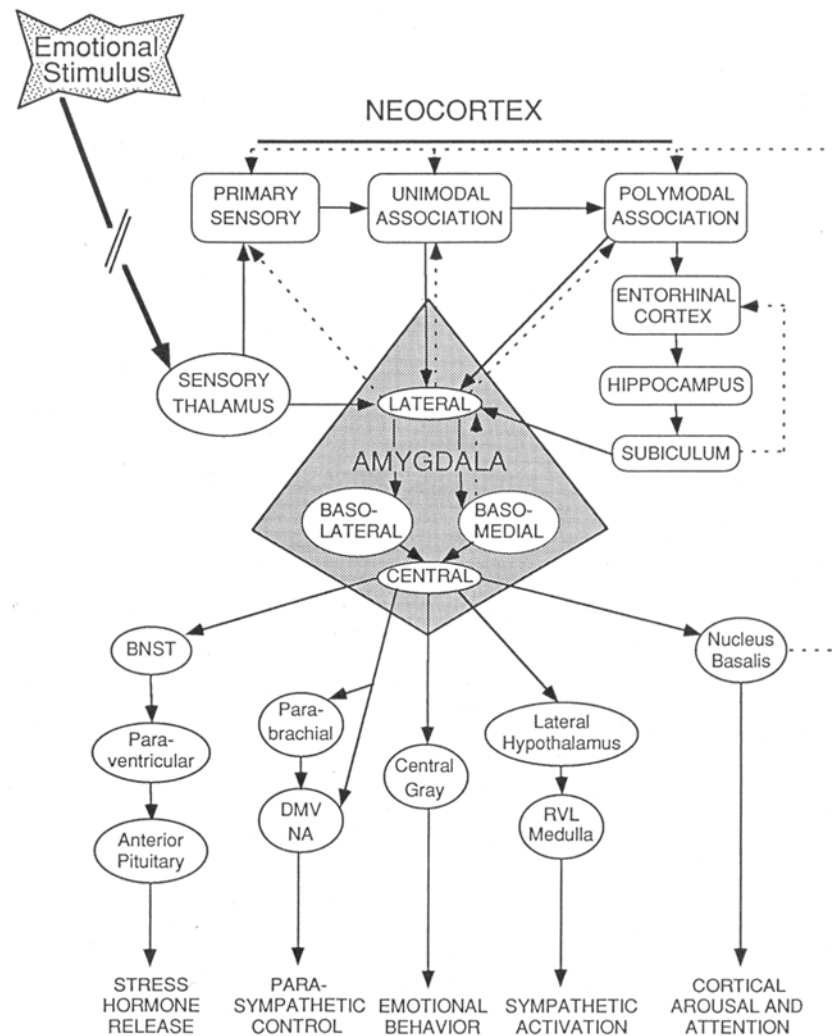
4b. SOCIAL PHOBIA ('social-anxiety'): normally it is the natural response generated by proximity to conspecifics. This could be generated by conflicts between approach and avoidance alternatives. The primary control centers are not even clear, but they should include amygdala and cingulate or prefrontal cortices. However there is likely to be excessive activity in the septo-hippocampal system.

5. GENERALIZED ANXIETY DISORDER: in this case the anxiety itself is a disorder, as opposed of being a normal reaction to outside stimuli. Neurological considerations suggest that there could be two different types: anxiolytic-sensitive (presumed to reflect overactivity in the septo-hippocampal system) and anxiolytic-insensitive (depending on descending inputs from the prefrontal and/or cingulate cortex to septo-hippocampal system and/or amygdala).

6. OBSESSIVE-COMPULSIVE DISORDER: they can be viewed as innate rituals generated both by specific environmental stimuli and also spontaneously. In the latter case they serve the function of defending the animal from threats which cannot be detected, such as disease organisms (infections). This could be linked to the 'checking' function of the septo-hippocampal system; but the key control centres are the cingulate (obsessions) and the basal ganglia (compulsions). But the neurally induced spread of activity or conditioning can result in increased anxiety (involving so the septo-hippocampal system and symptoms of anxiety).

A large body of literature has extensively described the different neuronal circuits, the main centers and the connections in the brain thought to be involved in the control of anxious states. Pharmacological studies, clinical investigations and, more recently, analysis of genetically-modified mice have also shown a great variety of mechanisms for the correct development of those brain areas and their connections (Griebel, 1999; Hood, 2000; Belzung and Griebel, 2001; Blanchard et al., 2001; Lesch, 2001; Wood, 2001; Kent et al., 2002). All these analysis have shown how defects in these mechanisms can be related to disorders in anxiety-like behaviors.

In the last 50 years literature has implicated the amygdala in assigning emotional significance or value to sensory information. In particular, the amygdala has been shown to be essential as a component of the circuitry underlying fear-related responses. Disorders in the processing of fear-related information are likely to be the underlying cause of some anxiety-related disorders in humans such as the Panic Disorder (PD) or the Post-Traumatic Stress Disorder (PTSD) (Grillon et al., 1998; LaBar et al., 1998). Analysis of fear conditioning in rats has suggested that long-term synaptic plasticity of inputs to the amygdala underlies the acquisition and perhaps storage of the fear memory (LeDoux et al., 1986; Davis, 1990; 1992). In agreement with this proposal, synaptic plasticity has been demonstrated at synapses in the amygdala both in *in vitro* and in *in vivo* studies (Sah and Lopez De Armentia, 2003). The amygdaloid complex contains two main divisions: the phylogenetically older corticomedial area and the newer basolateral area. Unlike other limbic structures it has a close relationship with basal ganglia. As it is composed of many different separated nuclei, with irregular boundaries, and it is long and narrow, it has always been a big effort to study the functional role of its different components (Pratt, 1992). Different experimental approaches have been used to assess the specific role of each nucleus of the amygdala; and it is not surprising that a variety of responses have been reported, as amygdala also has many interrelationships and connections with other brain structures through many fibers which pass in this area (Fig 3). Electrical stimulation of the amygdala produces effects on autonomic activity including changes in heart rate and respiration. But also orientation, habituation and exploratory behaviors are affected. And stimulation of the amygdala also evokes fear behaviors and defense reactions in animals (for a review, see Millan, 2003). While initial studies on the role of the amygdaloid complex used avoidance conditioning and instrumental learning, the study of emotions reached a new level with the introduction of the study of fear conditioning. This learned behavior is rapidly acquired and long lasting. The simple nature of this learning task and the readily measured physiological changes that accompany it, have made fear conditioning an interesting model for the study of learning and memory consolidation. Furthermore, because of the physiological similarities between animal and human fear, fear conditioning is seen as relevant to the genesis of anxiety disorders in humans. Davis (1998) reports the example of patients (Vietnam veterans) showing post-traumatic stress disorder: in these patients the startle reflex is increased in the dark to a greater extent than in control combat subjects (Grillon et al., 1998). Usually, to



(from Feinberg and Farah, Behavioral neurology & neuropsychology, 2003)

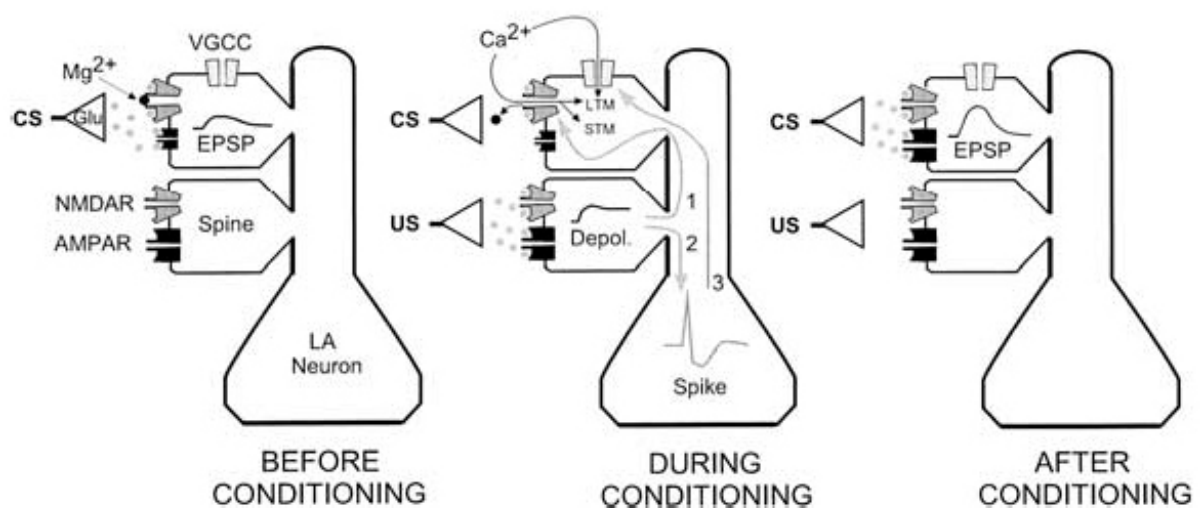
Fig 3 Schematic representation of the organization of structures involved in the integration and induction of anxious states. Note the central importance of the amygdala which can be subdivided into four major subnuclei: lateral, basolateral, basomedial and central. The lateral nucleus displays reciprocal projections with many structures from which it receives afferents. While the central nucleus shows projections to hindbrain regions through which it coordinates the behavioral, autonomic and endocrine responses to fear, a role to which—according to the concept of an “extended amygdala”—the adjacent bed nucleus of the stria terminalis (BNST) also contributes. Other abbreviations are as follows (more or less clockwise). DMV, dorsal motor nucleus of the vagus; NA, nucleus ambiguus; RVL medulla, rostral ventrolateral nuclei of the medulla.

be validated, a model should meet three major criteria: 1) face validity; 2) construct validity; 3) predictive validity. Regarding the face validity, the fear potentiated startle (FPS) responses to cue or contexts are considered to be a valid model for the re-experiencing of traumatic events or heightened startle responses, which are typical features of patients suffering of Panic Disorder (PD) or Post-Traumatic Stress Disorder (PTSD) (Grillon et al., 1998; reviewed in Cryan and Holmes, 2005). Indeed, the FPS has also shown already its good construct validity in rats as models of anxiety in humans, as the neural circuits underlying the startle responses have been well characterized in both species and showed strong similarities (Brown et al., 1951; Davis, 1992; LaBar et al., 1998; Phelps et al., 2001). Moreover, studies done in rats clearly demonstrated also the predictive validity of the FPS to study anxiety disorders, as pharmacological treatments of rats with the anxiolytics used in humans could show reduction of FPS in rats (Patrick et al., 1996; Bitsios et al., 1999). Thus, the FPS has been proven to be a valid model for anticipatory anxiety or fear in both humans and rodents.

Davis (1998) summarized some advantages of the use of a startle reflex response to study the effects of a fear-conditioning stimulus: 1. this involves the modulation of the acoustic startle reflex, a characteristic reflex observed in many different species, including humans (Grillon et al., 1991; Grillon and Davis, 1997); 2. there is a big knowledge about the neural circuits for the acoustic startle response and the FPS in rodents (Davis, 1994; Yeomans and Frankland, 1995; Lee et al., 1996). Despite the advantages shown, only in recent years researchers have developed procedures to examine FPS in mice (Falls et al., 1997; Sundin, 1998; Willott et al., 1998). During the past years, the Pavlovian fear conditioning paradigm has emerged as a leading behavioral paradigm for studying the neurobiological basis of learning and memory. Usually fearful experiences are rapidly acquired and thus easily consolidated into long-term memory (LTM), probably because they convey vital information about danger in the environment that might be important for survival. A large body of evidence suggests that the amygdala, and in particular the lateral amygdala (LA), is likely to be the site of the plasticity underlying storage of fear memory. LeDoux (1986) has reviewed the result of lesion studies aimed at identifying the circuits necessary for the expression of conditioned fear in response to acoustic stimuli. The model used typically involves pairing an auditory tone (conditioned stimulus, CS) with foot shock (unconditioned stimulus, US). The general model accepted to explain

plasticity in amygdala involves the activation of specific responses during fear conditioning in the neurons of the LA (Fig 4).

The pairing of CS and US is the input which alters synaptic transmission and neuronal activity: these activate glutamate receptors (NMDAR and AMPAR), favoring the entrance of Ca^{2+} , which in turn activates also Ion channels, like Voltage Gated Calcium Channels (VGCC); these series of events lead to the phospho-activation of specific kinases (like CaMKII, PKC, ERK/MAPK, PKA) in a cascade which leads to short-term memory (STM, lasting from few minutes to few hours) or long-term memory (LTM, lasting from few hours to months or even years), the latter if it ends with RNA/protein synthesis; this synthesis of new molecules inside neurons is considered the molecular mechanism on the basis of LTM and storage of information, as it causes structural modifications of the synapses.



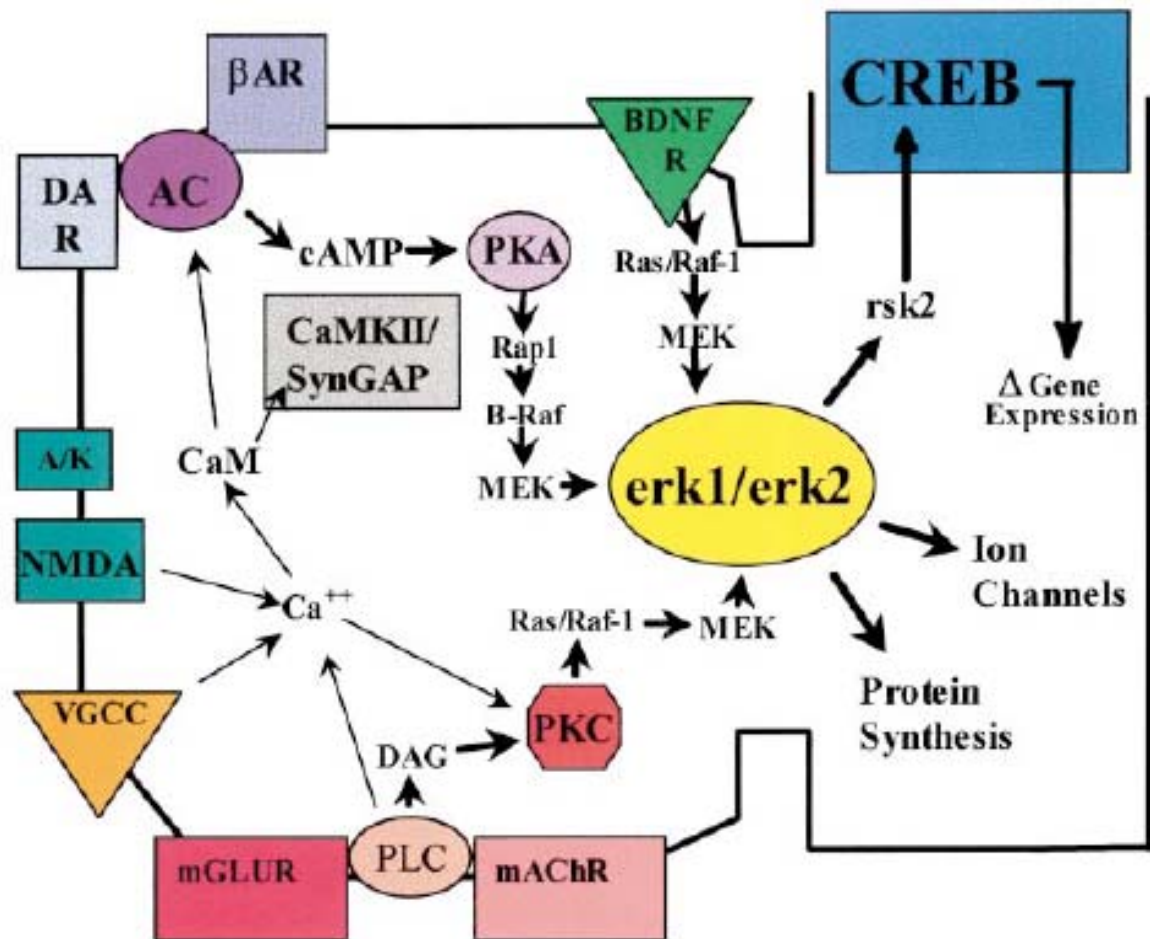
(from Blair et al., Learn Mem, 2001)

Fig 4 Cellular hypothesis of fear conditioning in LA. When the tone CS is presented before fear conditioning (left), glutamate is released at sensory synaptic inputs to LA neurons, and binds to AMPARs and NMDARs. The CS elicits only a small EPSP from the LA neurons, but it binds glutamate to NMDARs, making them eligible to pass calcium in the event of strong postsynaptic depolarization by the US (middle, arrow 1). Calcium entry through NMDARs induces short-term LTP at the synapse, but to stabilize these changes into long-term memories, VGCCs must be activated by a back propagating action potential, which occurs when the US elicits a spike from the LA neuron (middle, arrow 2) that back propagates into the dendrites to collide with CS-evoked EPSPs and open VGCCs (middle, arrow 3). After fear conditioning, the CS-evoked EPSP is larger, possibly due to an increase in AMPA currents following LTP (right).

2.2 The signalling pathways involved in fear learning

Among the signalling pathways extensively studied for their role in fear learning, the MAPK signalling pathway is one of the best characterized in the lateral amygdala (LA) of the rat in consolidation and extinction of fear memory (Schafe et al., 2000; Lu et al., 2001). The model proposed for acquisition of fear memory shows that the MEK1/2→ERK1/2 signalling pathway is activated downstream of N-methyl-D-aspartate (NMDA) receptors and voltage-gated calcium channels (VGCCs) in neurons of the LA in response to sensory stimuli as tone and footshock, when these are presented in paired association during Pavlovian fear conditioning. The mammalian family of mitogen-activated protein kinases (MAPKs) is a large group of serine/threonine terminal kinases, which consists of three well described subgroups: the extracellular signal-regulated kinases (ERK1 and ERK2) and the two stress-activated protein kinases (SAPKs) c-Jun NH₂-terminal kinases (JNKs) and p38. More recently eight different ERK isoforms with high similarity with ERK1/2 were described, among which only ERK1, ERK2, ERK3, ERK4, ERK5 and ERK7 were found to be expressed in the adult rodent brain. Among these eight proteins ERK1, ERK2, ERK3 and ERK5 belong to the canonical MAPK signalling pathway. ERK3 and ERK5, were described and included in this family (Sweatt, 2001; Johnson and Lapadat, 2002; for review, see Bogoyevitch and Court, 2004). However, despite the high degree of structural similarities with the previously described ERK1 and ERK2, they show functional features which distinguish them from all the other members of MAPKs, defining two more distinct subgroups of kinases (Turgeon et al., 2000; Cavanaugh et al., 2001). MAP kinases are evolutionary conserved from yeast to humans and are involved in the transduction of extracellular signals to cytoplasmic and nuclear effectors (see Fig 5 for a schematic representation), thus regulating a variety of cellular functions, like cell growth, proliferation, differentiation and stress responses (Pages et al., 1993; Kyriakis and Avruch, 1996; Weber et al., 1997; Refojo et al., 2005; Werry et al., 2005).

But, whereas the ERK1/2 pathway is a signalling cascade activated by mitogens through their binding to specific cell-type receptors (like hormones, growth factors and neurotransmitters, as schematized in Fig 5; see Pages et al., 1993; Vouret-Craviari et al., 1993; Weber et al., 1997), the JNK/SAPK and p38 pathways are mainly activated by cellular stresses (like UV-irradiation and anoxia or proinflammatory cytokines; see Dickinson and Keyse, 2006). The activation of these



(from Sweatt, J Neuroch, 2001)

Fig 5 Erk integration of diverse cell surface signaling mechanisms. VGCC, voltage-gated calcium channels; A/K, AMPA/Kainate subtype of glutamate receptor; PLC, phospholipase C; AC, adenylyl cyclase; NMDA, N-methyl-D-aspartate subtype of glutamate receptor; DAR, dopamine receptor; β AR, β -adrenergic receptor; BDNFR, brain-derived neurotrophic factor receptor; PKA, protein kinase A; CaMKII, Calcium calmodulin kinase II; mAChR, muscarinic acetylcholine receptor; mGLUR, metabotropic glutamate receptor; PKC, protein kinase C; CREB, cAMP response element-binding.

ERKs is mediated by their phosphorylation on tyrosine and threonine residues via the action of MEKs (MAPK/ERK kinases). Regarding the MEK proteins, MEK1 and MEK2 were identified as specific activators of ERK1 and ERK2, while MEK5 was described as the specific upstream activator of ERK5 (Bogoyevitch and Court, 2004). As activators of the MEKs, RAF kinases were identified (Catling et al., 1994; for a review, see Wellbrock et al., 2004). Among the RAF proteins, BRAF and CRAF were found to be expressed in the adult rodent brain. BRAF expression is mainly restricted to the brain in adult tissue and is described as the main activator of MEK1/2 (Storm et al., 1990; Papin et al., 1996; Morice et al., 1999).

It has also been shown that the MAPKs are phosphorylated and activated in a variety of cells, but with some regional and cell-type specificity. In fact, it has been recently shown that the activation of the BRAF→MEK1/2→ERK1/2 signalling cascade is restricted to neurons in contrast to astrocytes in the brain of rats (Dugan et al., 1999). Moreover it has been described that a direct interaction of BRAF with ERK3 occurs in protein extracts from pyramidal hippocampal neurons, suggesting that also this signalling pathway is restricted to neurons (cell-type specificity), and to hippocampus (regional specificity) (Kim and Yang, 1996).

Given the role of MAPKs in promoting proliferation and differentiation processes in neural tissues during embryonic development (Furthauer et al., 2002; Corson et al., 2003), this suggests that in the mature forebrain they could play a role in regions where adult neurogenesis takes place, as in the olfactory bulb (OB) and in the hippocampal dentate gyrus (DG) (Kuhn and Svendsen, 1999; for review, see Galli et al., 2003).

Several recent studies focused on understanding the mechanisms regulating activity-dependent synaptic plasticity in the Central Nervous System (CNS) which is the basis of acquisition, storage and utilization of information coming from the sensory world. The sensory pathways in the brain generally develop from crude wired networks to more refined systems through the organization of synaptic connections. And the refinement of synaptic connections has been shown to be based on neural activity, mostly driven by the function of N-methyl-D-aspartate (NMDA) receptors. These are thought to transduce synaptic activity to Ca²⁺-dependent cellular processes that result in refinement of neuronal circuits. In this process the activation of ERK1 and ERK2 seems to be essential (for reviews, see Constantine-Paton et al., 1990; Shatz, 1990).

In recent years the activation of MAPKs was studied to unravel new properties of these molecules in regulating both activity-dependent synaptic plasticity processes and behavioral responses, as learning and memory. Among these, worth to be mentioned are adaptive responses of mature neurons as long-term potentiation (LTP) and memory formation, which were shown to depend on activation of MAPKs components downstream of NMDA receptors (English and Sweatt, 1997; Atkins et al., 1998; Impey et al., 1998; Impey et al., 1999; Schafe et al., 1999; Arendt et al., 2004). In order to get more insight into the function of the MAPK signalling pathway in the adult brain a precise knowledge of the *in situ* expression pattern of genes implicated in this pathway is necessary to suggest possible functional interactions

among activator and effector proteins. The expression of MAPK signalling pathway components in the adult central nervous system has been shown by Northern or Western blot analysis; however, the precise spatial distribution of each of these genes within the adult brain had still to be determined. Therefore, I assessed the detailed expression pattern of *Mek1*, *Mek2*, *Erk1* and *Erk2* as the main members of the MAPK signalling pathway in the adult murine brain involved in regulating learning and memory processes.

2.3 The mouse as a model to study fear-based anxiety disorders

As the anxiety disorders affect a high percentage of the population, with increasing burdens on the health systems all over the world, it is clear that a better understanding of the pathophysiology of these disorders and the development of novel therapeutic treatments are medically desirable. On the other hand, due to the high costs of the clinical trials for the development of new pharmaceutical drugs, there is a strong interest for assurance that any identified biological target is really relevant to the disease. Thus, the availability of valid preclinical animal models for searching new potential pharmacological targets is of central importance. The advent of transgenic technologies in mice to further characterize the role of specific genes in complex behaviors, in the past years created the need for a detailed characterization of the mouse for its validity as animal model to study anxiety and fear-related behaviors in humans. As already described before, the FPS is a good paradigm to model anticipatory anxiety in rodents. But it was mostly used in rats. Only in recent years, the work of the Falls laboratory has started to characterize the FPS in mice, comparing the efficiency in acquisition of fear potentiation in different strains of inbred mice (Falls et al., 1997; Falls, 2002). They could also show that it is amygdala dependent, as lesions in this region in C57BL/6J mice can impair the acquisition of FPS (Heldt et al., 2000). Moreover they also showed that the FPS model can be used to characterize the involvement of specific molecules in the acquisition of fear-related behaviors (Falls, 2000). Thus, this strongly supports the FPS as a behavioral paradigm to unravel the role of new molecules and signalling pathways in the regulation of acquisition and extinction of learned fear in mice.

As mentioned above, among the signalling pathways extensively studied for their role in fear learning, the MAPK signalling pathway is one of the best characterized in the lateral amygdala (LA) of the rat in consolidation and extinction of fear memory

(Schafe et al., 2000; Lu et al., 2001). However, even though mechanisms on the basis of survival responses as fear conditioning are strongly conserved, the molecules which regulate those processes can be differentially expressed in the brains of evolutionary even highly related species as the rat and the mouse. As an example of this, I have recently shown that the expression pattern of components of the MAPK signalling pathway can differ in the adult brain of the rat and the mouse, at least at the mRNA level (Thomas and Hunt, 1993; Di Benedetto et al., 2007).

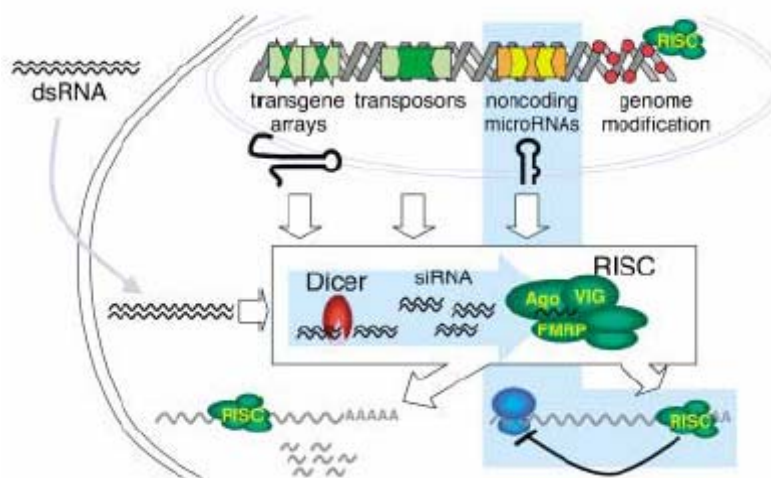
Moreover, in recent years some studies started proposing an active participation of glial cells in the regulation of stimulus-dependent synaptic activity (Nishiyama et al., 2002; Todd et al., 2006). In particular, it was shown that astrocytes can release glutamate in response to intracellular increases in Ca^{2+} concentrations, thus regulating the activity of neighboring neurons (Parpura and Haydon, 2000). As Ca^{2+} modulates in neurons the activation of intracellular signalling pathways as the MAPK pathway, for acquisition of fear memories, it is possible to hypothesize that MAPKs could be activated in glial cells during processes responsible for fear memory formation.

Taken together, these arguments stress the importance of further characterizing the mouse as a model to study the neurobiological basis of anxiety disorders. In particular, I aimed at (1) determining the pattern of expression of the MEK and ERK proteins (MEK1, MEK2, ERK1 and ERK2) in the LA of the mouse; (2) analyzing the time course of activation of ERK/MAPK in the LA of the mouse after fear conditioning; (3) identify the cell-type specificity of activated ERK/MAPK in LA after fear conditioning; (4) further characterize FPS in mice, analysing how the pharmacological inhibition of the ERK/MAPK signalling pathway in the LA can affect acquisition of FPS in this animal model.

2.4 RNA interference (RNAi) to study anxiety disorders: silencing of gene expression and application in downregulation of the ERK/MAPK signalling pathway

Since it was first described, RNA interference (RNAi) has become one of the most powerful techniques in the attempt of down-regulating the expression of specific genes in a variety of organisms in the past years. As a technique that only requires short stretches of sequence information to generate loss-of-function alleles of any

gene, it holds enormous promise in the functional analysis of new genes found in the recently completed genome sequences. And it is especially a great advantage for the analysis of gene function in those organisms in which traditional gene-knockout strategy is not feasible. In mammals, in which traditional gene knockouts are time-consuming lab-work, the advent of RNAi has generated a great deal of excitement in its application to identification of drug-target; but more than this, for its application in the generation of new tools to be used by gene therapy. RNAi was first described as a startling phenomenon in which exogenously supplied double-stranded RNA (dsRNA) had potent and specific effects in reducing the expression of homologous endogenous genes (Fig 6).



(from Conklin, ChemBioChem, 2003)

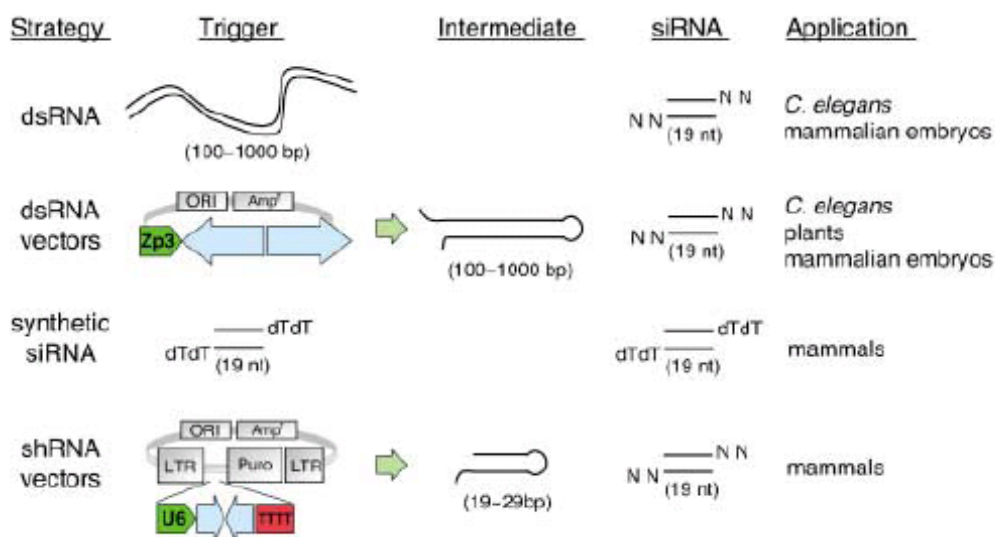
Fig 6 Schematic drawing representing the cellular processing of the RNA interference (RNAi) machinery. Exogenous dsRNA and transgene-derived RNAs are processed into small interfering RNAs (siRNAs), which silence mRNA by degradation. RISC, RNA-induced silencing complex.

The studies aimed at discovering the molecular mechanisms behind this phenomenon have described RNAi as a cellular mechanism of defense: it should inhibit infection by (and replication of) RNA viruses, as well as hopping of transposable elements, through recognition and cleavage of dsRNAs. The results of these studies, including genetic and biochemical evidences from *C. elegans* and *Drosophila*, have provided a model in which RNAi occurs through a two-step mechanism:

1 STEP: dsRNAs are recognized by the enzyme DICER (a RNase III family nuclease) and cleaved into 21-nt RNA fragments (siRNA), with 2-nt 3'-overhangs on both strands.

2 STEP: these siRNAs are then incorporated into a multicomponent nuclease complex termed RISC (RNA-Induced Silencing Complex), which contains the proteins necessary for unwinding the double-stranded siRNAs; then, directed by the antisense strand of the siRNA duplex, RISC recognizes and cleaves the target mRNA at complementary sites.

Despite the doubtless importance and power of RNAi as a useful genetic tool, as shown for genome-scale RNAi-mediated gene function analysis in *C. elegans*, it is still hard to perform similar studies in mammals. This is mainly due to the large impediments both to trigger enough siRNAs into the mammalian cells and to avoid the negative physiological responses to dsRNAs by these cells. Different strategies have been tried to circumvent these impediments. These involve 3 main approaches used so far (schematized in Fig 7):



(from Conklin, ChemBioChem, 2003)

Fig 7 RNA-interference delivery strategies . Four major methods of introducing RNAi triggers are listed with schematics and typical applications of each. A representative long dsRNA and short hairpin RNA (shRNA) vector are shown. The elements depicted in the shRNA vector are typically included to improve the gene-transfer efficiency and stability of the silencing effect. Note that a siRNA or siRNA-like molecule is generated in each approach.

1. use of “naked” siRNAs synthesized *in vitro* and annealed as RNA duplexes → they can be directly triggered into the cells → “dsRNA” or “synthetic siRNA”.
2. use of DNA plasmids containing sequences coding for siRNAs in the form of “small hairpin RNAs” (shRNAs) → plasmids are triggered into cells, where they encode for

shRNAs, which are recognized by the Dicer/RISC complex like siRNAs → “dsRNA vectors” or “shRNA vectors”.

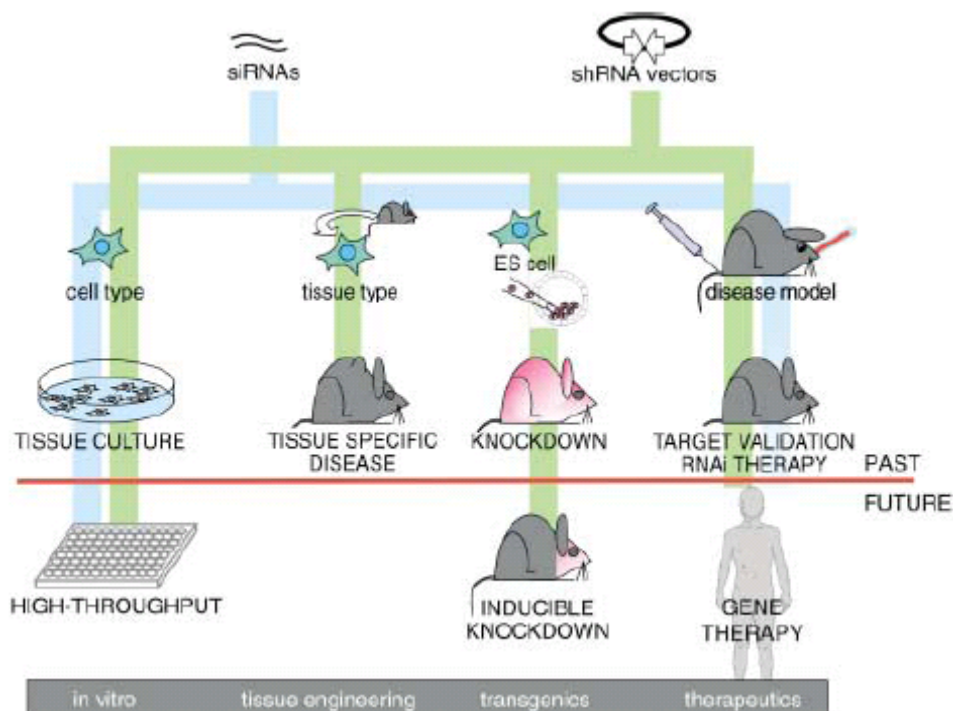
3. use of viral vectors containing sequences coding for siRNAs in the form of “small hairpin RNAs” (shRNAs) → vectors are triggered into cells, where they encode for shRNAs, which are recognized by the Dicer/RISC complex like siRNAs → “dsRNA vectors” or “shRNA vectors”.

Every one of them shows advantages and disadvantages which have to be taken into consideration when planning RNAi experiments.

In general a concept has emerged from the extensive use of siRNAs in gene silencing which regards the variable susceptibility of target genes to siRNAs. The central event in RNAi-mediated gene silencing is the interaction of the siRNA contained in RISC with its complementary sequence within an mRNA. However, it appears that not all interactions between siRNAs and target sequence are equal.

Even if highly useful already, a number of improvements to the current technologies are likely to emerge in the near future. Inducible hairpin promoters that express shRNAs only in response to small molecule inducers or in specific tissue types would be valuable in the analysis of genes that are essential, have multiple roles in development, or that are related to behavior. In Fig 8 are shown some examples of the applications in mammals so far. As mentioned in 2.2, one of the signalling pathways which is highly studied for its involvement in the regulation of memory formation, and especially in fear learning, is the MAPK signaling pathway. But a great limitation in the pharmacological dissection of the specific role of the different components in this signaling cascade lays in the lack of availability of specific pharmacological compounds to target single molecules. As a deep analysis of the role of single molecules in normal and pathological fear or anxious states is necessary, with the advent of RNAi it became immediately clear that one of the major advantages could be in circumventing this problem of lack of pharmacological compounds. Several reports already showed the feasibility of the RNAi approach, even *in vivo*, using different strategies to trigger the siRNAs into the mammalian cells (Caplen et al., 2001; Elbashir et al., 2001; Hannon, 2002). Among the different methods used, the viral approaches seemed to be more effective to reach sufficient levels of downregulation to perform subsequent behavioral studies (Rattiner et al., 2004; Musatov et al., 2006). Nevertheless, a major concern still requires attention: the choice of the best viral vector for the different scopes. In fact, there are several

types of viruses which can be used. Just to mention few, the retroviral vectors were found to be very effective in the introduction of siRNA-expression units into transfection-resistant cells as primary cells (Barton and Medzhitov, 2002; Devroe and Silver, 2002). However, the retroviral systems show major disadvantages, among which, one is the very low infection efficiency of non-dividing/post-mitotic cells. Some of these problems could be overcome by the use of the adenoviral (AV), adeno-associated viral (AAV) or lentiviral (LV) systems (Davidson et al., 2000; Hommel et al., 2003; Rubinson et al., 2003; Tiscornia et al., 2003). All of them efficiently triggered shRNAs into mammalian cells *in vivo* even in the adult mouse or rat brains. So, I decided to take the advantages of these different vectors for our aims. The choice of the best one was naturally based on some considerations dependent on the specificity of the goals. Namely, our major aim was to dissect the specific role of ERK1 and ERK2 in the acquisition of long-term memory as measured by Fear Potentiated Startle, to clarify the role of these two genes in fear-based anxiety disorders. To get further insight into this topic, I decided to: 1) select and test specific short hairpin sequences which could target either Erk1 or Erk2 mRNAs separately; 2) clone the selected hairpin sequences into viral backbones for the production of the viral vectors.



(from Conklin, ChemBioChem, 2003)

Fig 8 Applications of RNA-interference-based silencing in mammals. Schematic summary of current (above red line) and probable future (below red line) uses of RNA interference. siRNAs are typically used in cell cultures, but have also been used in some therapeutic studies in mice. shRNA vectors are especially useful in the generation of stable, hypomorphic alleles of genes in tissue culture cells, in specific cell types within mice, and in entire animals. High-throughput, inducible knockouts and gene therapy are under development.

2.5 Conditional inactivation of Pink1 in the mouse: an application to study the role of amygdala in fear-based anxiety behaviors in other pathologies of the Central Nervous System – the Parkinson's Disease case

Several recent neuropsychological studies have reported dysfunctions that impair the recognition of emotions. Patients with lesions of the amygdala (Adolphs et al., 1994; Adolphs et al., 1995; Adolphs et al., 1999) show severe defects in recognition of facial expressions of fear. People with Huntington's Disease (Sprengelmeyer et al., 1996) are poor at recognizing facial expression of disgust. In the case of Parkinson's Disease (PD), things are not so clear yet. Jacobs et al (1995) reported that PD patients exhibit deficits in comparing emotional facial expressions; but Adolphs et al (1998) could not reproduce the same findings. In another study, Kan et al (2002) found that PD patients do show deficits in recognizing fear and disgust in photographs and video recordings of facial expressions, but the recognition of emotions was not impaired in these patients when subjected to written verbal stimuli. As neuroimaging studies showed already that amygdala and striatum are activated in processing expressions of fear and disgust, and there is evidence that these areas are functionally impaired in PD patients, (Mattila et al., 1999; Ouchi et al., 1999), it is possible to hypothesize that the disturbance of emotional recognition can be attributed to pathological changes in these regions of the brain.

Several loci have been already associated with the neuropathology of Parkinson's disease. Moreover, linkage studies have identified some of the genes involved in the development of this disorder. Recently, Pink1 was associated with the PARK6 locus and studied for its role in one of the autosomal recessive forms of PD (Valente et al., 2004). To get more insight into the neuropathology of PD and its behavioral dysfunctions in humans, I decided to generate a conditional mutation of the Pink1 gene in the mouse. The use of the conditional approach to generate a null mutation

of Pink1 could allow to circumvent the eventual lethality of this mutation; and it could help a more precise dissection of the role of this gene in different areas of the brain with the use of different tissue- or region-specific Cre lines. Moreover, if Cre lines were not available for some areas, it would be possible to conditionally delete the gene in those areas via their viral-mediated transduction with Cre-expressing vectors, as shown already (Ahmed et al., 2004). The goal was to generate a mouse model of PD which could be further analysed to cast light on the role of PD genes in the neuropsychiatric dysfunctions shown by some PD patients; thus, this could help to clarify association between PD and defects in processing emotional cues. For this aim, a targeting vector bearing two loxP sites flanking the region containing exon 2 and exon 3 of the Pink1 gene was generated as part of this work.

3 RESULTS

3.1 Expression analysis of mRNAs coding for components of the MAPK signalling pathway in the adult mouse brain

The expression study of ERK/MAPK in the brain of adult mice was performed on adjacent sections, in order to be able to compare the expression of the different genes in different regions of the brain. Judged was the “presence” or “absence” of a hybridisation signal. However, no attempt was made to compare the signal intensities of different probes. The spatial distribution of the signals was evaluated on coronal sections and it was confirmed on sagittal and horizontal sections (Fig 9-12). The signal intensity of a specific antisense probe was judged as being absent (-), very weak (-/+), weak (+), weak-to-moderate (+/+++), moderate (++), moderate-to-strong (++/+++), strong (+++), or very strong (++++) (see Tab 1). The judgement was made relative to the signal intensity of the background.

	Mek1	Mek2	Erk1	Erk2
Olfactory bulb				
Periglomerular layer	-	-	++	++
External plexiform layer	-	-	+	-
Mitral cells	+ / ++	-	+++	+++
Granule cells	++	-	+	+++
Anterior olfactory nucleus	++	-	+ / +++	+++
Cerebral cortex	++ / +++	-	++	+++
Piriform cortex	+++	-	+++	+++
Hippocampus				
CA1 pyramidal cells	++	-	-	+++
CA2 pyramidal cells	++	- / +	-	+++
CA3 pyramidal cells	++++	- / +	+	++++
Dentate gyrus	++	-	++	+++
Tenia tecta	++	-	++	+++
Nucleus of olfactory tract	+	-	+	++
Ventral tegmental area	- / +	-	- / +	+
Amygdala				
Basal amygdaloid nuclei	++	-	+	+++
Lateral amygdaloid nuclei	+++	-	+++	+++
Central amygdaloid nucleus	+++	-	++	+++

	Mek1	Mek2	Erk1	Erk2
Basal ganglia				
Caudate putamen	++	-	+	++
Lateral striatal stripe	++	-	-/+	+++
Nucleus accumbens	++	-	+	+++
Olfactory tubercle	++	-	+	+++/+
Globus pallidus	+	-	-/+	-/+
Endopiriform nucleus	+++	-	++	+
Clastrum	+++	-	++	++
Zona incerta	-/+	-	-	++
Substantia nigra, pars reticulata	-	-	-	+
Substantia nigra, pars compacta	++	-	+	+++
Septum				
Bed nucleus stria terminalis	++	-	+++	++/+
Lateral septum	++	-	-/+	++
Medial septum	-	-	-	+
Diagonal band	-	-	+	+
Habenula, medial part	+	-	++	++
Habenula, lateral part	-	-	-	+
Thalamus (general)	+	-	+/>++	++
Pretectal nucleus	-/+	-	-/+	+/>++
Lateral geniculate nucleus	+	-	-	++
Hypothalamus (general)	++	-	+	++
Mammillary nuclei	-/+	-	-/+	++
Mid- and hindbrain				
Superior colliculus	-/+	-	+	+/>++
Inferior colliculus	-/+	-	-	++
Periaqueductal gray	+	-	-/+	+/>++
Oculomotor nucleus	-/+	-	+++	++
Red nucleus	-	-	++	+++
Cerebellum				
Molecular cell layer	-	-	-	-/+
Purkinje cell layer	++	+	-/+	+/>++
Granule cell layer	-	-	-/+	-/+
Raphe nuclei	+	-	+	+/>++
Locus coeruleus	++	-/+	+++/>++	+++
Pontine reticular nucleus	-/+	-/+	-/+	+
Pontine nuclei	+	-	+/>++	+++
Tegmental nuclei	-/+	-	+/>++	+/>++
Cochlear nucleus	-	-	-	+
Superior olive	-/+	-	-	+/>++
Inferior olive	-/+	-/+	-	+
Trapezoid body	-	-	-	+/>++
Formatio reticularis	-/+	-/+	-/+	+/>++
Nuclei of cranial nerves (5, 7, 10, 12)	-/+ to ++	- to -/+	- to ++	+/>++ to ++

Tab 1 Expression levels of the MAPKs in all analysed regions in the adult mouse brain. Regions are listed in the left column. Expression levels for Mek1, Mek2, Erk1 and Erk2 are listed in the following columns. “-“ means no expression detectable, “-/+” indicates a faint expression, up to “++++” for a strikingly high expression; referred to the background signal. When the distribution of expression signal throughout one region was not uniform, the intensity depicted here corresponds to an estimated overall mean in this region. The 5th, 7th, 10th and 12th nucleus of cranial nerve were analyzed individually but pooled in this table.

Acb	nucleus accumbens
Amy	amygdala
C	cochlear nucleus
CA	field of Ammon’s horn, hippocampus
CA1	CA1 region, hippocampus
CA2	CA2 region, hippocampus
CA3	CA3 region, hippocampus
CeA	central nucleus, amygdala
Cb	cerebellum
Co	cerebral cortex
CPu	caudate putamen
DG	dentate gyrus
GL	granule cell layer, cerebellum
Hy	hypothalamus
IC	inferior colliculus
LA	lateral nucleus, amygdala
ML	molecular cell layer, cerebellum
OB	olfactory bulb
PC	purkinje cell layer, cerebellum
Pn	pontine nuclei
PnR	pontine reticular nucleus
Rt	formatio reticularis
SN	substantia nigra
SNC	substantia nigra pars compacta
SNR	substantia nigra pars reticulata
Su	superior colliculus
Th	thalamus

Tab 2 List of abbreviations used in the Figures and text for the expression analysis of components of the MAPK signalling pathway.

3.1.1 *Mek1* expression

The expression of *Mek1* mRNA (summarized in Tab 1) in the olfactory bulb shows moderate signals in the anterior olfactory nucleus and in granule cells. Also the mitral cell layer of the bulbs shows the signals, at weak-to-moderate levels (Fig 9B). The cerebral as well as the piriform cortex express *Mek1* mRNA at moderate-to-strong and strong levels, respectively. Also some regions of the basal ganglia show strong

signals for *Mek1* mRNA, as the claustrum and the endopiriform nucleus. All the other parts of the basal ganglia are only weakly to moderately labelled; with exception of the zona incerta, showing only very weak signals, and the pars reticulata of the substantia nigra since this region is completely devoid of any *Mek1* labelling (Fig 9H). Also the lateral habenula does not show any signals for *Mek1*, while the medial part does at weak levels.

In the hippocampal formation signals are quite prominent, as in the dentate gyrus granule cells are moderately labelled, as well as the CA1 and CA2 regions. The CA3 region shows even a very strong *Mek1* expression. These differences in the intensity of the signals can be detected at a closer view. Fig 9D shows the very strong

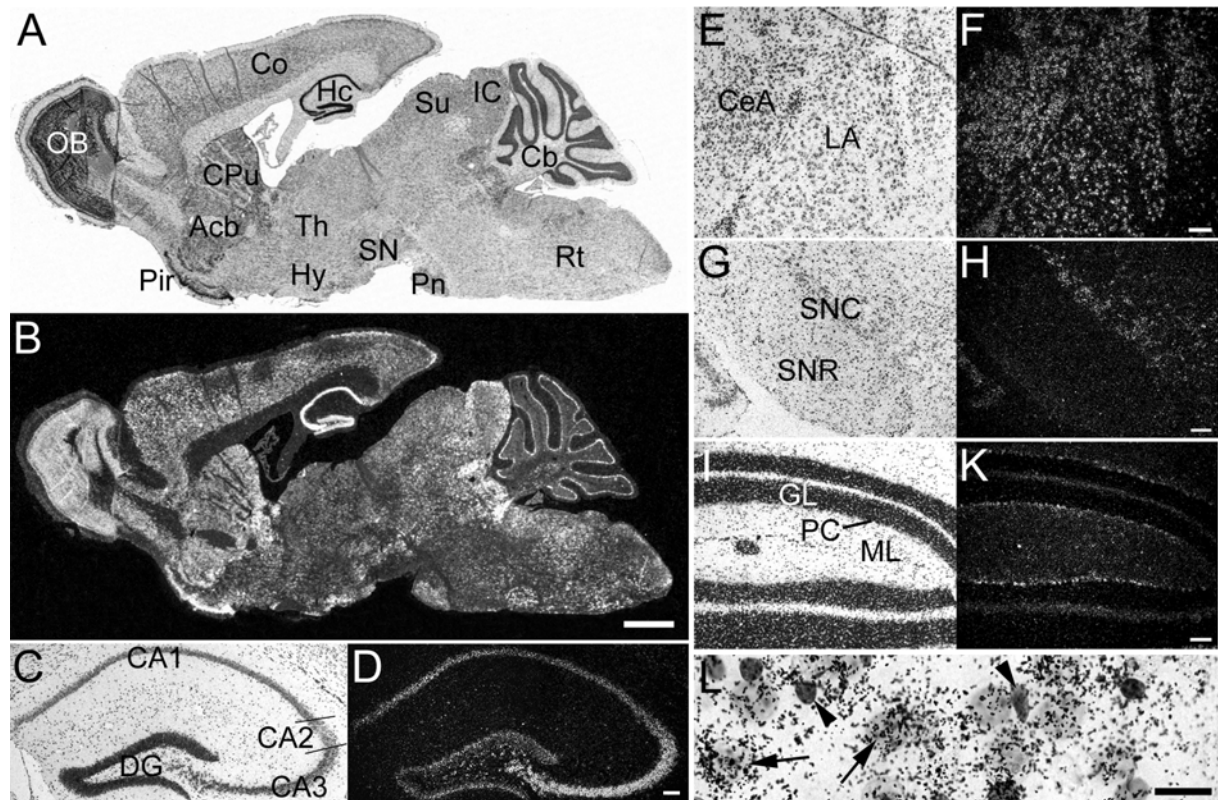


Fig 9 Sections of adult mouse brain labelled with the *Mek1* in situ probe. Darkfield photomicrographs (B, D, F, H, K) and corresponding brightfield images of Nissl stained sections (A, C, E, G, I) are displayed. A and B show a high exposed complete sagittal section at a glance. Magnifications of the hippocampus (C, D), the amygdala (E, F), the substantia nigra (G, H) and the cerebellum (I, K) from coronal sections present the expression pattern of *Mek1* mRNA in more details and with more graduations (especially in D). For abbreviations see Tab 2. In the brightfield image of a high magnification of striatal cells (L) expression signal is visible mostly in big neuron-like cells (arrows) and only weak, but well detectable, in some smaller, darker Nissl stained glia-like cells (arrowheads). Scale bar = 1 mm in B; 0.1 mm in D, F, H, K; 0.016 mm in L.

labelling in CA3 in contrast to the slightly weaker signals in CA1 and CA2 (that is not readily distinguishable on the highly exposed picture in the overview of Fig 9B). Also in the amygdala high levels of *Mek1* mRNA are expressed, particularly the lateral and central parts show strong signals, whereas the basal nuclei show only moderate labelling (Fig 9F).

Furthermore, the hypothalamus is moderately labelled with the *Mek1* probe, while the thalamus shows only a weak expression. In more posterior areas *Mek1* mRNA is not so prominent any more. Only the locus coeruleus and the VII cranial nerve show moderate signals whereas other regions in the posterior parts of the brain express *Mek1* only at weak or even very weak levels. Moreover the red and cochlear nuclei and the trapezoid body do not express it at all. In the cerebellum only Purkinje cells show moderate signals (Fig 9B and K).

Mek1 expression in the brain is not restricted to one specific cell type. Although strong signals for *Mek1* mRNA are visible on almost all neurons, also some glia cells, identified by the smaller size and dark Nissl-staining, show weak expression (arrowhead in Fig 9L).

3.1.2 *Mek2* expression

In line with previous reports (Brott et al., 1993) showing Northern blot analysis in which very low levels of *Mek2* mRNA were present in the adult murine brain, the probe for the in situ detection of *Mek2* mRNA shows barely detectable levels of the hybridisation signal in our slices of adult brain (Fig 10). The very weak signal is confined to CA2 and CA3 hippocampal regions (Fig 10B, barely visible). More

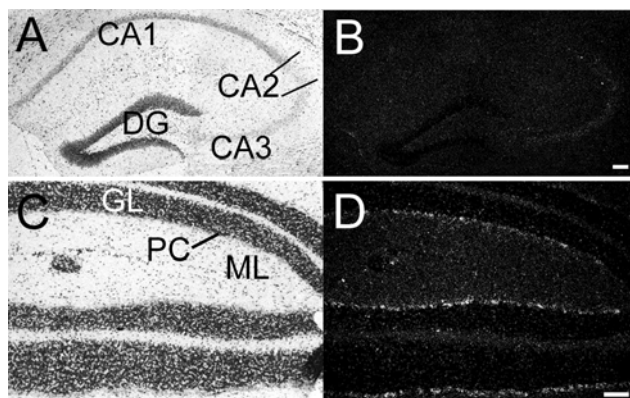


Fig 10 Sections of adult mouse brain labelled with the *Mek2* in situ probe. Darkfield photomicrographs (B, D) and corresponding brightfield images of Nissl stained sections (A, C) are displayed. A and B show in a complete sagittal section the absence of *Mek2* mRNA in most of the regions. Magnifications of the hippocampus (A, B) and the cerebellum (C, D) from coronal sections visualize the very weak signal. For abbreviations see Tab 2. Scale bar = 1 mm in B; 0.1 mm in D, F.

posterior very weak signals are present in the locus coeruleus, in the pontine reticular nuclei, in the inferior olive, in the formatio reticularis and in the X and XII cranial nerves. In the cerebellum a weak labelling of Purkinje cells is visible (Fig 10D).

Due to the weakness of the signal, it is not possible to get an impression of the cell types expressing *Mek2*. But to confirm the functionality of our probe, I performed an *in situ* hybridisation on slices cut from the brain of newborn mice, known to express high levels of *Mek2*, where I could observe a widespread labelling signal (data not shown). Thus, the expression level of *Mek2* mRNA in adult mouse brain is in fact very low.

3.1.3 *Erk1* expression

The hybridisation signal for *Erk1* is widespread present in all the regions of the murine brain but shows major differences in the level of expression (as summarized in Tab 1). In the olfactory bulbs strong signals can be seen in mitral cells and weak signals in granule cells and in the external plexiform layer. All cortical cells express *Erk1* mRNA with strong signals in the piriform cortex and moderate labelling in cells of the cerebral cortex. The regions of the basal ganglia show weaker signals with still moderate intensity in the endopiriform nucleus and in the claustrum but no signals in the zona incerta and in the pars reticulata of the substantia nigra (Fig 11G).

Furthermore the cells of the hippocampus express *Erk1* barely; more precisely, the dentate gyrus shows moderate and the CA3 region weak signals, whereas the neurons of the CA1 and CA2 regions do not label for *Erk1* mRNA (Fig 11D). But the amygdala gives strong signals in the lateral nuclei with descending intensities in the central and basal nuclei (Fig 11F). Conspicuous is also the strong *Erk1* expression in the bed nucleus of the stria terminalis. On the contrary, striking due to the absence of *Erk1* signal is the medial septum and the lateral part of the habenula.

The thalamic areas express low to mediocre levels of *Erk1* mRNA. And in posterior regions more areas are devoid of *Erk1* expression as the inferior colliculus, the olives, the cochlear nuclei and the V cranial nerve. Here, only the locus coeruleus and the oculomotor nuclei show moderate-to-strong and strong signals (for more details see Table 1). In the cerebellum only a very weak signal can be detected in the granule and in the Purkinje cell layer (Fig 11K). On the cellular level there is no restriction of *Erk1* mRNA to a specific cell type.

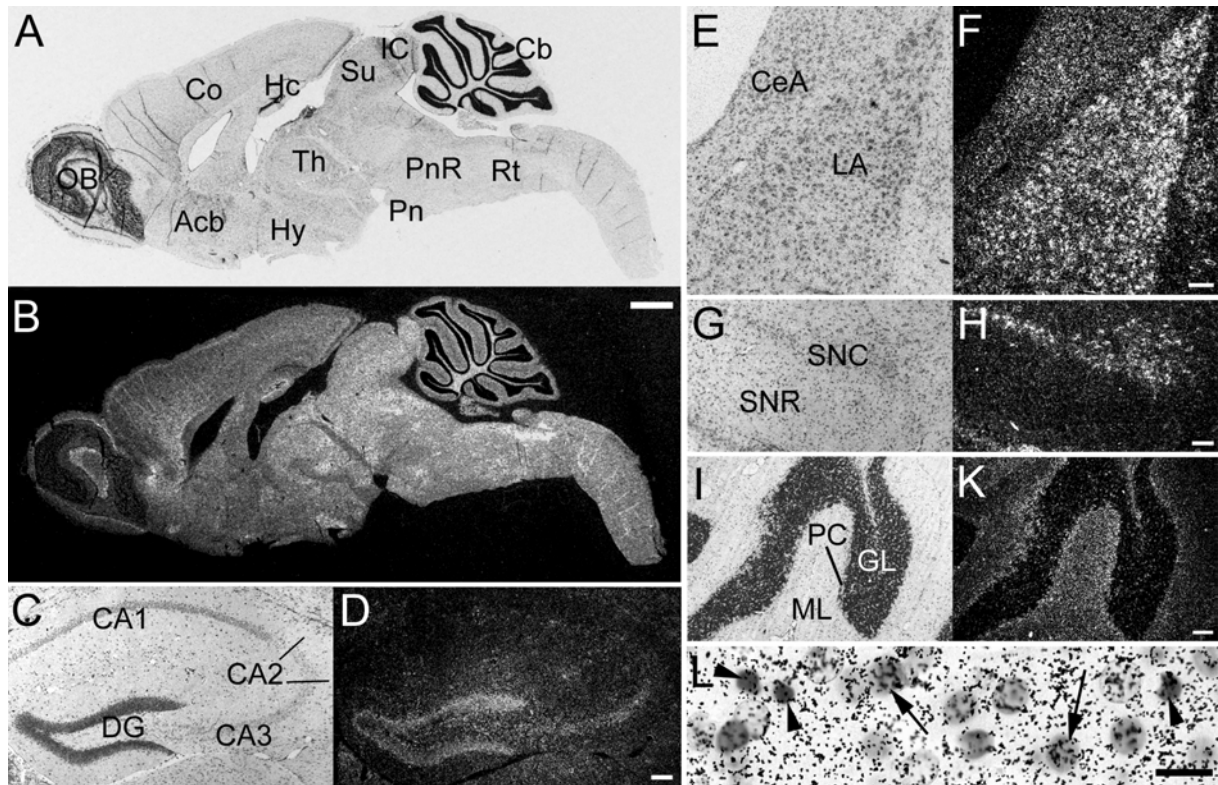


Fig 11 Sections of adult mouse brain labelled with the Erk1 in situ probe. Darkfield photomicrographs (B, D, F, H, K) and corresponding brightfield images of Nissl stained sections (A, C, E, G, I) are displayed. A and B show a complete sagittal section at a glance. Magnifications of the hippocampus (C, D), the amygdala (E, F), the substantia nigra (G, H) and the cerebellum (I, K) from coronal sections present the expression pattern of Erk1 mRNA in more details. For abbreviations see Tab 2. In the brightfield image of a high magnification of striatal cells (L) expression signal is visible as well in big neuron-like cells (arrows) as in smaller, darker Nissl stained glia-like cells (arrowheads). Scale bar = 1 mm in B; 0.1 mm in D, F, H, K; 0.016 mm in L.

On the Nissl stained tissue the larger neurons show a similar amount of signals as the smaller and darker glia cells (Fig 11L).

3.1.4 *Erk2* expression

Also the mRNA for *Erk2* is widely distributed in all regions of the brain of the adult mouse (Fig 12). In the olfactory bulb only the external plexiform layer is devoid of any *Erk2* hybridisation signal whereas all the other parts show strong or moderate signals. Also in the cortical fields *Erk2* mRNA is strongly expressed and in the hippocampal formation signals are strong throughout the different subregions but even very strong in CA3 neurons (Fig 12D). In the basal ganglia signal intensities

vary from very strong, as in the olfactory tubercle, to very weak in the globus pallidus. Remarkable is the pattern of *Erk2* expression in the substantia nigra where strong signals are found in the pars compacta but only weak signals are detected in the pars reticulata (Fig 12H). The cells of the amygdala express *Erk2* mRNA at equally strong levels in all the nuclei (Fig 12F). Further the thalamic areas show moderate *Erk2* signals. All regions in the mid- and hindbrain express *Erk2* mRNA but at different levels. Cells with strong signal intensities are found in the red nucleus, the locus coeruleus and the pontine nuclei (for more details see Tab 1). Moreover in the cerebellum *Erk2* shows, together with the weak-to-moderate expression in Purkinje cells, very weak but clear signals in the molecular cell layer and in granule cells (Fig 12K).

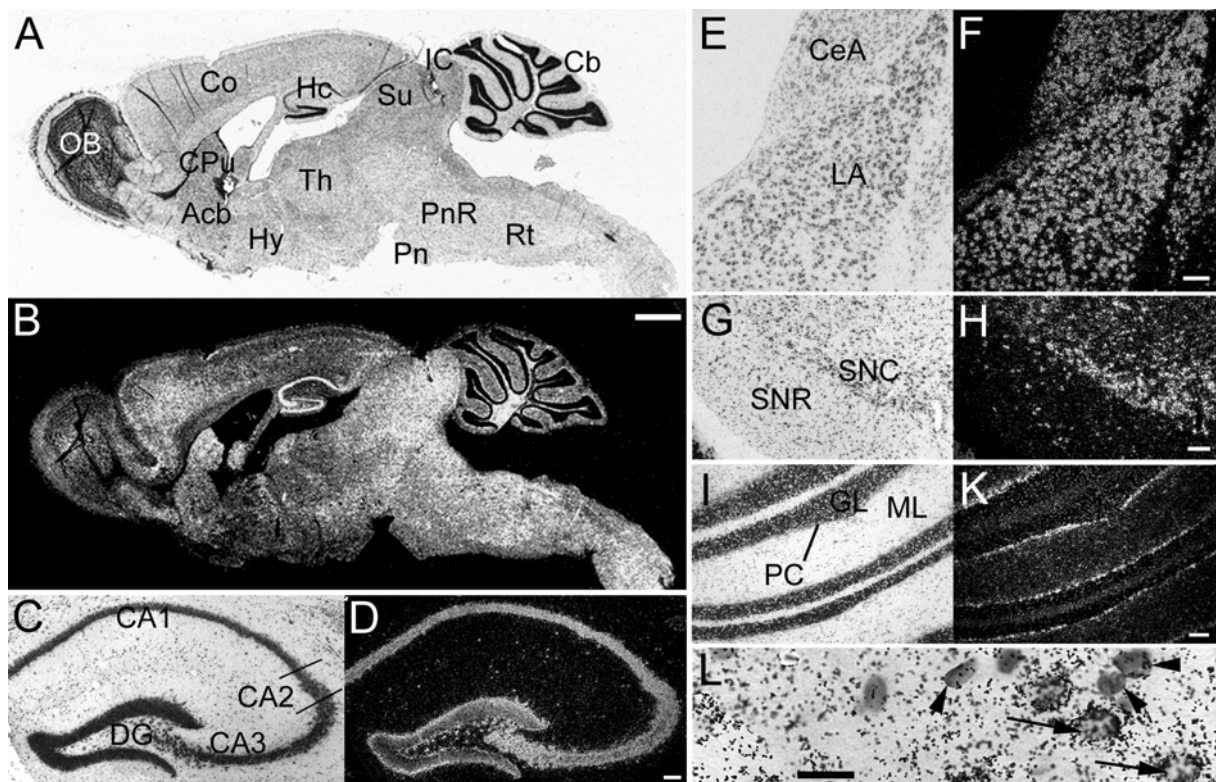


Fig 12 Sections of adult mouse brain labelled with the *Erk2* in situ probe. Darkfield photomicrographs (B, D, F, H, K) and corresponding brightfield images of Nissl stained sections (A, C, E, G, I) are displayed. A and B show a complete sagittal section at a glance. Magnifications of the hippocampus (C, D), the amygdala (E, F), the substantia nigra (G, H) and the cerebellum (I, K) from coronal sections present the expression pattern of *Erk2* mRNA in more details. For abbreviations see Tab 2. In the brightfield image of a high magnification of striatal cells (L) expression signal is very strong visible in big neuron-like cells (arrows), whereas the faint signal in the dark glia-like cells may also be background staining (arrowheads). Scale bar = 1 mm in B; 0.1 mm in D, F, H, K; 0.016 mm in L.

At the single cell level, silvergrains marking *Erk2* mRNA are almost exclusively found on larger, weakly Nissl stained cells, the neurons, in accordance with what has already been described for *Erk2* in rat neurons (Boulton et al., 1991). Even if also the darker stained, smaller glia-cells show a weak labelling signal, it cannot be excluded to be background staining in these cells (Fig 12L).

3.2 Protein expression of ERK/MAPK signalling pathway components in the lateral amygdala of the adult mouse

To examine the expression of MEK1, MEK2, ERK1 and ERK2 at the protein level, I performed a Western blot analysis. Total proteins were extracted from tissue of the LA nucleus after dissection of amygdalae from adult mouse brains (for a detailed protocol, see 5.3.1). As shown in Fig 13, all four proteins were present in the LA. To our knowledge, it was never shown that these four MAPK signalling pathway components were co-expressed specifically in the LA nucleus of the adult mouse brain. Moreover, I observed that the mRNA for *Mek2* was absent from most of the regions of the adult mouse brain (Tab 1). Thus, I decided to check whether this was also reflected in eventual absence of the MEK2 protein. Data shown in Fig 13 are coming from three independent brains, which confirmed one another the observed results, which will be discussed later.

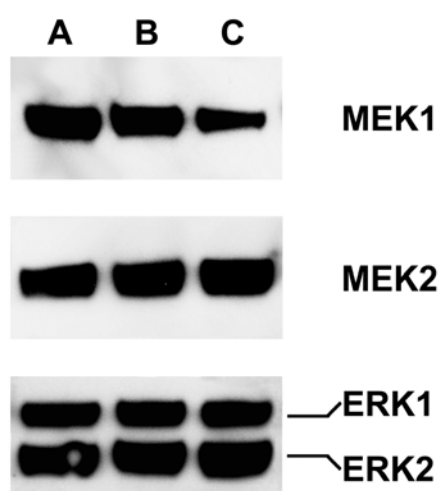


Fig 13 Western blot of LA samples to characterize the expression of MEK1/2 and ERK1/2 proteins. Lanes A-C show the results of the immunoblotting analysis from three independent dissection experiments (n=3). Total protein extracts were taken from LA nucleus tissue, after dissection from vibratome 400- μ m-thick sections of adult mouse brains.

3.3 Establishment of the Fear Potentiated Startle in mice

As shown in Fig 14 (Group3-4), the protocol of 10 trials, starting after a 5 min acclimation period and terminating with a 0.5 sec foot shock of 0.5 mA gave a significant increase in fear potentiation. Indeed, also the protocol which consisted of 5 trials and 0.5 sec foot shock of 0.4 mA showed a significant fear potentiation (Fig 14, Group1); but it was not reliable enough, as far as the second group of animals treated with it (Fig 14, Group2), did not show the same result. On the other hand, the protocol with 10 repetitions and 0.5 mA foot shock was more reliable, as it gave significant fear potentiation and the results were reproducible in both groups of animals treated (Group3-4).

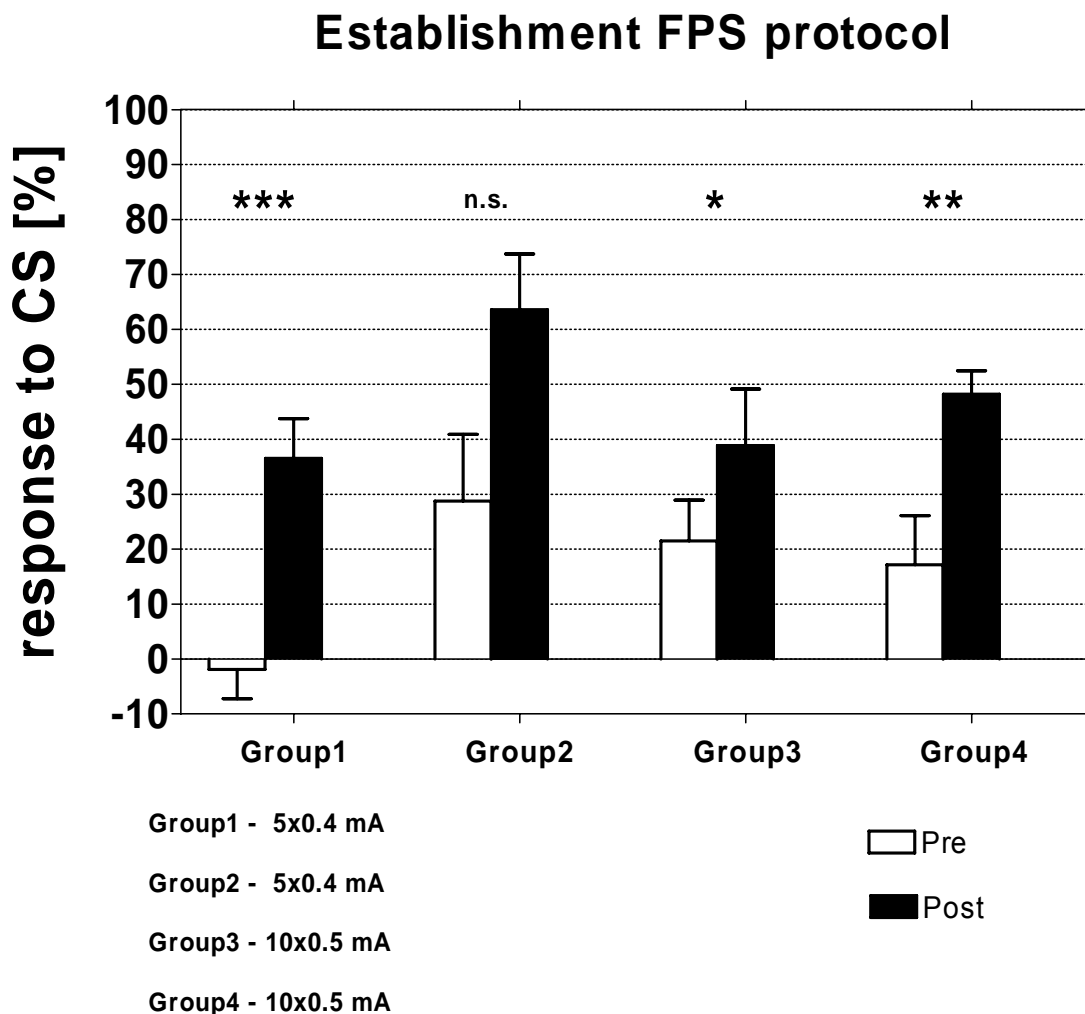


Fig 14 Graph showing the results of different protocols tested to establish the FPS protocol. Results are described in details in the text. Pre, pre-conditioning; Post, post-conditioning. * $p \leq 0.05$; ** $p \leq 0.01$; *** $p \leq 0.001$; n.s. not significant.

3.4 ERK/MAPK is transiently activated in the amygdala after Pavlovian fear conditioning

I used immunohistochemistry to anatomically localize expression of phospho-activated ERK/MAPK (pMAPK) to particular amygdala nuclei.

The pMAPK were found scattered throughout the LA, as shown in Fig 15. Some labelled cells could be seen also in adjacent regions around the LA. But for our study, I took only the pMAPK in the nuclei of the LA into account for statistical analysis. To date, no study was performed using stereological methods to count the total numbers of phospho-activated MAPK labelled cells in the LA of rodents.

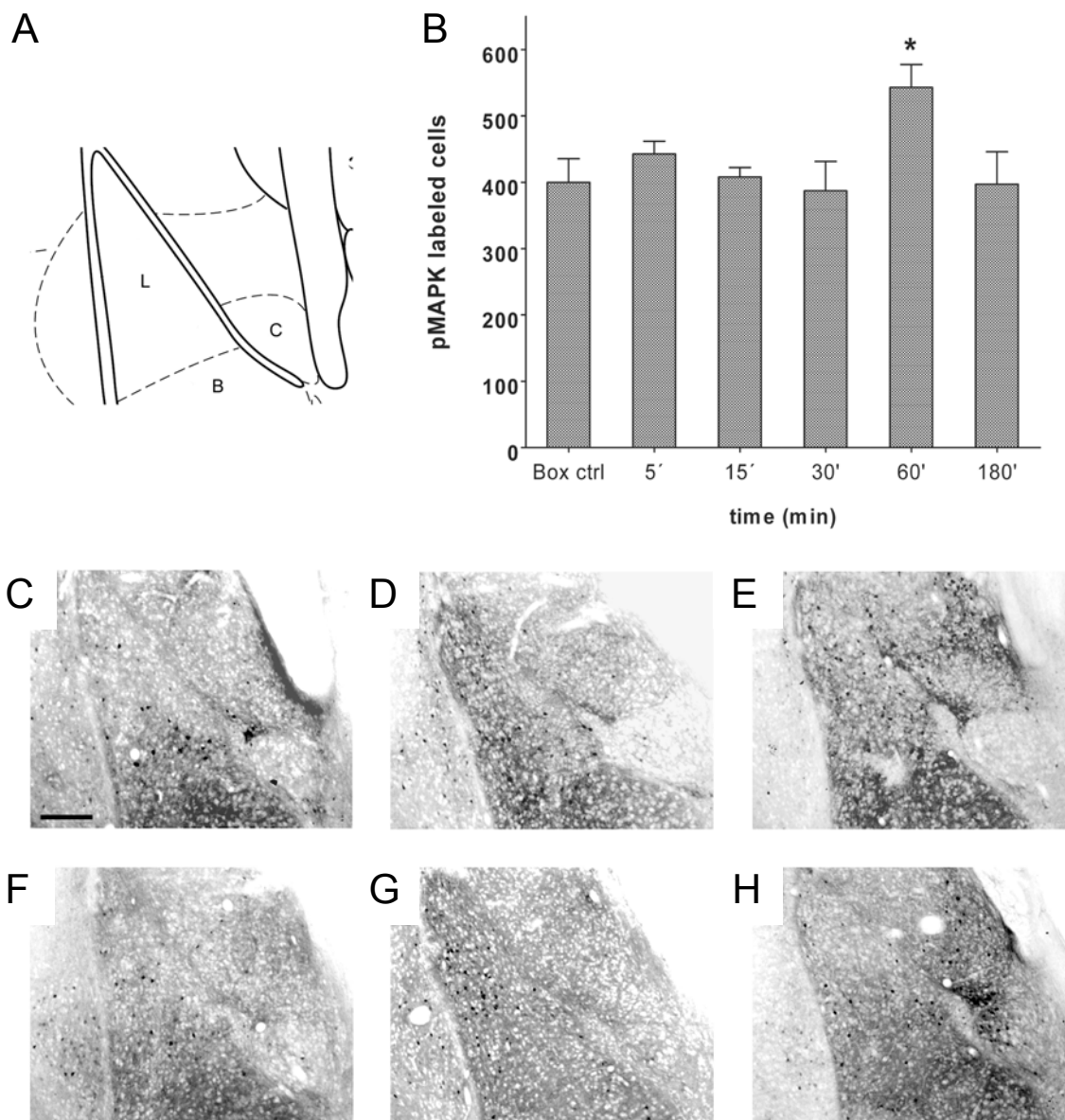


Fig 15 Time course of activation of pMAPK in LA after fear conditioning. (A) schematic representation of the amygdala at approximately -1.82 from bregma (according to Paxinos and Franklin, 1989); (B) Mean \pm SEM of pMAPK immunoreactive cells in: sham-trained controls (Box control, ctrl) ($n=3$) and 5 min ($n=3$), 15 min ($n=4$), 30 min ($n=5$), 60 min ($n=6$), 180 min ($n=4$) after conditioning ($* p \leq 0.05$); (C) Representative photomicrographs of pMAPK labelling in the LA in sham-trained controls (Box ctrl); (D, E, F, G, H) Representative photomicrographs of pMAPK labelling in the LA at 5 min (D), 15 min (E), 30 min (F), 60 min (G), 180 min (H) after fear conditioning. Scale bar = 200 μm .

This method allows an unbiased estimate of the total numbers of the cells of interest within a fraction of a selected tissue, involving a systematic, uniformly random sampling of that tissue.

As controls, I decided to use animals which were exposed to the conditioning boxes, but not to tones and shocks. Thus, any eventual unspecific activation of pMAPK due to the influence of handling or context-exposure would be included in baseline controls cell counts.

A student t test was performed against control values ("Box ctrl") for each time point. Our results showed that only the number of pMAPK at 60 min after fear conditioning was significantly higher than that in the control group (Fig 15B; $* p \leq 0.05$). Consistent with the results shown in rats (Schafe et al., 2000; Paul et al., 2007), there was an increase in the number of phospho-labelled cells that reached a peak at 60 min after fear conditioning and went down again to basal levels by 180 min. But in contrast to Paul et al (2007), where they found in the rat a second peak of activation at 5 min after fear conditioning, even higher than the one at 60 min, in the mouse there was no evidence of this second peak of phospho-labelled cells (Fig 15B).

3.5 Characterization of the expression of activated ERK/MAPK in different cell types: neuronal or glial?

I used fluorescent immunohistochemistry to investigate the colocalization of pMAPK with either a specific neuronal or glial marker. To label neurons, I chose the antibody NeuN, which recognizes a nuclear protein (Baekelandt et al., 2000); and for glial cells, I used an antibody against the calcium-binding protein S100 β (Nishiyama et al., 2002). Mice were trained with the conditioning protocol and were sacrificed 60 min after conditioning, when the increase in pMAPK in LA was most prominent. Brains were prepared to be processed for fluorescent immunohistochemistry (IHC) as

described in Materials and Methods. The IHC was performed on parallel sections, each of which was labeled with one of the two antibodies's combination, namely pMAPK/NeuN or pMAPK/S100 β . After proceeding and mounting the sections, brains were analysed at the confocal microscope. The analysis did not show any colocalization signals of pMAPK with the S100 β antibody; while all the pMAPK positive cells appeared to be co-labelled with NeuN (Fig 16B). Thus, this strongly suggested that the activation of pMAPK at the peak of 60 min after fear conditioning was exclusively neuronal, without involvement of pMAPK in glial cells at this time point.

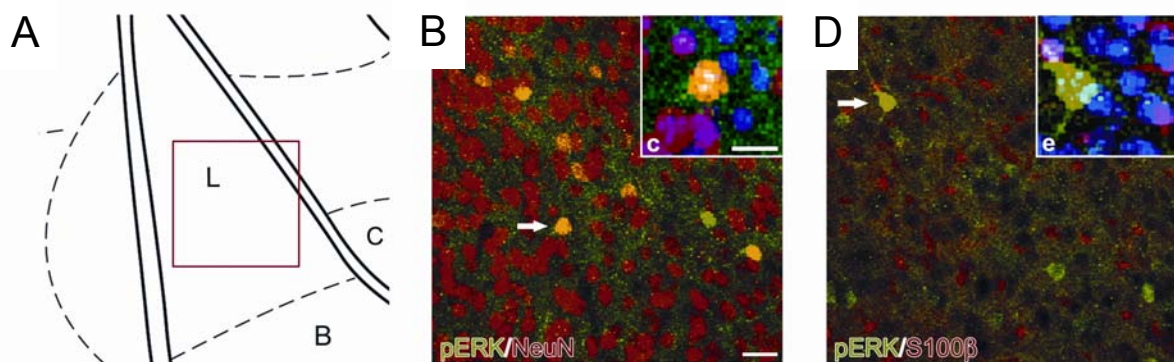


Fig 16 Cell-type specificity of phospho-activated MAPK after fear conditioning. (A) Schematic drawing of lateral (L), basal (B) and central (C) amygdala; (B) Representative photomicrograph (20X) of a portion of the LA (red square in (A)) immunostained with pMAPK (green) and NeuN (red) at 60 min after fear conditioning; the yellow colour of the “merge” between the green pMAPK immunostaining with the red NeuN shows the co-localization of the two signals; (c) Higher magnification of labelled cells (white arrow in b), in which the counterstaining with DAPI (blu) shows the single-cell nuclei; (D) Representative photomicrograph (20X) of a portion of the LA (red square in (a)) immunostained with pMAPK (green) and S100 β (red) at 60 min after fear conditioning; in contrast with (b), the “merge” between the green pMAPK immunostaining with the red S100 β shows no co-localization of the two signals; (e) Higher magnification of labelled cells (white arrow in c), in which the counterstaining with DAPI (blu) shows the single-cell nuclei. Scale bar = 20 μ m in B, D; 10 μ m in c, e.

3.6 Evaluation of the acquisition of the Fear Potentiated Startle after surgery

Ketamine is often used as the anaesthetic of choice in surgical experiments. Several studies already reported that the action of ketamine is mediated through its antagonism on NMDA receptors in mice (Petrenko et al., 2006; Visser and Schug,

2006; Klein et al., 2007). As far as the acquisition of long-term fear memories is shown to involve the activation of NMDA receptors in rats (for a review, see Blair et al., 2001), it was very important to verify the eventual influence of ketamine used for surgery on the performance of the FPS. I compared two groups of animals with 12 individuals each; one of them was left completely naïve, while the other one was subjected to surgical procedure for the implantation of guiding cannulas aimed at the amygdala. After one week of recover, animals were run through an FPS protocol, as described in 5.4.2. A paired *t* test was used to evaluate separately the significance of the fear potentiation in the group of naïve animals and in the group of operated ones. Then a *t* test with unequal variances was used to compare the two fear potentiations with each other. As shown in Fig 17, even after the use of ketamine to anesthetize animals, they could still acquire the task and show significant levels of potentiation.

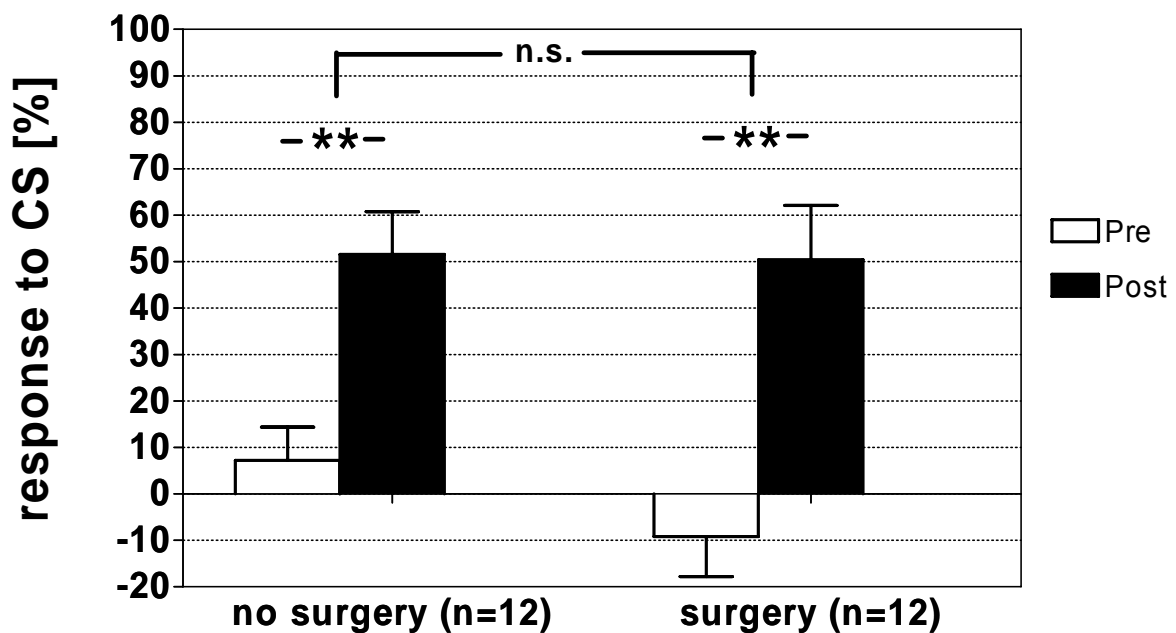


Fig 17 Graph showing the acquisition of FPS in animals after surgical procedure. Details about results are described in the text. Pre, pre-conditioning; Post, post-conditioning. ** $p \leq 0.01$; n.s. not significant.

3.7 Pharmacological blockade of ERK/MAPK activation in the amygdala impairs fear learning in the mouse

I asked whether activation of ERK/MAPK in the LA was obligatory for acquisition of Fear Potentiated Startle in mice. I performed pharmacological inhibition of the MEK1/2 proteins via the injection of U0126, a specific inhibitor of these molecules

which are directly upstream activators of ERK/MAPKs. As shown in Fig 18B, the bilateral injection of the compound 30 min before conditioning could impair the acquisition of the fear potentiation. A two-way ANOVA (group x conditioning) followed by Bonferroni *post hoc* test, showed a significant effect of treatment. But no significant difference was found between the two groups before conditioning. These differences in acquisition of fear potentiated startle produced by pretraining infusions of the U0126 were not attributed to permanent damage of the amygdala. Indeed, one week after the pharmacological manipulations, the same animals were retrained without infusions and tested again, 24 hrs later, to check the specificity of pharmacological inhibition. As shown in Fig 18B, the fear potentiation in the reconditioning

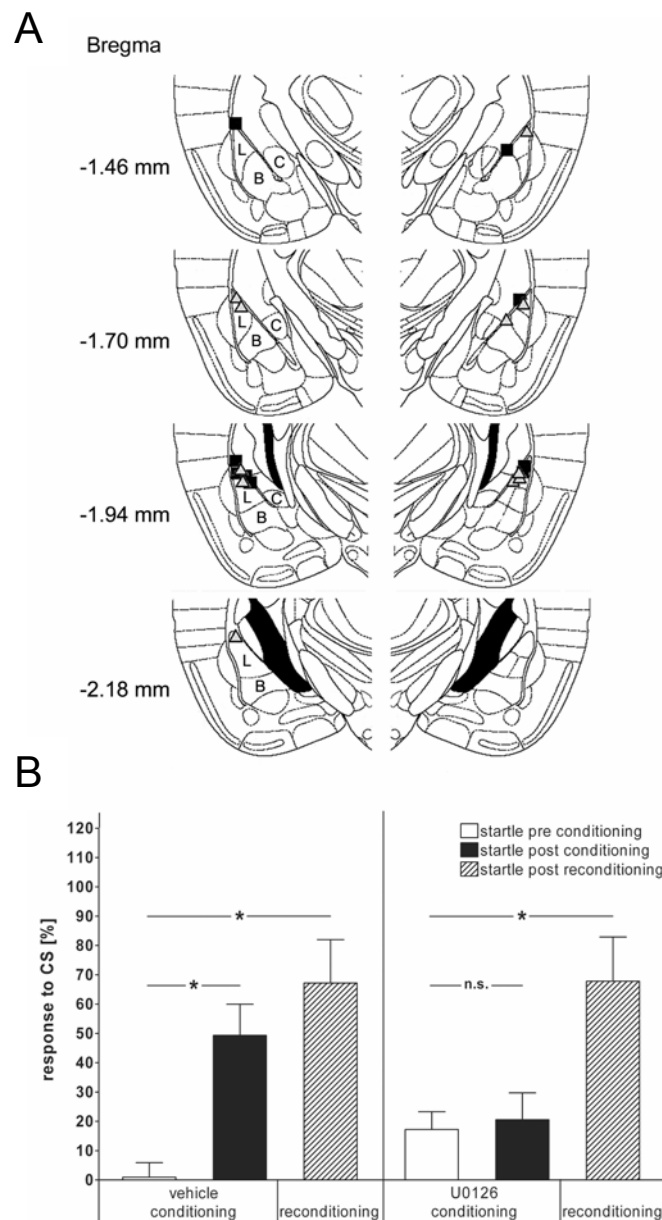


Fig 18 Impairment in acquisition of the FPS after intra-LA infusions of the MEK inhibitor U0126. (A) Schematic drawing representing the sites of injections of the vehicle (black filled square) or the pharmacological inhibitor U0126 (grey filled triangle). L=lateral amygdala; B= basal amygdala; C=central amygdala. (B) Mice received bilateral intra-LA injections of either 50% DMSO in aCSF (vehicle) or U0126 in 50% DMSO in aCSF 30 min before a fear conditioning session and were tested 24 hrs later. Vehicle-injected mice (n=5) showed acquisition of fear potentiation (as increase in % of response to CS) that was not seen in U0126-injected mice (n=7) (t-test; * $p \leq 0.05$; n.s. not significant). As described in the text, these differences in acquisition of fear potentiated startle produced by pretraining infusions of the U0126 were not attributed to permanent damage of the amygdala, but to a specific, transient effect of the pharmacological inhibition, as verified by a reconditioning experiment.

session was highly significant in both groups; a two-way ANOVA (group x re-conditioning) showed a significant effect of conditioning in both groups, but no difference between groups. Thus, I could confirm that the previously observed inhibition was due to the specific, transient effect of the pharmacological compound and not to a permanent damage of the amygdalae as a consequence of the injections.

3.8 Generation of a tool to study the specific role of the MAPK ERK2 in amygdala of mice via viral-mediated RNA interference

3.8.1 Selection and testing of shRNAs for efficient downregulation of ERK1/2 *in vitro*

For the efficient downregulation of genes *in vivo*, it is necessary to have first some hairpin sequences which can work efficiently at least *in vitro*. We established an *in vitro* test for the evaluation of hairpin efficiency in our lab. This was based on transient transfections of ES cells with plasmids coding for the hairpin of interest against endogenous genes. After 48 hrs post-transfection, cells were lysed and total RNAs and proteins were extracted. To check the downregulation at the RNA level, samples were sent to a collaborator, the company Cenix, which was in charge of performing qRT-PCR. To check the efficiency at the protein level, we performed Western blot analysis with specific antibodies directed against our targeted molecules. Results were compared with controls, namely mock-transfected ES cells. As shown in Fig 19A, all five selected hairpin sequences specifically downregulated

Erk1; and out of five tested hairpin sequences, one showed a good downregulation of Erk2, without measurable downregulation of Erk1 (erk2sh4, Fig 19B). Thus, I used erk2sh4 to proceed for *in vivo* experiments i.e. integration in an AAV viral backbone and testing of virus tropism and Erk2 downregulation *in vivo*.

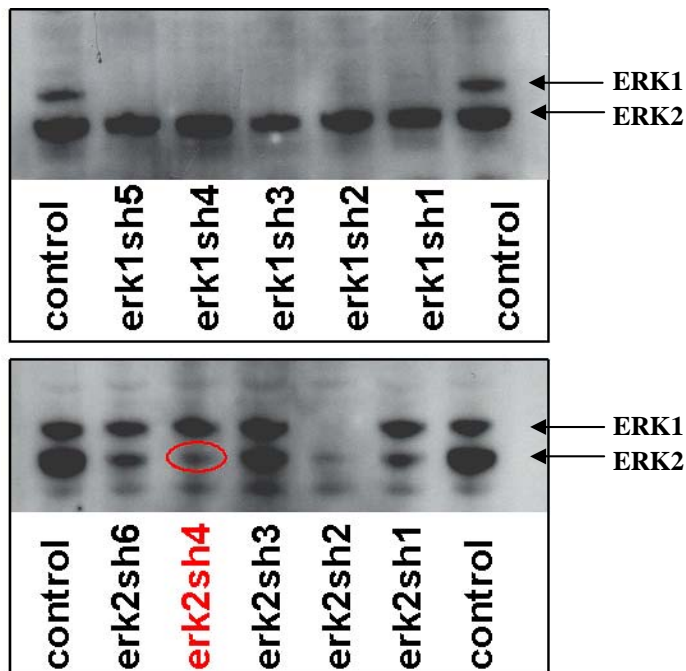


Fig 19 Western blot for the analysis of efficiency of downregulation of short hairpin *in vitro*. (A) Results of five different hairpin in downregulation of ERK1; (B) Results of five different hairpin in downregulation of ERK2; the hairpin sh4 was chosen for further experiments (red circle).

3.8.2 Testing for the tropism of the virus - the adeno-associated virus (AAV)

As shown in Fig 20, our viral preparation was selectively infecting neurons (Fig 20E) and not glial cells (Fig 20I) after injection into the amygdala. The results are from mice sacrificed seven days after viral injection. As far as our previous results showed that the activation of pMAPK is specifically neuronal (Fig 16B, C), without involvement of glial cells at 60 min after fear conditioning (Fig 16D, E), I decided that this virus could fulfill our requirements for the specific downregulation of *Erk2* in neurons.

3.8.3 Testing of downregulation efficiency *in vivo* after viral-mediated infection with shRNA against *Erk2* mRNA

Seven days after injection of 1 μ l of each virus bilaterally into the amygdala of the

adult mouse brain, animals were sacrificed and the specificity of downregulation was tested. As shown in Fig 21D and E, the cells which were infected with the control virus (CMV-venus-LacZsh), indicated by the GFP signal (in green, white arrowhead

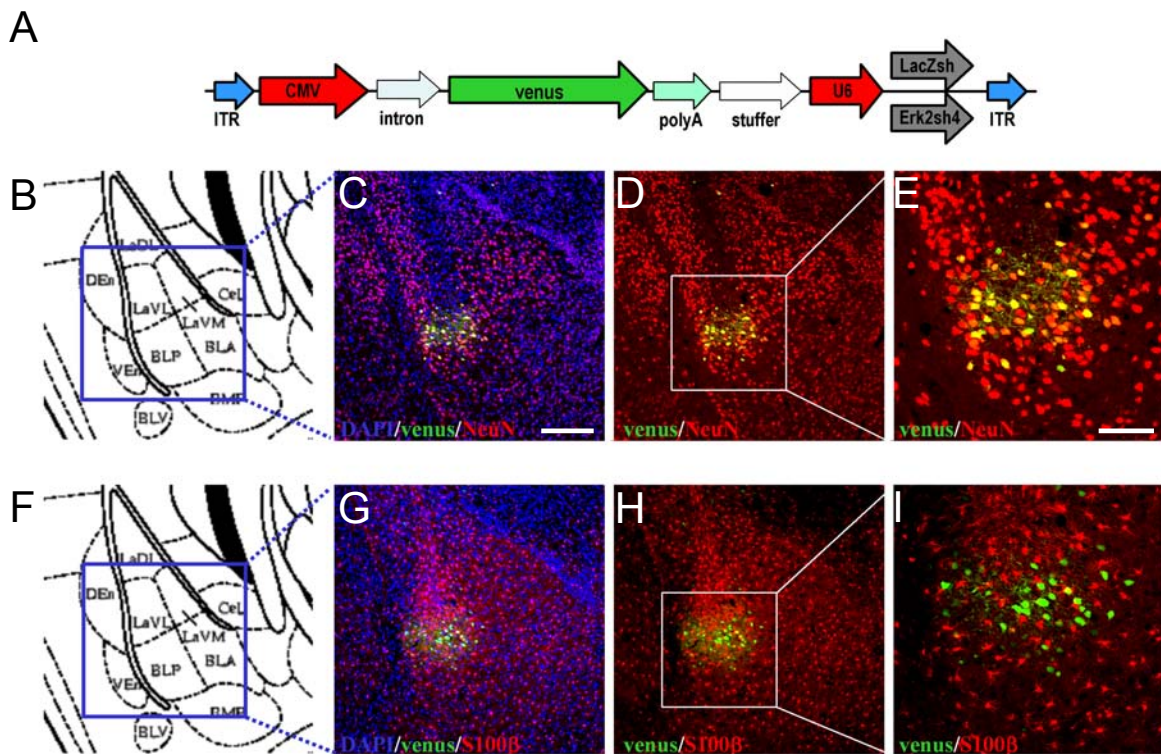


Fig 20 Test injection to analyse the tropism of the AAV carrying the short hairpin against Erk2. (A) Schematic drawing representing the structure of the viral backbone. ITR, inverse terminal repeats; CMV, Citomegalovirus promoter; (B, F) Drawing from Paxinos and Franklin (1989) to pinpoint the site of injection; (C, D) Confocal pictures showing the cell-type localization of the signals for venus (green) and NeuN (red), to identify the tropism of the AAV (reported by the expression of the Venus gene); (E) Higher magnification (40X) of the site of viral injection to highlight the yellow color derived from the “merge” of the venus (green) and NeuN (red) in (D); (G, H) Confocal pictures showing the cell-type localization of the signals for venus (green) and S100 β (red), to characterize the tropism of the AAV; (I) Higher magnification (40X) of the site of viral injection to highlight the lack of co-localization of the venus (green) and S100 β (red) in (H). Scale bar = 200 μ m in C, G, D, H; 60 μ m in E, I.

in D), did show a clearly detectable signal for *Erk2* mRNA (in black, red arrowhead in E); to verify the *in situ* signal, a neighbouring cell which does not show a GFP signal (white arrow in D; in blu DAPI labels the nucleus) but is positive for an *in situ* signal (in black, red arrow in E) is shown. On the other hand, cells infected with the virus bearing the Erk2sh4 (CMV-venus-Erk2sh4) in Fig 21H and I, did show a clear depletion of the *in situ* signal (red arrowhead in I) where the GFP signal was present (in green, white arrowhead in H); also here, neighbouring cells not infected (white

arrow in H; in blu DAPI labels the nucleus), show the signal for *Erk2* mRNA (in black, red arrow in I), indicating the specificity of downregulation and ruling out the possibility of a side effect due to the injection itself in the region.

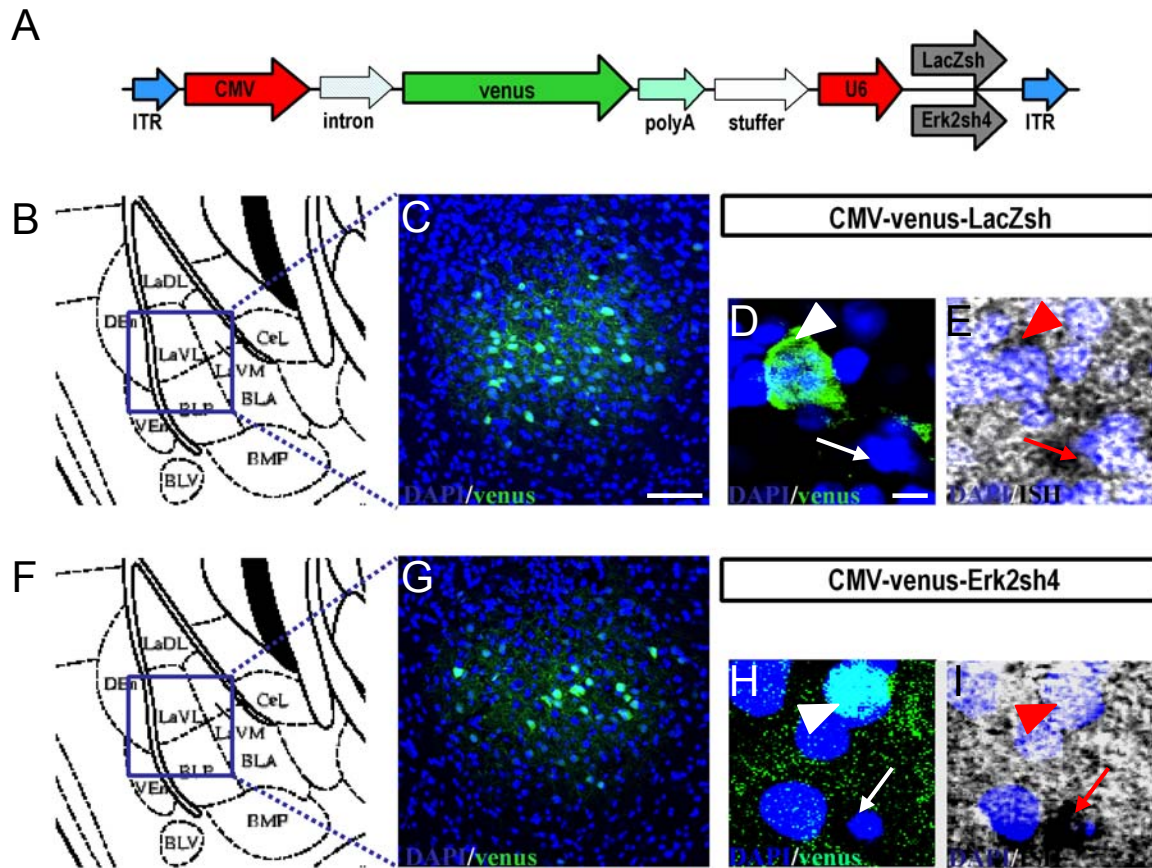
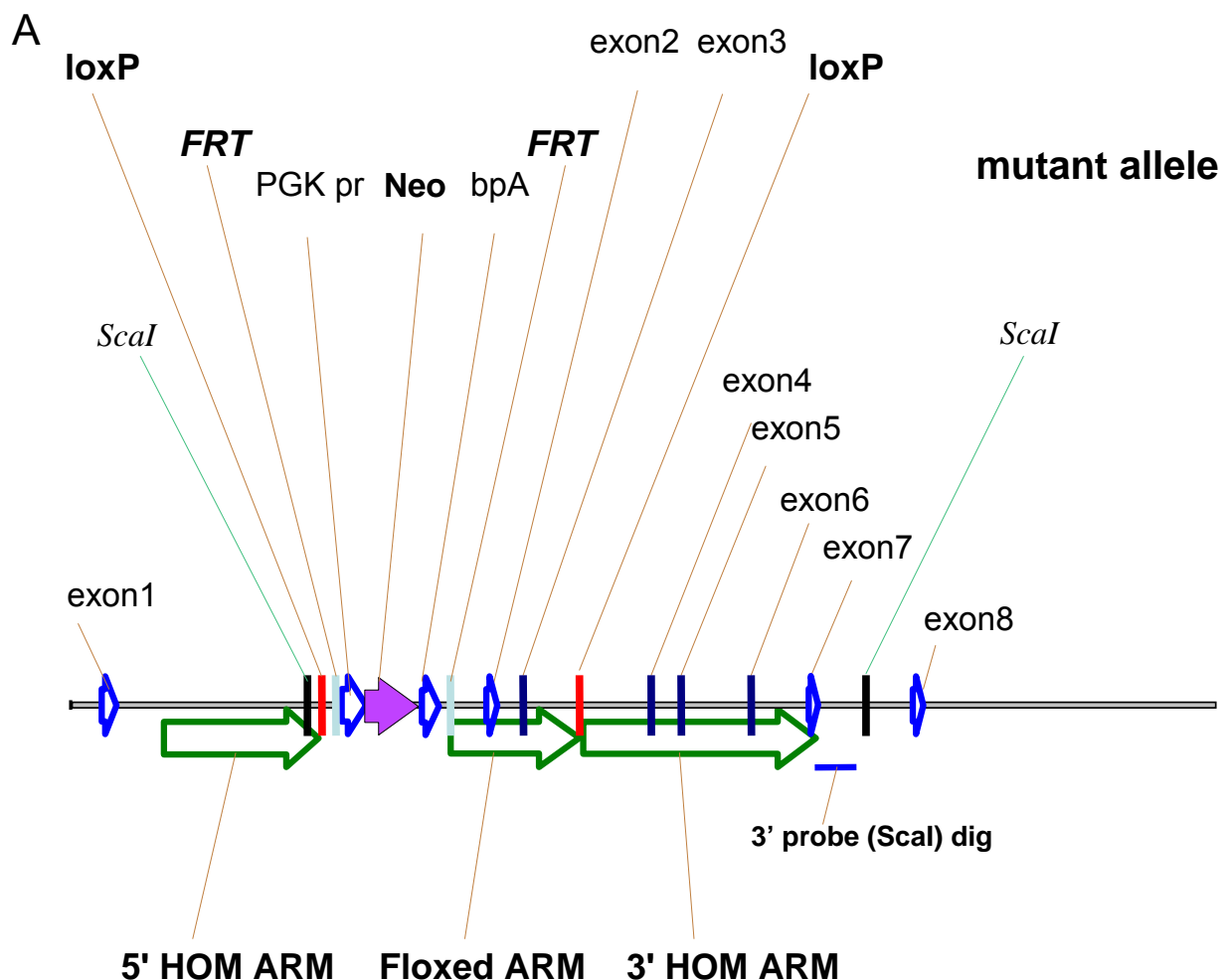


Fig 21 Test injection to analyse the efficiency of downregulation of the AAV carrying either the short hairpin against LacZ, as control injection, or the hairpin against Erk2. (A) Schematic drawing representing the structure of the viral backbone. ITR, inverse terminal repeats; CMV, Citomegalovirus promoter; (B, F) Drawing from Paxinos and Franklin (1989) to pinpoint the site of injection; (C, G) Confocal pictures showing the sites of injection of the two viral preparations, indicated by the signal of the reporter gene (venus, green); (D, E) Higher magnification (40X) of the site of injection with the control virus, to show that cells infected with this virus (in D, white arrowhead: venus, green) still maintain expression of Erk2 (in E, red arrowhead: ISH, black) as compared with not infected neighbouring cells (in D, identified with DAPI, blu, white arrow; in E, the red arrow shows the corresponding *in situ* signal); (E) Higher magnification (40X) of the site of injection with the virus containing the short hairpin against Erk2, to show that cells infected with this virus (in H, white arrowhead: venus, green) do not show anymore the expression of Erk2 (in I, red arrowhead) as compared with not infected neighbouring cells which still express Erk2 mRNA (in H, identified with DAPI, blu, white arrow; in I, the red arrow shows the corresponding *in situ* signal). Scale bar = 60 µm in C, G; 5 µm in D, E, H, I.

3.9 Targeted conditional deletion of the *Pink1* gene in the mouse as a model to study Parkinson's Disease

The Southern blot was performed as described in 5.11.3 with the probe recognizing the 3' region external to the site of insertion of the targeting vector in the *ScaI* digestion (Fig 22A). The result showed a clear efficiency of this probe in detection of a band of expected size in wildtype DNA (~7 kb), and could then be used for subsequent experiments.



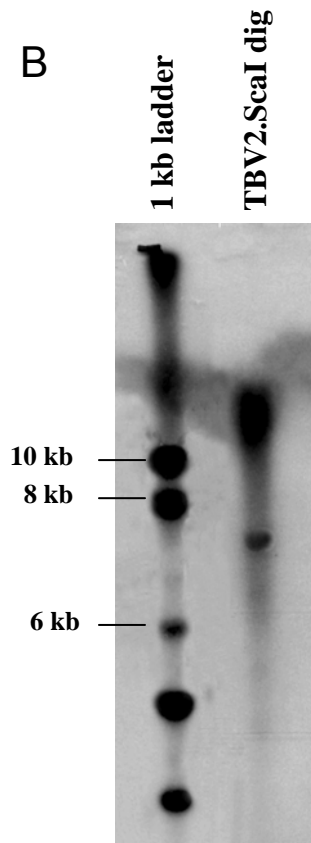


Fig 22 (A) Schematic drawing representing the structure of the mutant allele in the Pink1 genomic locus. The different parts of the construct are represented in different colors. The loxP sites flank a region containing the exons 2 and 3. The expression of the resistance gene neomycin (Neo) is driven by the promoter for the phospho-glycerate kinase, PGK (PGK pr) and regulated by the bovine polyA signal (bpA). FRT sites are added to allow the excision of the selection marker via Flippase recombination, if necessary; (B) Southern blot on wt genomic DNA to test the 3' probe for the selection of the ES cells positive for the homologous integration of the construct for the conditional inactivation of Pink1. As expected from a ScaI digestion, the probe is binding to a DNA fragment of approximately 7 kb. The mutant allele will be distinguished from the wt by a difference in length of about 2 kb, with the mutant DNA fragment being around 9 kb.

4 DISCUSSION

4.1 Expression analysis of mRNAs coding for components of the MAPK signalling pathway

From our expression analysis, signalling interactions between particular regions of the brain could be suggested. From these descriptive data, and based on what is known about MAPK functions, several hypotheses can be proposed which can be subject to further functional studies.

4.1.1 MAPK and neurogenesis: expression in the olfactory bulb

Recently, new findings have shown that in the adult mammalian brain, the genesis of new neurons continues throughout life within two 3-layered cortical regions, the hippocampus and the olfactory bulb (OB), where it is sustained by endogenous stem cells (for a general review see Ming and Song, 2005).

The most active neural stem cell (NSC) compartment is found in the subventricular zone (SVZ). This area represents a remnant of the embryonic germinal neuroepithelium, which persists throughout life as an active mitotic layer in the wall of the telencephalic lateral ventricles; this generates interneurons of the OB, after migration of NSCs to reach their target region via the rostral migratory stream (RMS). In the OB the progenitor cells coming along the RMS arrive in the ependymal lining of the olfactory ventricle (E/OV) and then ascend radially into the overlying granule (Gr) and glomerular (GI) cell layers to become, respectively, granule cells and periglomerular interneurons (Altman, 1969; Betarbet et al., 1996; Belluzzi et al., 2003; Carleton et al., 2003).

Notably, *Mek1* expression is confined to the granule cell layer of the OB (Fig 9B); while *Erk1* and *Erk2* are present in both granule (Gr) and glomerular (GI) cell layers (Tab1, Fig 11B and 12B), both being sites of active neurogenesis of local circuit neurons throughout life. Given the role of MAPK signalling pathways in regulating differentiative processes (Cowley et al., 1994), it is not astonishing that some

components of this pathway are expressed in neurogenic regions of the adult mouse OB where terminal differentiation of newly generated neurons occurs.

Recently the role of neurotrophin-3 (NT-3) has been elucidated in the maintenance of homeostasis between precursor and mature neuronal populations in the olfactory epithelium. Using primary olfactory neuronal culture, NT-3 has been shown to activate directly the PI3K/Akt pathway and indirectly the MAPK signalling pathway; the PI3K/Akt cascade promoting the survival of mature neurons and the release of secondary factors which activate the MAPK pathway; this in turn reduces the neuronal precursor population and inhibits neuronal maturation (Simpson et al., 2003). The expression of *Erk1* and *Erk2* in the glomerular layer suggests that these molecules could be the possible downstream effectors of NT-3 function in regulating neuronal maturation in this neurogenic area. A similar mechanism of action could be true for other members of the neurotrophin family in the granular cell layer where *Mek1*, *Erk1* and *Erk2* are expressed. Indeed, recent studies show that neurotrophins are good candidates to contribute to regenerative processes in the OB (Linnarsson et al., 2000; for review see Mackay-Sim and Chuah, 2000).

Moreover, the expression pattern of some components of the WNT signalling pathways could also suggest the existence of functional interactions occurring between the WNT and the MAPK signalling pathways within the OB of the adult mouse to regulate its plasticity (Shimogori et al., 2004).

In a different model system, namely the bone system, indeed it has been shown that WNT signalling prolongs the survival of uncommitted osteoblast progenitors and osteoblastic cells via activation of the canonical pathway as well as the Src/ERK and PI3K/Akt cascades, with GSK-3 β representing at least one convergence point between the two signalling cascades (Almeida et al., 2005). This suggests that the WNTs can regulate the homeostasis of the precursor/mature cells in the bone development via the MAPK signalling pathway, as shown for neurotrophins in olfactory neuronal cells. Further this leads to the possibility that the same functional interaction may also occur in the OB, where actually it has been shown that Wnt1, the canonical family member, is expressed in the granule and glomerular cell layers (Shimogori et al., 2004). These are the same regions where I found expressed *Mek1*, *Erk1* and *Erk2* (in Gr) and *Erk1* and *Erk2* (in Gl), respectively. Interestingly, some other WNT signalling components as Frizzled receptor 3 (*Fz3*) and the soluble Frizzled related proteins (*sFrp*) 1 and 2 are also expressed in the E/OV, the site of

arrival of the progenitor cells migrating from the lateral ventricle (LV) along the RMS; and *Fz3* and *sFrp1* can be found in the LV itself, thus leading to the hypothesis of WNTs being possibly involved in the regulation of proliferation of progenitor cells. On the contrary, none of the MAPK signalling components seems to be expressed in these regions, prompting the idea that the MAPK signalling could rather interact with WNTs to regulate the survival or maturation of uncommitted neuronal progenitors in granule and glomerular cell layers, than to modulate their proliferation. Therefore these results suggest that, depending on the cellular context, activation of MAPKs can be involved in cell survival and differentiation more than in proliferation. But future studies may reveal if co-localization of these molecules occurs in the same cellular compartments and if there are possible functional interactions.

4.1.2 MAPK and neurogenesis: expression in the hippocampal formation

A second NSC compartment is the subgranular zone (SGZ) of the DG in the hippocampus, from which new granule neurons can be generated to replace the eventually damaged cells in the CA regions (Gage, 2000; Alvarez-Buylla et al., 2002; Doetsch, 2003; Alvarez-Buylla and Lim, 2004; Zhou et al., 2004). In the DG, proliferating progenitor cells divide along the border between the hilus and the granule cell layer; the daughter cells differentiate into granule cell neurons, migrate into the already existing granule cell layer and integrate into functional neuronal circuits. Also in this region it clearly appears that the MAPK pathway via BRAF→MEK1/2→ERK1/2 can not be activated, as far as BRAF is not expressed (Di Benedetto et al., 2007). Similar findings as for the OB neurogenic areas can be described here; also in the DG, in fact, only *Mek1*, *Erk1* and *Erk2* are expressed. The absence of some of the canonical activators of this signalling pathway suggests that also in this neurogenic region alternative upstream factors interact with the expressed MAPK components to regulate their physiological role. As previously observed for the OB, also in the DG gene expression of WNT signalling components appears at hippocampal sites of neurogenesis, new axon growth and synaptogenesis. *Wnt5a*, *7a* and *8b* are expressed in hilar cells lining the DG blades in the adult hippocampus; furthermore, cells in similar positions express *Fz1*, *2* and *9* as well as *sFrp3*. Moreover, *Wnt7b*, *Fz1* and *3* and *sFrp3* are expressed in the DG blades (Shimogori et al., 2004). But in the case of the DG, further studies should be performed to clearly

distinguish if expression of MAPK components is in the active mitotic layer, along the border of the hilus, in the granule cell layer, where maturation and differentiation of newly generated neurons occur, or in both.

4.1.3 MAPK and the limbic system: expression in forebrain areas

There is increasing evidence that the RAS-activated RAF→MEK→ERK pathway can perform critical roles also in terminally differentiated cells, besides the regulation of growth and differentiation in proliferating cells. Moreover, recent findings suggest that mechanisms that control proliferation and differentiation of neuronal progenitor cells during development, subserve the regulation of synaptic plasticity in the adult nervous system, i.e. cell cycle activation in neurons and synaptic plasticity might be alternative effector pathways (Arendt et al., 2004; Bichler et al., 2004). Recently, especially in the limbic system, the NMDA receptors have been shown to be responsible for activity-dependent synaptic plasticity which leads to acquisition and storage of fear memory in the amygdala and long-term potentiation (LTP) in the hippocampus through the activation of the ERK/MAPK signalling pathway (Blair et al., 2001; Schafe et al., 2001; Bauer et al., 2002). Our findings actually support these models of activation, as far as I could find that in both, the hippocampus and the amygdala, various MAPK components are expressed; thus suggesting that also in the adult brain of the mouse, similar modes of activation could occur as in the adult brain of the rat (English and Sweatt, 1997; Atkins et al., 1998; Schafe et al., 1999; Schafe et al., 2000). Interestingly, I could find that in the hippocampus, the different MAPKs show a restricted regional expression. Moreover, among the *Meks* only *Mek1* is expressed in the CA1 field, as it is only *Erk2* among the *Erks* (Fig 9D and 12D); thus strongly supporting the idea that the activation of *Erk2* occurs through *Mek1*, and not through *Mek2* (Xu et al., 1999; Bardwell et al., 2001; Robinson et al., 2002). Conversely, *Mek2* and *Erk1* are completely excluded from CA1 and CA2 regions (Table 1 and Fig 11D).

Regarding another region of the limbic system, the amygdala, it is interesting that most of the components of the canonical MAPK pathway are present in the lateral nucleus (LA), namely *Mek1*, *Erk1/2*; notably, *Mek2* is absent at the mRNA level (Table 1), but it is detectable in tissue's extracts at the protein level (Fig 13), which will be discussed below. It was already shown that ERK/MAPK are phosphorylated in

the LA in response to fear memory formation in the adult rat brain (English and Sweatt, 1997; Impey et al., 1998; Atkins et al., 1998; Impey et al., 1999; Schafe et al., 2000; Schafe et al., 2001). My results suggest that this mechanism could also occur in the adult mouse brain.

4.2 Activation of the ERK/MAPK in the lateral amygdala of the mouse is required for acquisition of a fear potentiated startle response

4.2.1 General consideration

Several studies done in rats have shown that the amygdala, and in particular the lateral nucleus of the amygdala (LA), is involved in processing sensory stimuli into synaptic changes responsible for acquisition/consolidation of associative fear memories. Moreover, some of the intracellular pathways or receptors which are activated in rats in LA for acquisition of fear conditioning have been identified, as for example the ERK/MAPK signalling pathway or the TrkB receptor (Schafe et al., 2000; Blair et al., 2001; Bauer et al., 2002; Rattiner et al., 2004). And it was also shown that the activation of the ERK/MAPK in LA of rats is characterized by a specific time course (Schafe et al., 2000; Paul et al., 2007). But all these studies were based on the use of the freezing paradigm as a read-out to measure inhibition of specific behavioral responses (memory acquisition) after pharmacological treatments (Schafe et al., 2000; Paul et al., 2007). Moreover, the studies which were addressing questions via injection of pharmacological compounds in specific regions were mostly done in rats, due to the bigger size of the brain, which obviously allows a more precise targeting of the injection itself.

On the other hand, the mouse can be efficiently genetically modified to perform further experiments to characterize the specific role of genes in the aetiopathogenesis of mental diseases. In particular, the C57BL/6J is usually the strain of choice among inbred strains for backcrossing genetically engineered mice for the performance of behavioral studies. Given this, a careful molecular and behavioral characterization of the mouse to set baselines for subsequent analysis of mutants has become necessary. In particular, since our present knowledge of fear learning is mainly based on studies performed in rats, it is necessary to assess

similarities and possible differences between mice and rats. First, my aim was to molecularly characterize the LA nucleus in terms of MAPK signalling pathway components expressed in this specific region in the adult mouse brain. In fact, in our study to analyse the expression pattern of the mRNA coding for various components of the classical MAPK signalling pathway $\text{Braf} \rightarrow \text{MEK1/2} \rightarrow \text{ERK1/2}$, I saw that, for example, the mRNA for *Mek2* was absent from most of the regions of the adult brain (Tab 1). Given that the model accepted for fear conditioning is always considering the MEK1 and MEK2 proteins responsible for activation of the ERK1 and ERK2 via phosphorylation in the LA for acquisition/consolidation of long-term memory (LTM), I thought it was fundamental to check whether these proteins were all co-expressed in the LA of the mouse as well.

Second, I wanted to study the time course of activation of the ERK/MAPK signalling pathway in the LA of the mouse after fear conditioning.

Third, I aimed at analysing the cell-type specificity of activated pMAPK in the LA. Much is known, in fact, about the role of neurons in fear conditioning. But only in recent years, also an active role of glia cells in the processes which lead to synaptic plasticity was suggested. Thus, I supposed that the pMAPK could also be activated in glia cells in response to signals which lead to synaptic plasticity responsible for memory formation.

Fourth, I decided to develop molecular tools to study the involvement of the ERK/MAPK in acquisition of FPS. As this paradigm was shown to be a valid model of anticipatory anxiety in humans, I found it worthwhile to validate it in the mouse to study the role of specific molecules in the amygdala for fear memory acquisition. This would then allow the use of mutant mice to identify possible new molecules involved in fear memory acquisition, helping to identify new possible molecular targets for drug discovery to treat anxiety disorders in the clinic.

4.2.2 Analysis of expression of MEK1/2 and ERK1/2 shows the presence of all these proteins in the lateral amygdala of the mouse

The actual model for fear memory formation (for a review, see Schafe et al., 2001) sees the activation of the ERK/MAPK signalling pathway downstream of N-methyl-D-aspartate (NMDA) receptors in response of a conditioned stimulus (CS) and an unconditioned stimulus (US) when these are presented in pairings during Pavlovian

fear conditioning. Usually, what is postulated is that the ERK/MAPK are phosphorylated-activated by their upstream activator proteins MEK1 and MEK2. As I mentioned before, so far, there was no formal proof that both MEK1 and MEK2 were co-expressed in the LA of the mouse. So, I performed a Western Blot analysis on amygdalae's tissue extracts to check whether these activator (MEKs), but also the effector (ERKs), proteins were present. The results showed that they are all present, allowing to rule out a major difference between the mouse and the rat in the expression of these molecules, considered the basis of neural processing leading to LTM in the LA. It could very well be that in our previous study the mRNA for MEK2 was not enough to be detected by ISH analysis, as it could be quickly degraded after translation; thus, making its level too low for detection via ISH, but allowing enough protein to be produced for detection via WB. It is indeed described that the turnover of mRNAs can vary depending on their 3'UTRs (for a review, see Chen and Shyu, 1995 and Mitchell and Tollervy, 2000). Thus, in this line, depending on their mRNA structures, these different four molecules could show such a differential expression between transcriptional and translational levels. But only further biochemical studies could eventually clarify this point.

4.2.3 Time course of ERK/MAPK activation after fear conditioning in the lateral amygdala of the mouse

In order to be able to interfere with specific processes responsible for acquisition or consolidation of fear memories, it is fundamental to identify where and when they are activated to regulate memory formation. To know the site of action of molecules like the ERK/MAPK signalling pathway components, I used the Western Blot on dissected tissue from the LA nucleus. But to study when those processes occur, it is necessary to perform a time course of activation of pMAPK in the LA after fear conditioning. This analysis could reveal that there is indeed a difference between the rat and the mouse in the peaks of activated pMAPK in LA. In fact, in the mouse I could see only one peak of activated pMAPK at 60 min after fear conditioning; but, different from the rat, I could not detect any peak at 5 min after conditioning in the mouse (Paul et al., 2007). This shows again clearly the importance of the validation of the models chosen to study human diseases, in terms of construct validity. Unfortunately, the functional role of the 5 min peak is not known yet. As reviewed in

(Whishaw et al., 2001), several comparative studies already described differences between the mouse and the rat in their performance in various behavioral tests. As explanation for this observation it is argued that these two species occupied different ecological niches during evolution. Thus, the necessity of coping with different environmental stimuli made these rodents diverge already 10 million years ago (Bonhomme, 1985; Boursot, 1993). Based on these comparisons, the mouse seems to exhibit a simpler behavioral repertoire and much less flexibility in dealing with novel situations. These findings suggest that also a "simplification" in the molecular pathways involved in behavioral responses could occur. And the absence of a first peak of activation of pMAPK at 5 min after conditioning could represent a molecular aspect of that "simplification".

4.2.4 The activation of ERK/MAPK after fear conditioning is specifically neuronal

In recent years the involvement of glial cells in active processes regulating neuronal function at the synaptic level has become more and more evident. Namely, it was shown that glial cells participate actively in regulating Ca^{2+} -mediated glutamate release/recycling during synaptic communication (Parpura and Haydon, 2000; Ge, 2006). My results show that the pMAPK activated in the LA after fear conditioning are not in glial cells, but only in neurons. But the analysis was limited to the time point in which this activation is most prominent, namely at 60 min after conditioning. As far as glial cells are involved in regulating neuronal activity (for a review, see Seifert et al., 2006), acting for example on the regulation of synaptic strength, it is possible that MAPKs still play a role in glial cells, but at different time points after conditioning; the latter serving as, for example, a protective mechanism to restore baseline conditions after a peak of activity, reducing the excess of inter-synaptic glutamate which could result in neurotoxic effects (Nicholls and Attwell, 1990; Rothstein et al., 1996; Gegelashvili and Schousboe, 1997; Kanai, 1997; Tanaka et al., 1997).

4.2.5 The activation of ERK/MAPK in the lateral amygdala is necessary for the acquisition of a fear potentiated startle response

The MAPK signalling pathway is already considered a pharmacological target in the

clinic in some neuropsychiatric diseases as the Bipolar Disorder. Among the treatments of choice, the mood stabilizers Valproic acid or Lithium have shown their effects in inhibiting the MAPKs (for a review, see Coyle and Duman, 2003). The present finding of pharmacological inhibition of FPS acquisition by a MEK inhibitor shows that the ERK/MAPK signalling pathway is directly involved in the acquisition of the FPS paradigm in mice. This goes in line with a previous report where the analysis of the CREB knockout, a known target of the ERK/MAPK, shows impairment in the acquisition of FPS (Falls, 2000). Taken together, these findings suggest that the ERK/MAPK signalling pathway can also be a valid biological target in the attempt to intervene in anxiety disorders.

4.2.6 Generation of a tool to study the specific role of the MAPK ERK2 in amygdala of mice via viral-mediated RNA interference

To study the specific role of the ERK/MAPK, several mouse mutants were generated for the inactivation of the genes coding for the various components of this signaling cascade. The classical transgenesis could cast light on some basic functions of these genes during development (Giroux et al., 1999; Pages et al., 1999; Belanger et al., 2003; Hatano et al., 2003). But on the one hand, the early lethality of some of the mutations prevented the further analysis of the role of these genes in adulthood. On the other hand, the lack of promoters specific for restricted areas of the CNS to be used as Cre-drivers, prevented the use of the Cre/LoxP technology in clarifying the function of genes in specific brain regions. To circumvent these problems, I decided to use the RNAi technology coupled with stereotactic injections to control the timing and the regional specificity of gene inactivation. Moreover, to increase the efficiency of targeting, I developed viral vectors to trigger shRNAs into neurons of the amygdala. Among the ERK/MAPK ERK1 and ERK2, I focused my efforts on analyzing the role of ERK2 in fear-based anxiety responses, as far as the knockout mouse for ERK1 was already available and did not show any impairment in emotional learning (Selcher et al., 2001). The results show the validity of the method in region-specific targeting and efficiency of downregulation of the *Erk2* mRNA. Thus, this technique offers a new, valid tool for the analysis of gene function confined in time and space.

4.3 Targeted conditional deletion of the *Pink1* gene in the mouse as a model to study Parkinson's Disease

The presence of comorbidity among neuropsychiatric diseases as, for example, depression and anxiety is already known (Kaufman and Charney, 2000). But in other cases the extent of comorbidity among neuropsychiatric diseases and other brain diseases, as Parkinson's Disease (PD) or Huntington's Disease, is still under debate. Nevertheless, it was already observed that PD patients show impairment in recognition of fear and disgust in facial expressions, a function typically mediated by amygdala and striatum (Morris et al., 1996; Krolak-Salmon et al., 2003). One of the last genes associated with PD was the *Pink1*, for which there was not any model available. So, I decided to generate a conditional mutation of this gene to have a valid tool to be used for further analysis of association between PD and neuropsychiatric diseases as fear-based anxiety disorders.

4.4 Summary and further plans

The scope of this work was to characterize the mouse as a model for studying fear-based anxiety disorders and establish new methods to analyze the molecular mechanisms of fear-based anxiety in the mouse. To date, the results of studies in mice were most often interpreted on the basis of findings in rats. However, researchers have an increasing awareness that anatomical and behavioral differences between these two species may complicate and limit the use of rat studies to interpret findings in mice. For this goal, first I deeply characterized the pattern of expression of the mRNAs coding for some components of the ERK/MAPK signalling pathway in the adult mouse brain, specifically *Mek1*, *Mek2*, *Erk1* and *Erk2*. Indeed, this pathway was shown to be crucial as a downstream effector of glutamate NMDA receptors signalling during synaptic transmission (English and Sweatt, 1997; Atkins et al., 1998; Impey et al., 1998; Impey et al., 1999; Schafe et al., 1999; Arendt et al., 2004). The results showed a quite widespread pattern for all the four mRNAs, which was expected for molecules involved in many basic intracellular functions (see Pages et al., 1993; Vouret-Craviari et al., 1993; Weber et al., 1997). Surprisingly, the mRNA for *Mek2* was absent from most of the regions of the adult murine brain (see Tab 1). As the studies made in rats to clarify the mechanisms on the basis of synaptic

plasticity always consider MEK1 and MEK2 as co-mediators of the NMDA receptors activity, it was striking to observe, at least at the mRNA level, the absence of *Mek2* in most regions of the adult mouse brain. As further plans, when working antibodies were available, an immunohistochemistry on tissue sections could better show how these genes are expressed in the adult CNS of the mouse at the protein level.

Moreover, I was interested in analysing the role of these molecules in the amygdala of the mouse in the acquisition of the Fear Potentiated Startle, as a model of anticipatory anxiety in humans. In rats, it was shown that the ERK/MAPK signalling pathway is involved in the acquisition of the fear responses, as measured with freezing (Schafe et al, 2000; reviewed in Blair et al, 2001). But the neural circuits on the basis of the freezing responses are not as much known as the ones responsible for FPS responses. Moreover, it was already shown that the neural circuits which regulate FPS are very similar in rodents and humans, making this paradigm a better choice in terms of construct validity to study anxiety disorders in humans (Brown et al., 1951; Davis, 1992; LaBar et al., 1998; Phelps et al., 2001). As I discussed, several results came out from my analysis. First of all, I could show that there is a difference in the amygdala of adult mice between the mRNA and protein levels of MEK2. I postulated that this could be due to the differential regulation on the mRNA turnover. But only further biochemical studies could really clarify this point, offering maybe a better explanation for the differences observed. Second, I found out that a major difference between the mouse and the rat occurs in the peaks of activated phospho-MAPK after fear conditioning. As I discussed, this could be due to evolutionary major complexity of the rat in respect to the mouse, so that it shows a second peak of activation. But further investigations would be necessary also to check if the differences in the fear conditioning protocols could influence the results observed. Third, I analysed the cell-type specificity of activated phospho-MAPK in the amygdala of the adult mouse. As the analysis was restricted to the time point when the activation is more prominent, it would be interesting to verify how this occurs at the other time points after fear conditioning. Fourth, I investigated the specific role of MAPK in the acquisition of FPS. To perform the experiments, I used the pharmacological inhibitor U0126 injected into the amygdala of mice before fear conditioning. But this approach does not allow a differentiation to characterize the specific role of the two MAPK ERK1 and ERK2 in fear-based anxiety disorders. To do this, I established another approach, using stereotactic injections of viral vectors

carrying shRNAs against these two molecules separately. In this way, it would be possible to dissect the role of each of them separately in the acquisition of the FPS as a model to study anxiety disorders in human. Moreover, I generated a construct for the conditional inactivation of Pink1, a recently discovered Parkinson's Disease's associated gene, to analyse the possible comorbidity between neuropsychiatric and neurological pathologies of the Central Nervous System.

5 MATERIALS AND METHODS

5.1 Animals

C57BL/6J male mice (Charles River, Sulzfeld, Germany) were used for the experiments. They arrived in our animal house at the age of 7 weeks and were maintained group housed in individually ventilated cages (IVC, four mice per cage) when received from the provider; they were let acclimate for three days before separation. On the third day they were singly housed in IVC cages, but provided with a paper tissue in the cage to relief a bit the stress from separation. They were maintained on a 12 hr light/dark cycle (lights on at 7:00 A.M.) with food and water available *ad libitum* until the day of the experiment. Only the age of the mice at time of the experiment differed depending on the specific requirements of the various experimental procedures, and therefore will be each time specified. Experiments on animals were carried out in accordance to the European Communities Council Directive of 24 November 1986 (86/609/EEC).

5.2 Expression analysis of mRNAs coding for components of the MAPK signalling pathway

5.2.1 Tissue preparation for *in situ* hybridization

Mice 10 weeks old were used for the experiments. On the day of the experiment, between 10:00 A.M and 12:00 P.M., mice were asphyxiated with CO₂ and perfused intracardially, after a brief rinse with ice-cold PBS, with ice-cold 4% paraformaldehyde in 0.1 M phosphate buffer (PB, 0.1 M Na₂HPO₄/NaH₂PO₄, pH 7.5). Brains were dissected and post-fixed for 2 hours in 4% paraformaldehyde-PB. For embedding the brains were then dehydrated through an ascending ethanol scale (30%, 50%, 70%, 95%, 2 x 100%, 1 hour each passage), clarified in Rotihistol (Roth, # 6640) 2 x 45 minutes, equilibrated in 50% Rotihistol/ 50% paraffin for 1 hour, and then transferred into paraffin at +65°C, 2 x 1 hour; they were equilibrated to room temperature in the last paraffin passage and kept at +4°C until cutting. Eight-

micrometer sections were cut in three planes (coronal, sagittal and horizontal) and mounted on SuperFrost® Plus slides (Menzel-Gläser, # J1800AMNZ); slides were dried overnight at 37°C and put at +4°C until proceeding with *in situ* hybridization.

5.2.2 Cloning of the probes for *in situ* hybridization

DNA templates for probes were prepared by RT-PCR on total RNA extracted from adult brains of 10 weeks old mice. Total RNA was extracted using Trizol (Invitrogen, # 15596-026) following manufacturer's instructions. RT was performed using random hexameres and SuperScriptII (Invitrogen Kit, # 11904-018) following manufacturer's instructions. PCR amplifications were performed with the following oligonucleotides: *Mek1*: 5'-GTCTGAGAGGGAGCCTTGTG-3' and 5'-GCCAGCATCTGAGCCTTTAG-3' (from NCBI acc # BC051137, nt 1303-2151); *Mek2*: 5'-CCATGCATTTGAAAACCAAA-3' and 5'-ATTCAGATTGTGGGCAGGAG-3' (from NCBI acc # NM_023138, nt 1522-1965); *Erk1*: 5'-CTGAAGGAGTTGATCTTCCAG-3' and 5'-CCATATACACATCTCTATATTTATAT-3' (from NCBI acc # NM_011952, nt 1095-1765); *Erk2*: 5'-CAGCAGTATCTGTTGTTCTGCAG-3' and 5'-CAT TCTCTTCATGGAATACTC-3' (from NCBI acc # NM_011949, nt 1964-2700). A PCR thermal cycler (Eppendorf) was used with the following amplification conditions: 95°C, 5 min, 1 cycle / 95°C, 30 sec-60°C (45°C for *Mek1* and *Mek2*), 30 sec-72°C, 60 sec, 35 cycles / 72°C, 10 min, 1 cycle. PCR products were purified (Gel extraction Kit, QIAGEN, # 28704), cloned into a pCRII vector (TOPO TA Cloning Kit, Invitrogen, # K4600-01) and transformed into TOP10 chemically competent cells (provided with TOPO TA Cloning Kit, Invitrogen), following manufacturer's instructions. Plasmids containing cDNA fragments coding for the probes were isolated, sequence-verified and linearized with appropriate restriction enzymes to generate DNA templates for *in vitro* transcription of antisense radiolabeled RNA probes.

5.2.3 Preparation of radiolabelled RNA probes and *in situ* hybridization

After linearization with the appropriate enzyme and purification (PCR purification Kit, QIAGEN, # 28704), the DNA templates were used to generate antisense probes labeled with ³⁵S. *In situ* hybridization (ISH) was performed according to a modified version of Dagerlind et al. (1992). For the preparation of radiolabeled probes and ISH

procedures detailed protocols are given at <http://www.empress.har.mrc.ac.uk/EMPreSS/servlet/EMPreSS.Frameset>.

5.2.4 Figure preparation

Photomicrographs were taken on a Zeiss Axioplan microscope equipped with a Zeiss AxioCam MRc digital camera. Image processing in Adobe Photoshop included adjustment of tonal value, brightness, contrast, sharpness (not in all images) and image size. The background especially of the darkfield overview images was made uniform via the copy stamp function of Photoshop.

All photomicrograph images (Fig 9-12) were mounted and labeled with Adobe Photoshop.

5.3 Analysis of the ERK/MAPK signalling pathway components expressed in the lateral amygdala of the adult mouse

5.3.1 Tissue preparation for Western blot analysis

At the age of 10 weeks, mice (n=3) were asphyxiated with CO₂ and brains were removed. Amygdalae were rapidly dissected on ice from 400- μ m-thick sections taken on a vibratome. The dissection was performed with visual inspection under a binocular microscope, with the help of a pair of very sharp tweezers used as scalpels; the lateral and medial boundaries of the LA were identified by the fiber bundles (external capsule) surrounding it; the basal boundary could not be recognized in the same way, so it is highly likely that even parts of the basal nucleus were included in the preparation, together with possibly also part of the central nucleus, or some cortical and striatal tissue around the LA nucleus. Samples were immediately homogenized in ice-cold RIPA buffer (50 mM Tris-HCl, pH 7.5, 1% NP-40, 0.25% Na-Deoxycholate, 0.15 mM NaCl, 1 mM EDTA and a protease inhibitor cocktail). Concentrations of samples were determined with BSA standards and Laemmli buffer was added to the homogenates.

5.3.2 Western blot procedure

Equal amount of proteins (15 μ g) were boiled at 95°C for 10 min, electrophoresed on a 10% SDS-PAGE gel and proteins were then blotted on PVDF membrane (Pall, Pensacola, FL, USA, # P/N 66543). Western blots were blocked in TBST (50 mM Tris-HCl, pH 7.5, 150 mM NaCl, 0.05% Tween 20) with 5% skim milk O/N at 4°C and then incubated with the rabbit anti-MEK1 (C-18, Santa Cruz Biotechnology, # sc-219) (dilution 1:1000) or the mouse anti-MEK2 (BD Transduction Laboratories, NJ, USA, # 610235) (dilution 1:2500) or the rabbit anti-ERK1/2 (Cell Signaling Technology, Beverly, MA, USA, # 9102) (dilution 1:1000), all in TBST with 5% skim milk, for 1 hr at room temperature (RT). Blots were washed in TBST and incubated with goat anti-rabbit or goat anti-mouse conjugated with horseradish peroxidase (Jackson ImmunoResearch, Cambridgeshire, UK, respectively # 111-065-003 and # 115-035-003) (dilution, respectively 1:5000 and 1: 1000) in TBST for 1 hr at RT. After washing with TBST, they were visualized with enhanced chemiluminescence (Amersham Biosciences, Arlington Heights, Illinois) and films were scanned and processed with Adobe Photoshop.

5.4 Behavioral procedure: the Fear Potentiated Startle

5.4.1 Fear Potentiated Startle apparatus

Fear Potentiated Startle (FPS) was assessed using the startle apparatus and software from Med Associates Inc. (VT, USA, Startle Stimulus Package PHM-255A, ANL-925C Amplifier). The apparatus included 4 identical sound-attenuating cubicles (64 x 40 x 42 cm). The animal holders consisted of a transparent plastic cylinder (length 12.5 cm, inner diameter 4.3 cm, 0.5 cm thick wall) where one long side of the cylinder contained 17 holes (0.3 cm diameter, 1 cm space between the holes) in three lines. Each cylinder was fixed in the center of a plastic platform (25 cm x 9 cm) (Fig 23B). Per cubicle, one animal holder was mounted on the top of a load cell platform with the holes facing the two speakers of the stimulus panel (in 7.5 cm distance from the middle of the tube), one for background noise and one tweeter for the stimuli. Cylinder movements were detected and measured by a piezoelectric element mounted under each cylinder (Fig 23A). Startle responses were transduced

by the load cell, amplified and digitized over a range of 4096 arbitrary units. The protocols for FPS were written using the “Advanced Startle” software. For FPS, foot shocks were delivered by Stand Alone Shockers (ENV-414s-SR) and the shock intensity was calibrated by using the PHM-265 Shock Current Test Package.

5.4.2 Behavioral procedure

Pavlovian fear conditioning was used to study learning and memory. In Pavlovian fear conditioning a neutral stimulus such as a tone is paired with an aversive stimulus such as a foot shock (unconditioned stimulus, US).

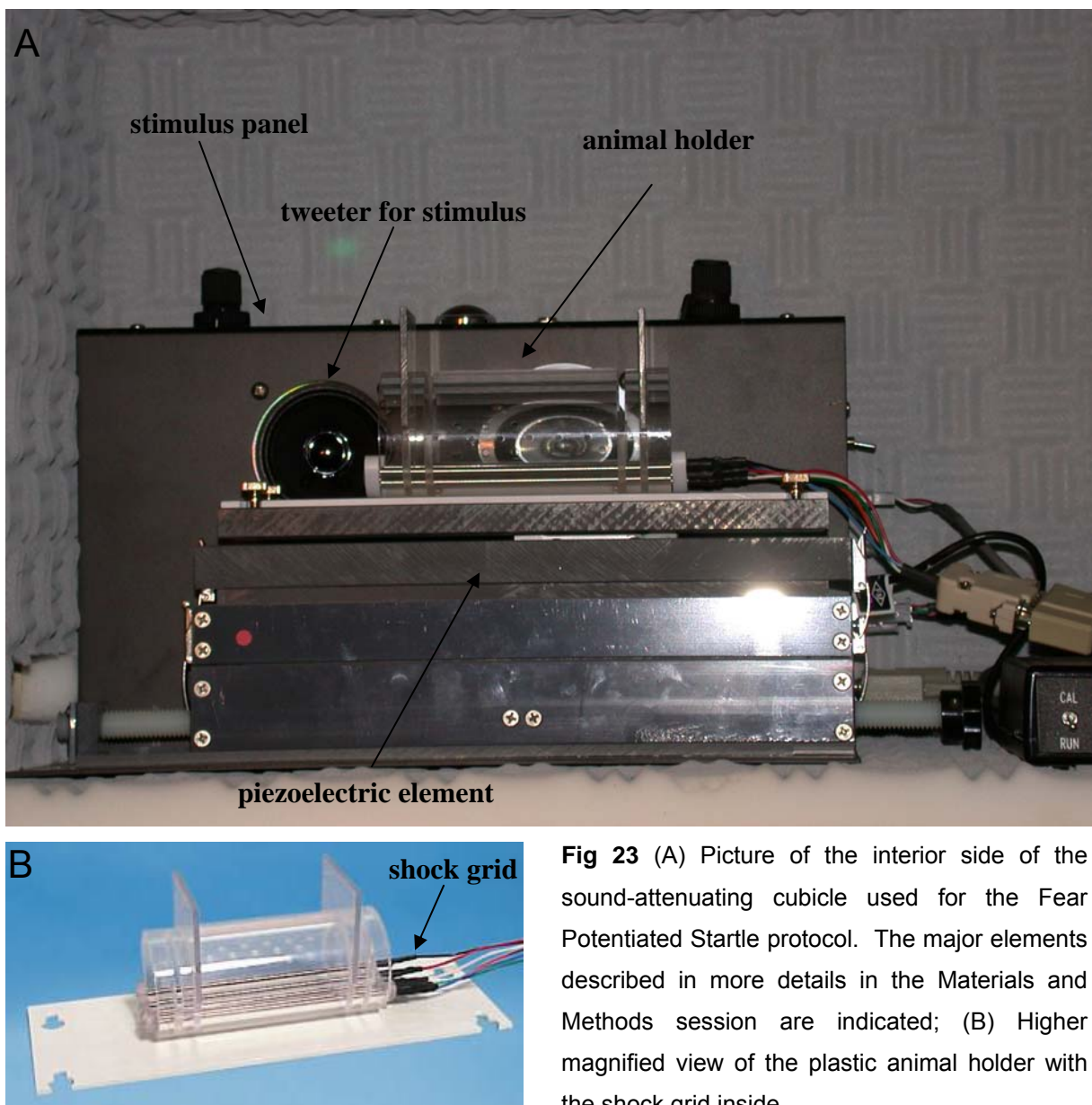


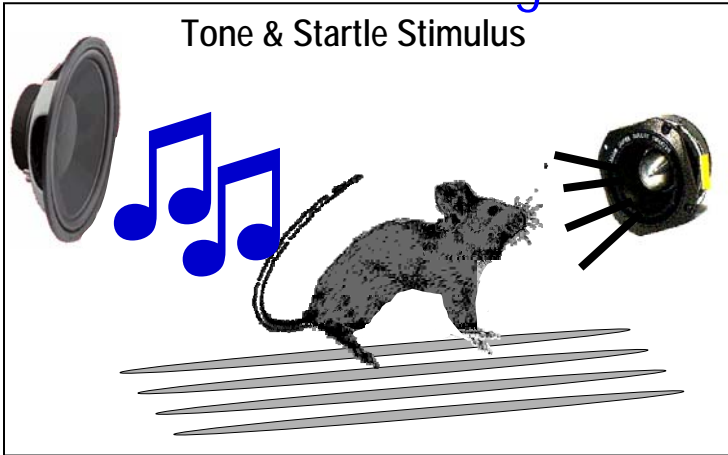
Fig 23 (A) Picture of the interior side of the sound-attenuating cubicle used for the Fear Potentiated Startle protocol. The major elements described in more details in the Materials and Methods session are indicated; (B) Higher magnified view of the plastic animal holder with the shock grid inside.

After a few of these pairings the tone becomes a conditioned stimulus (CS) that elicits the same reaction as the unconditioned stimulus, indicating successful conditioning or learned fear. In the FPS paradigm conditioned fear is defined as elevated startle response to the CS after conditioning in comparison to the response to the CS before conditioning.

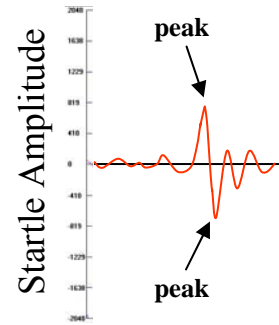
FPS experiments were carried out between 12:00 and 2:00 P.M. on 9 weeks old mice. The FPS protocol consisted of three sessions: pre-conditioning, conditioning and post-conditioning, with a 24 h delay between conditioning and post-conditioning sessions (Fig 24A, C, D). A constant current shocker was placed outside of each sound-attenuating cubicle and shock grids were present in the acrylic tubes in each session. White noise bursts were used as startle pulses (stimulus duration: 20 msec), and FPS was determined in the absence of background noise. The pre-conditioning session was initiated with 5 min acclimation period followed by 9 presentations of startle pulse alone trials (stimulus intensities 95, 100 and 105 dB, each presented three times in random order) that were excluded from statistical analysis. After these 9 leaders, baseline movement of the animal was assessed by three no stimulus (NS) trials, in which a measurement was taken without any stimulus presentation. Altogether, six different trial types were presented in random order with an inter trial interval (ITI) of 60 sec: three different CS trials, in which the CS (12 kHz tone, 60 dB, 30 sec duration) immediately preceded startle pulses of 95, 100 or 105 dB, and three different startle stimulus alone (STL) trials of 95, 100 or 105 dB intensity. Immediately after the session, the mice were removed from the holder. After each session, holders and grids were cleaned with a disinfectant (Pursept). The maximal peak-to-peak amplitude (Fig 24B, E) was used to determine the acoustic startle response occurring within 100 msec after the onset of the startle stimulus. Mean startle amplitudes were calculated over all three startle stimulus intensities. The unconditioned response to CS was calculated as follows: % response to CS = $\frac{[(CS+STL)] - STL \text{ alone}}{STL \text{ alone}} \times 100$.

For the conditioning session, different protocols were tested to choose the best parameters to achieve the highest fear potentiation, defined as a significant increase in the % response to CS during post-conditioning vs. pre-conditioning. The differences consisted in the number of trials and the intensity of the current for the foot shocks delivered to the animals. Namely, four independent groups of wildtype animals were tested (Fig 14, Group1-4), each of which consisted of 12 mice. The first

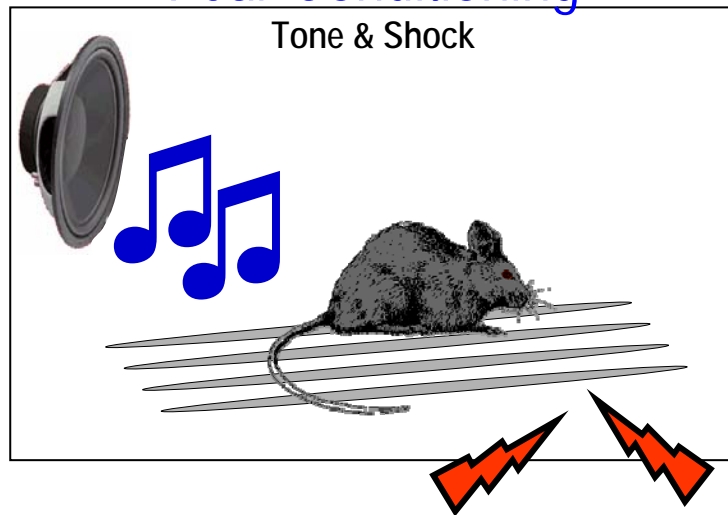
A Pre-conditioning



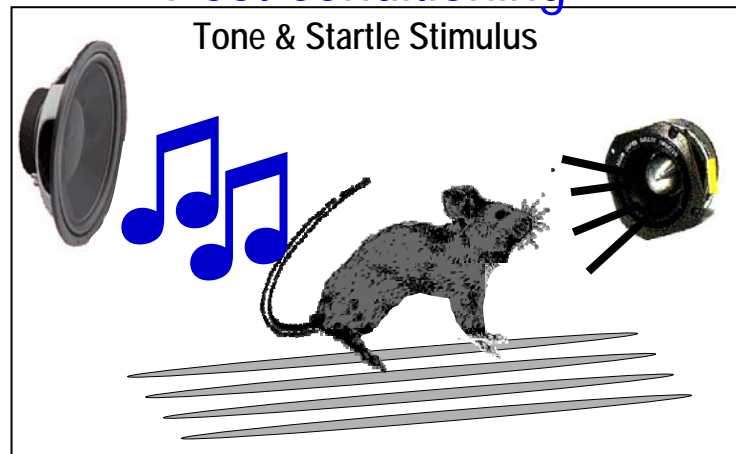
B



C Fear Conditioning



D Post-conditioning



E

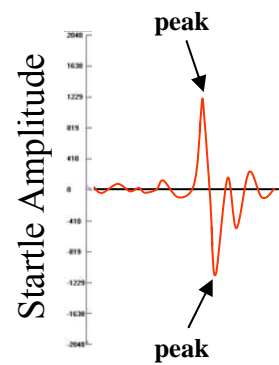


Fig 24 Schematic drawing to represent the three phases of the FPS protocol. (A) The pre-conditioning session, where the animals receive three different conditioned stimulus (CS) trials, in which the CS (12 kHz tone, 60 dB, 30 sec duration) immediately preceded startle pulses of 95, 100 or 105 dB, and three different startle stimulus alone (STL) trials of 95, 100 or 105 dB intensity; (C) The conditioning session, where the animals receive 10 pairings of CS and unconditioned (footshock, US, 0.5 mA, 0.5 sec duration) stimuli; (D) The post-conditioning session, where the animals receive the same protocol as in the pre-conditioning session; (B), (E) Graphs showing the appearance of the startle responses on the computer screen, when transduced by the load cell, amplified and digitized over a range of 4096 arbitrary units with the “Advanced Startle” software; it is shown how it would appear the increase in peak-to-peak amplitude after conditioning (compare (B) to (E)).

two groups (Fig 14, Group1-2) were subjected to a protocol consisting of 5 trials, starting after a 5 min acclimation period. For each trial a 30 sec, 12 kHz, 60 dB tone terminated with the onset of a 0.5 sec foot shock of 0.4 mA. The ITI varied between 60 and 180 sec. The other two groups (Fig 14, Group3-4), instead, received a conditioning protocol of 10 trials, terminating with a 0.5 sec foot shock of 0.5 mA. The most satisfactory conditioning protocol consisted of 10 trials and a foot shock of 0.5 mA (Fig 14; *, $p < 0.05$; **, $p < 0.01$). The protocol and data calculation for post-conditioning were exactly the same as in the pre-conditioning session.

5.5 Analysis of the time course of activation of the ERK/MAPK in the amygdala of mice after fear conditioning

5.5.1 Behavioral procedure and tissue preparation for immunohistochemistry to quantify phospho-MAPK labelled cells

At the age of 9 weeks, between 12:00 and 2:00 P.M., mice were trained with ten conditioning trials consisting of a 30 sec, 12 kHz, 60 dB tone coterminating with the onset of a 0.5 sec foot shock of 0.5 mA (for details, see 5.4.2). Control mice were handled and exposed to the conditioning box for an equivalent amount of time (23 min), but were not exposed to tones and shocks (sham-trained, “Box ctrl”). At the appropriate time intervals after training (5', 15', 30', 60', 180'), mice were asphyxiated with CO₂ and perfused intracardially, after a brief rinse with ice-cold PBS, with ice-cold 4% paraformaldehyde in 0.1 M phosphate buffer (PB, 0.1 M Na₂HPO₄/NaH₂PO₄, pH 7.5) for 7 minutes. Brains were removed, post-fixed in the same fixative solution

for 24 hr at 4°C and cryoprotected in 0.1 M phosphate buffer containing 25% sucrose for 24 hr at 4°C. Sections (30µm) were cut on a cryostat (Leica, Germany) and kept in a solution containing 30% ethylene glycol, 30% glycerol and 0.1 M phosphate buffer at –20°C until they were processed for immunohistochemistry.

5.5.2 Immunohistochemistry (IHC)

The immunohistochemical procedure was adapted from protocols previously described (Sgambato et al., 1998) except that for the detection of phosphorylated proteins, 0.1 mM NaF was included in all buffers and incubation solutions.

For the detection with anti-phospho-ERK1/2:

Day 1: Free-floating sections were extensively rinsed in Tris-buffered saline (TBS; 0.05 M Tris and 0.15 M NaCl, pH 7.5). Endogenous peroxidase was quenched with incubation for 5 min in TBS containing 3% H₂O₂ and 10% methanol. Sections were then rinsed three times for 10 min each in TBS. Cell membranes were permeabilized with incubation for 15 min in 0.5% Triton X-100 in TBS. After three washes for 5 min each in TBS, sections were incubated with the rabbit anti-phospho-ERK1/2 (Cell Signaling Technology, Beverly, MA, USA, # 9101) (dilution 1:400) in TBS, overnight at 4°C.

Day 2: After three rinses of 10 minutes each in TBS, the sections were incubated for 2 hr at room temperature with the secondary biotinylated antibody anti-rabbit (Jackson ImmunoResearch, Cambridgeshire, UK, # 111-065-003) (dilution 1:200) in TBS. After three washes for 5 min each in TBS, the sections were incubated for 90 min in avidin-biotin-peroxidase complex (ABC) solution (final dilution, 1:50; Vector Laboratories, Peterborough, UK, # PK-6100). The sections were then washed one time in TBS and twice in TB (0.05 M Tris, pH 7.5) for 10 min each, placed in a solution of TB containing 0.1% 3,3'-diaminobenzidine (DAB, 50 mg/100 ml; Sigma, # D5637), and developed for 30 min after H₂O₂ addition (0.02%). The reaction was stopped by washing the sections three times in TB. After processing, the tissue sections were mounted onto poly-L-lysine-coated slides, air-dried, dehydrated through ascending ethanol scale (30%, 50%, 70%, 95%, 2 x 100%, each for 5 min), clarified in Rotihistol (Roth, # 6640) 2 times for 10 min each, mounted with Rotihistokitt (Roth, # 6638.2) and covered with coverslips for light microscopic examination.

5.5.3 Microscopy data analysis

For the quantification of phospho-MAPK labeled cells, three to six different brains were analyzed for each time point and the resulting data compared to control values. In each brain, sections from comparable anteroposterior levels were selected for scoring, starting from -1.22 mm until -2.30 mm posterior to bregma. At these levels, the nuclei of the LA are clearly identifiable. Cell counts were taken from nine sections per mouse and scored after selection of the boundary around the LA in each section. Cells were counted only when their nuclei were clearly labelled. To estimate the total number of labelled cells, I used the Optical Fractionator design in which the counting strategy involves systematic, unbiased and uniformly random sampling of a known fraction of the tissue. The StereoInvestigator Software (Brightfield, Inc) was then used to elaborate the results. The actual cell counts were obtained with a 40x oil-immersion objective.

5.6 Characterization of the expression of activated ERK/MAPK in different cell types: neuronal or glial?

5.6.1 Behavioral procedure and tissue preparation for immunohistochemistry

At the age of 9 weeks, between 12:00 and 2:00 P.M., mice were trained with ten conditioning trials consisting of a 30 sec, 12 kHz, 60 dB tone terminating with the onset of a 0.5 sec foot shock of 0.5 mA (for details, see 5.4.2). Sixty minutes after training, mice were perfused and brains prepared and cut as described for the quantification of phospho-MAPK labelled cells after fear conditioning (for details, see 5.5.1).

5.6.2 Immunofluorescent-immunohistochemistry (IF-IHC)

To study the cell-type specificity of phospho-MAPK labelled cells, the procedure was as follows:

Day1: Free-floating sections were extensively rinsed in phosphate-buffered saline (PBS, 0.1 M $\text{Na}_2\text{HPO}_4/\text{NaH}_2\text{PO}_4$, pH 7.5). Endogenous peroxidase was quenched

with incubation for 5 min in PBS containing 3% H₂O₂ and 10% methanol. Sections were then rinsed three times for 10 min each in PBS. Cell membranes were permeabilized with incubation for 15 min in 0.5% Triton X-100 in PBS. After three washes for 5 min each in PBS, they were then incubated 48 hrs at 4°C with the rabbit anti-phospho-ERK1/2 (Cell Signaling Technology, Beverly, MA, USA, # 9101) together with one of the following: either mouse anti-Neuronal Nuclei (NeuN, Chemicon, # MAB377) (dilution 1:200) or mouse anti-glial protein S100 β (clone SH-B1, Sigma, # S2532) (dilution 1:1000) in PBS 1X containing 10% Normal Goat Serum (NGS) and 0.5% Triton X-100.

Day 2: After three rinses in PBS for 10 min each, the sections were incubated for 24 hrs at 4°C with the secondary fluorescent-conjugated antibodies (FITC-anti-rabbit, Dianova, # 111-095-003 and TRITC-anti-mouse IgG1, Southern Biotech, # 1070-03) (dilution 1:200) in PBS.

Day 3: after three washes for 10 min each in PBS, the sections were mounted onto poly-L-lysine-coated slides, covered with anti-fading AquaPolyMount (Polysciences, # 18606-20), protected with coverslips and let dry before confocal analysis.

5.6.3 Microscopy data analysis

The analysis was performed using a confocal microscope (Olympus, equipped with the FluoView1000 Software), scoring through amygdala's sections, from anterior to posterior levels, on both left and right sides, in at least two brains (n=2) for each antibody combination.

5.7 Surgical procedure: the stereotactic surgery in mice to target the amygdala

5.7.1 Stereotactic apparatus

Stereotactic surgery was performed using a stereotactic device (Stoelting, # 51600, Illinois, USA) (Fig 25A). The apparatus was equipped with a manipulator arm, fitted to keep different types of probe holders. Two lateral ear bars were provided to fix the skull and a mouse tooth-bar adaptor was used to fix the mouth of the mouse in the

device. In this way the head of the mouse was safely secured into the apparatus to prevent any kind of movement during surgical procedure.

5.7.2 Surgical procedure

The purpose was to identify the correct coordinates in the brain of mice to drive injection of pharmacological compounds (or other substances) in specific target areas, through the help of special stainless steel cannulas (PlasticOne), and perform afterwards behavioral studies. Different coordinates were extrapolated from The Mouse Brain Atlas (Paxinos and Franklin, 1989) and tested *in vivo* to establish the best fitting to target the lateral amygdala (LA). To check the injection sites, dil or Methylene blu were injected in different positions into the brains and animals sacrificed. Brains were removed, fixed by immersion in 4% paraformaldehyde in 0.1 M phosphate buffer (PB, 0.1 M Na₂HPO₄/NaH₂PO₄, pH 7.5) 24 hr at 4°C. Sections (30µm) were cut on a cryostat (Leica, Germany), mounted on SuperFrost® Plus slides (Menzel-Gläser, # J1800AMNZ) and processed with Nissl staining for histological analysis. Light microscopy was used to check the injection sites; the coordinates which were showing the injection site above or inside the LA were chosen to perform the subsequent experiments. Surgery was performed on animals 8 weeks old. Each mouse was placed on an elevated platform (ca. 4 cm) and its head secured to the stereotactic frame via the tooth bar and ear bar assembly (Fig 25A). An incision was made along the midline skull area and the skull was exposed, deviating the skin laterally with clamps and scraping the periosteum with a sterile blade. Rostrocaudal leveling was accomplished by measurements on the midline sagittal suture, ensuring that bregma and lambda (Fig 25B) were sitting at the same level. After leveling the skull, the coordinates of the bregma were identified, positioning the tip of the cannula on it and reading the resulting numerals on the scales on the manipulator arms. Then, on the basis of the desired coordinates, as established by the test experiments described above, the targeted coordinates could be calculated. The tip of the cannula was positioned on the skull at the position of the anteroposterior (AP) and mediolateral (ML) coordinates and the point on the skull was marked with a pencil; afterwards, an electric drill was used to make holes in correspondence of the marked points to allow the insertion of the cannulas (PlasticOne, # C313GS-5) in the mouse brain.

Once the correct dorsoventral position was reached, the cannulas were fixed on the skull with dental cement or glue (Fig 25C) and plugged with dummy cannulas (PlasticOne, # C313DCS-5) to prevent clogging. The skin was sewed up with special surgical sewing material and the mouse let to recover for at least 7 days before carrying on any other experimental procedures. In Fig 25D, a mouse is shown after the surgical procedure and recovery from anesthesia.

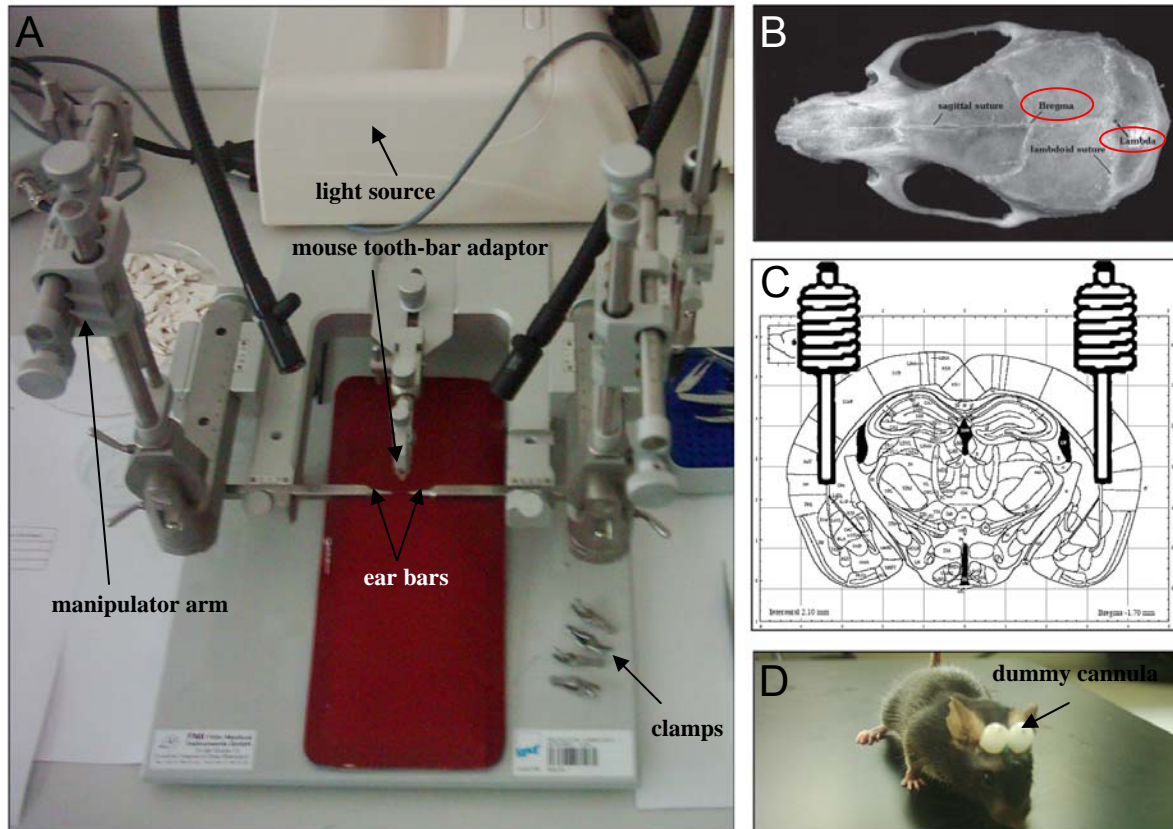


Fig 25 The stereotactic apparatus and the surgical procedure. (A) Picture of the stereotactic apparatus: arrows indicate the major tools used for surgery (for details, see text); (B) In the picture from Paxinos and Franklin (1989) bregma and lambda are indicated on the skull for the orientation during surgery; (C) schematic drawing to show the coordinates of insertion of the cannulas into the mouse brain; (D) picture of the mouse after surgery: indicated are the dummy cannulas used to plug the guiding cannulas to prevent clogging.

5.7.3 Histological analysis

Sections were stained in cresyl violet solution (Kresylviolett 2.5 gr, CH₃COONa 0.102

gr, CH₃COOH 1.55 ml, H₂O till 500 ml, pH 3.5) for 10-15 minutes. They were then rinsed in distilled water, dehydrated through an ascending ethanol scale (2 x 70%, 2 x 96%, 2 x 100%, 2 minutes each passage), clarified in Rotihistol (Roth, # 6640) 2 times for 10 min each, mounted with Rotihistokitt (Roth, # 6638.2) and covered with coverslips for light microscopic examination.

5.8 Pharmacological analysis of the role of the ERK/MAPK during acquisition of fear conditioning in amygdala of mice

5.8.1 Surgery

At the age of 8 weeks, mice were anesthetized with Ketamine/Xylazine and implanted bilaterally with 22-gauge stainless steel guiding cannulas (PlasticOne, # C313GS-5) aimed at the LA. Coordinates, taken from The Mouse Brain Atlas (Paxinos and Franklin, 1989), were: -1.7 mm anteroposterior, ±3.4 mm mediolateral, and -3.4 mm dorsoventral. The cannulas were anchored to the skull with glue and a 28-gauge dummy cannula (PlasticOne, # C313DCS-5) was inserted into each guiding cannula to prevent clogging. After surgery, mice were given at least 7 days to recover before proceeding with the subsequent experiments (for details, see 5.7.2).

5.8.2 Drugs

For behavioral studies, U0126 (Promega, Madison, WI, # V1121) was dissolved in 100% DMSO to a final stock concentration of 4 mg/ml. The drug was diluted 1:1 in artificial cerebrospinal fluid (aCSF, D-glucose, 5 mM; CaCl₂, 1mM, NaCl, 125 mM, MgCl₂, 1 mM, NaHCO₃, 27 mM, KCl, 0.5 mM, Na₂SO₄, 0.5 mM, NaH₂PO₄, 0.5 mM, Na₂HPO₄, 1.2 mM). U0126 is a specific inhibitor of MAP kinase kinase (MEK), an upstream regulator of ERK/MAPK activation (Favata et al., 1998). In a recent study using hippocampal homogenates, the effects of U0126 have been shown to be specific to ERK/MAPK and to have no effect at a range of concentrations on other kinases, such as PKA, calcium-calmodulin kinase II, or PKC (Roberson et al., 1999).

5.8.3 Behavioral procedure

After surgery, the day before conditioning, mice were tested for their baseline pre-conditioning responses as described in 5.4.2.

On the day of conditioning, mice were given a bilateral intra-BLA infusion of either 0.3 μ l 50% DMSO in aCSF (vehicle; 0.1 μ l/min) or 0.3 μ l U0126 in 50% DMSO in aCSF (1.0 μ g/side in 0.3 μ l; 0.1 μ l/min). Injectors remained in the cannulas for 1 min after drug infusion to allow diffusion of the drug from the tip. Thirty minutes after drug infusions, mice were trained with ten conditioning trials consisting of a 30 sec, 12 kHz, 60 dB tone that coterminated with a 0.5 sec, 0.5 mA foot shock (ITI between 60 and 180 sec randomly distributed among trials). Testing for conditioned fear responses (FPS) in mice was conducted 24 hr after conditioning. The post-conditioning protocol and data analysis were exactly the same as in the pre-conditioning session. All data were analyzed with ANOVA followed by Bonferroni *post hoc t* tests. Differences in % of response to CS (fear potentiation) between pre- and post-conditioning were considered significant if $p \leq 0.05$. One week after the pharmacological manipulations, the same animals were trained (reconditioning) and tested again, 24 hrs later, to check the specificity of pharmacological inhibition. The absence of fear potentiation after reconditioning was used as the first criterion to exclude animals from data analysis, as this could be a sign of permanent damage of the amygdalae following injections. At the end of each behavioral experiment, mice were asphyxiated with CO₂ and perfused intracardially, after a brief rinse with ice-cold PBS, with ice-cold 4% paraformaldehyde in 0.1 M phosphate buffer (PB, 0.1 M Na₂HPO₄/NaH₂PO₄, pH 7.5). Brains were removed, cryoprotected in 0.1 M phosphate buffer containing 25% sucrose for 24 hr at 4°C. Coronal sections (30 μ m) were cut on a cryostat (Leica, Germany) through the area of amygdala, stained with Nissl. Light microscopy was used to verify the location of injection sites within the amygdalae and as a second criterion, animals were excluded from data analyses when the tips of the injectors terminated outside of the amygdala.

5.9 Injections into the amygdala

5.9.1 Pharmacological inhibitor

On the day before conditioning, mice were habituated to dummy cannulas' removal for at least 10 minutes, immediately after the pre-conditioning session was performed, to avoid any interference with the testing session itself.

On the day of conditioning, mice were given a bilateral intra-BLA infusion of either the vehicle or the pharmacological compound. Injectors were connected through a tubing system (Polyethylene Tubing, Intramedic, Becton Dickinson, Sparks, MD, USA) to a Hamilton syringe (Hamilton, USA). The syringe was in turn connected to a manual micromanipulator to allow a precise control on injection rate (see Fig 26). Dummy cannulas were removed, the injector was placed into the guiding cannulas until it reached the bottom of it. Animals were then put into a fresh cage and injected while

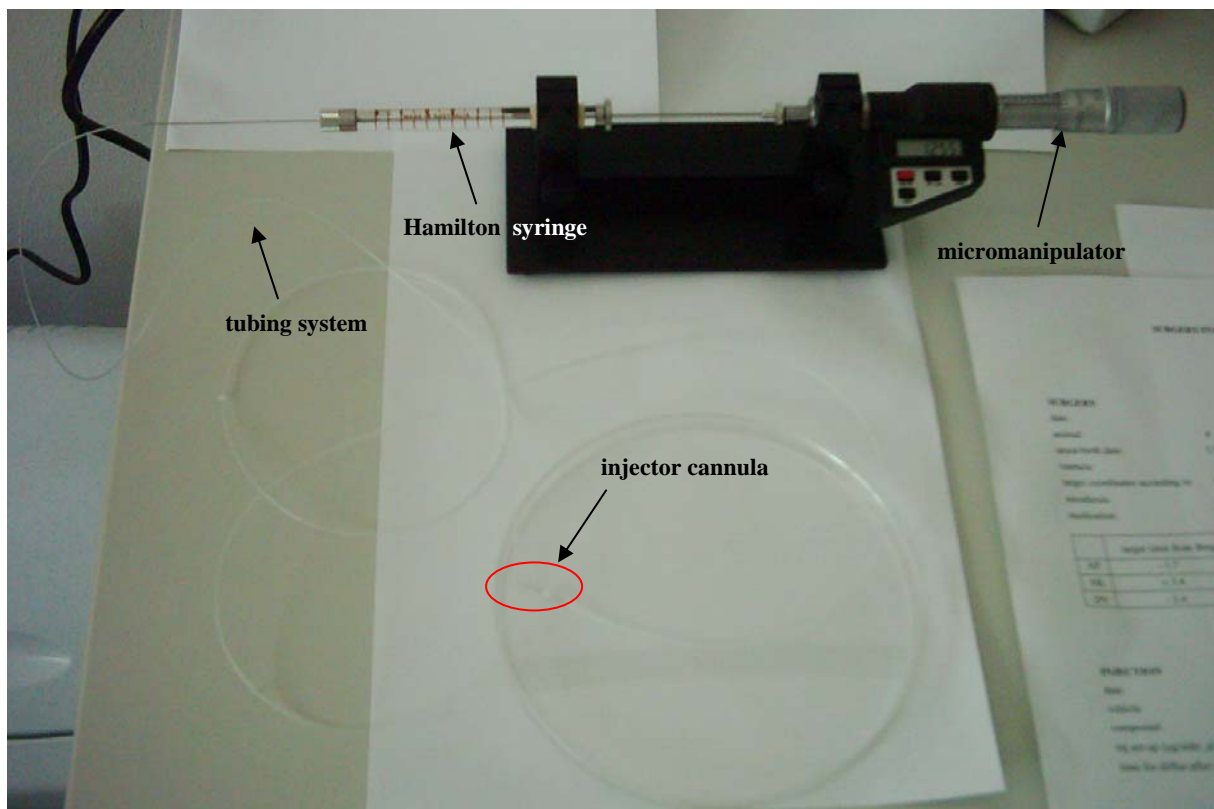


Fig 26 Picture of the injection set-up used for the pharmacological studies. The various components described in details in the text are indicated.

freely moving during the injection time. Afterwards, injectors were removed and dummy cannulas were put back into the guiding cannulas to prevent entrance of infectious material and to keep the guiding cannulas free.

5.9.2 Viral injections

Mice were anesthetized and fixed in the stereotactic apparatus. After having prepared the head of the mouse as described above in 5.7.2, the injection was performed via the use of glass capillaries fixed on the tip of the injector set-up (shown in Fig 27). Injectors were connected through a tubing system to a manual micromanipulator to allow a precise control on injection rate.

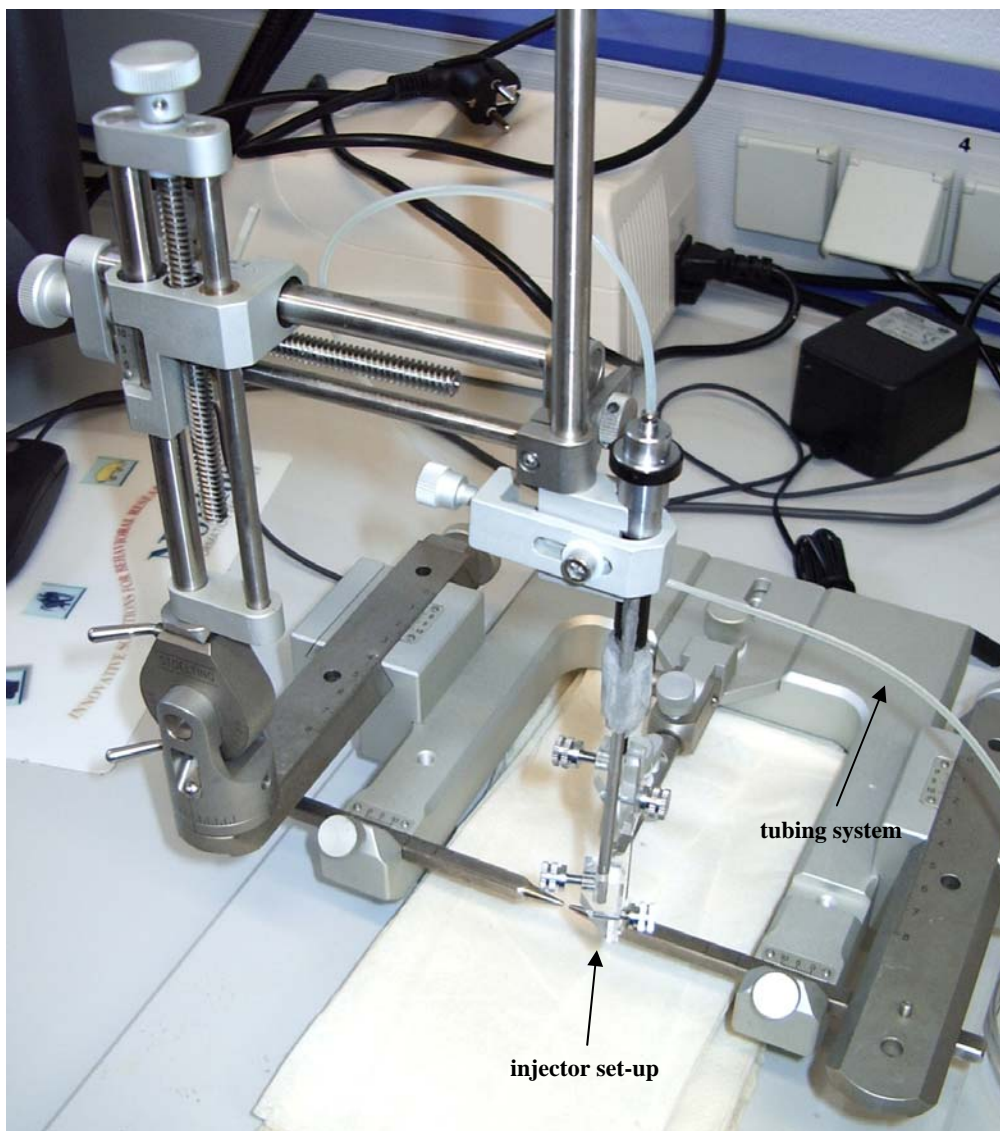


Fig 27 The stereotactic apparatus with the manipulator for viral injections. The components described in details in the text are indicated.

5.10 Analysis of the differential role of the ERK/MAPK ERK1 and ERK2 during acquisition of fear conditioning in amygdala of mice using RNAi

5.10.1 Selection and *in vitro* testing of shRNAs for efficient downregulation of Erk1/2 mRNAs

This experimental part was done in collaboration with Dr. Ralf Kühn, with the help of Christoph Birke. Briefly, after choosing the short hairpin sequences, as stretches of DNA sequences homologous to specific parts of the targeted genes, the corresponding oligos were designed, ordered and cloned into plasmid backbone vectors bearing the U6 promoter and the polyA sequences to drive their expression. Plasmids were transfected into ES cells and cells cultivated for 48 hours. They were then lysed in RIPA buffer (for receipt, see 5.3.1); total proteins were measured via BSA standards and Laemmli buffer was added to the homogenates. Western blots were carried out as described in 5.3.2, except that only the rabbit anti-ERK1/2 antibody was used.

5.10.2 Cloning of the viral construct and viral preparation

This part was done in collaboration with another PhD student, Benedikt Wefers, who took care of the cloning of the efficient short hairpin against ERK2 into the viral backbone (see Results session, 3.8.1); he then made the viral preparation which I used for testing the tropism and efficiency of downregulation *in vivo* (Results session, 3.8.2 and 3.8.3 respectively).

5.10.3 Surgery

At the age of 8 weeks, mice were anesthetized with Ketamine/Xylazine and injected bilaterally with 1 μ l of AAV preparation/side, aimed at the LA. Coordinates, taken from The Mouse Brain Atlas (Paxinos and Franklin, 1989), were: -1.7 mm anteroposterior,

±3.6 mm mediolateral, and –3.9 mm dorsoventral. After surgery, mice were given at least 7 days to recover.

5.10.4 Testing for the tropism of the virus - the adeno-associated virus (AAV)

Immunohistochemistry was carried out on free floating cryosections, prepared as described in 5.5.1. The immunohistochemical procedure was done as described in 5.6.2, except that on Day 1, after free-floating sections were extensively rinsed in PBS, they were then incubated 24 hrs at 4°C with the chicken anti-Green Fluorescent Protein (GFP, Aves Lab, # GFP-1020) together with one of the following: either mouse anti-Neuronal Nuclei (NeuN, Chemicon, # MAB377) (dilution 1:200) or mouse anti-glial protein S100 β (clone SH-B1, Sigma, # S2532) (dilution 1:1000) in PBS 1X containing 10% Normal Goat Serum (NGS) and 0.5% Triton X-100. And on Day 2, the appropriate FITC-conjugated anti-chicken secondary antibody was used, at the same dilution as used for the other secondary antibodies.

5.10.5 Preparation of DIG-labelled RNA probes and *in situ* hybridization

After linearization with the appropriate enzyme and purification (PCR purification Kit, QIAGEN, cat # 28704), two micrograms of DNA templates were used for the synthesis of DIG-labelled transcripts by *in vitro* transcription with DIG-UTP. After 20 min of DNase I (Roche, cat # 04716728001) treatment, the probes were purified by the RNeasy Clean up protocol (QIAGEN, cat # 74104) and measured in a dot-blot assay. Briefly, the following procedures were carried out. DNA template (4–6 μ l, 2 μ g) was added to an *in vitro* transcription reaction containing final concentrations of 1 mM CTP, ATP, GTP, 0.65 M UTP, 0.35 M Dig-UTP (Roche, # 11277073910) 2 units/ μ l of the appropriate RNA polymerase (Roche), 1x buffer and 1 unit/ μ l RNase inhibitor (Roche, # 03335402001). The reaction volume was brought up to 20 μ l per sample and was incubated for 2 h at 37°C. One microliter (10 units/ μ l) of RNase-free DNase (Roche, # 776785) was added to each reaction tube. This reaction was incubated for 15 min at 37°C. To precipitate the probes, the following was added in order: 2 μ l of 0.2M EDTA, 1 μ l of molecular grade glycogen, 2.5 μ l of 4 M lithium chloride and 75 μ l of cold ethanol. Samples were then placed at -70°C overnight. The probes were then

centrifuged at 12,000 x *g* for 20 min at 4°C and rinsed in 70% ethanol. The probes were resuspended in 50–100 µl of DEPC-treated water (containing 0.2 units of RNase inhibitor/µl water) and heated for 30 min at 37°C. Probe yield was determined by comparing serial dilutions of probe to Dig-labelled control RNA standards. Samples were serially diluted (50% DEPC–water, 30% 20x SSC, 20% formaldehyde) 1/10, spotted onto a nylon membrane. Membranes were then blocked in 1% blocking reagent in maleic acid buffer (0.1 M Maleic acid, 0.15 M NaCl, pH 7.5 with NaOH) for 30 min. Membranes were then incubated in sheep anti-Dig alkaline phosphatase-conjugated antibody 1/5000 in blocking reagent/maleic acid buffer for 1 h at room temperature, rinsed 3 times in maleic acid buffer and then incubated in NBT/BCIP (0.46 mM NBT (Roche, # 11383213001), 0.43 mM BCIP (Roche, # 1383221) in 50 mM MgCl₂/100 mM Tris in 100 mM 2 NaCl, pH 9.3) to visualize/quantitate the probe dilutions.

For the ISH procedures, detailed protocols are given at <http://www.empress.har.mrc.ac.uk/EMPreSS/servlet/EMPreSS.FrameSet>.

5.10.6 Testing for the efficiency of downregulation of the short hairpin against Erk2

For the ISH procedures, briefly:

Day 1: free-floating sections were extensively rinsed in PBS. Endogenous peroxidase was quenched with incubation for 30 min in PBS containing 0.3% H₂O₂. Sections were then rinsed three times for 5 min each in PBS. They were incubated for 15 min in 5X SSC (0.75 M NaCl, 0.75 M Na-citrate). After 1 hr incubation at 58°C in pre-hybridization solution (5X SSC, 50% formamide, pH 7.5 with HCl, 50 µg/ml salmon sperm), the sections were incubated O/N at 58°C in hybridization solution (the same as pre-hybridization, with 500 ng/ml of DIG-labelled probe).

Day 2: sections were washed for 1 hr at 65°C in 2X SSC, then rinsed three times for 5 min each in PBS and blocked 30 min in PBS-BB (PBS with 1% BSA, 0.2% powdered skim milk, 0.3% Triton X-100). They were then incubated for 1 hr in HRP-conjugated anti-DIG antibody (Roche, # 11207733910), washed two times for 5 min in PBS and two times in PBST (0.5% Triton X-100 in PBS). For amplification of the signal, sections were incubated in Tyramid Signal Amplification solution (TSA, Perkin Elmer, # SAT700) (dilution 1:50 in its own diluent solution). Sections were rinsed for

5 min in Maleic acid buffer (MB, 0.1 M Maleic acid, 0.15 NaCl, pH 7.5 with NaOH) and incubated for 30 min in a solution containing Neutravidin (Pierce, # 31000) (dilution 1:750 in Maleic acid blocking buffer (1% blocking reagent, Roche, # 11096176001 in MB)). After a wash for 5 min in MB, sections were rinsed two times for 5 min in Detection buffer (Tris-Cl 0.1 M, pH 9.5; MgCl₂ 0.05 M; NaCl 0.1 M) and developed in Developing solution (NBT 0.5 mg/ml (Roche, # 11383213001), BCIP 0.375 mg/ml (Roche, # 1383221) in Detection buffer). When a clear signal was visible, sections were washed three times for 5 min each in PBS, before incubation 24 hrs at 4°C with the chicken anti-Green Fluorescent Protein (GFP, Aves Lab, # GFP-1020).

Day 3: as described before, the appropriate FITC-conjugated anti-chicken secondary antibody was used, at the same dilution as used for the other secondary antibodies in IF-IHC (for details, see 5.6.2).

Day 4: sections were mounted as described in 5.6.2, to be ready for microscopical analysis.

5.11 Targeted conditional deletion of the Pink1 gene in the mouse as a model for Parkinson's Disease

5.11.1 Construction of the targeting vector

The Pink1 targeting vector was constructed from a genomic clone isolated from a 129/ola genomic library (RZPD, clone ID MPMGc121K0633Q2). To isolate the clone containing the Pink1 gene, a screening of a macroarray library was performed using a specific genomic fragment as a probe for the screening by Southern blot. The Southern blot on macroarray was performed following the RZPD's instructions. Once the correct clone was identified, the corresponding bacterial colony was ordered and plated on bacterial selective medium. The DNA was isolated and 1 µl was used to perform each of the three long-run PCR reactions to amplify the three fragments corresponding to the two homologous 5' and 3' arms and the floxed arm. The PCR reactions were performed with the following oligonucleotides: *5HA-for*: 5'-CCAAGGCGCGCCCTGTTCTTCCTATGGGGTTGCAAAC-3' and *5HA-rev*: 5'-GGAAGCGATCGCGGATCCGTGAGTGATATACTAACAACACTGACAGC-3' for the 5' homologous arm; *floxHA-for*: 5'-

GGACCTGCAGGCCAACGTGGCATTACACAGACTGG-3' and *floxHA-rev*: 5'-GGGAGTCGACGGCACCAGAGGTAGAATACAGAACC-3' for the floxed arm; *3HA-for*: 5'-CCAAGGCCGGCCGTGCCAAGGGTACTAGCTGAAATTC-3' and *3HA-rev*: 5'-GAACAGCCTCACCTTGCTGGCCTC-3' for the 3' homologous arm. The long-run proofreading BD TITANIUM™ Taq DNA Polymerase, the BD Advantage™ 2 PCR Kit (BD Biosciences Clontech, # 639207) and a PCR thermal cycler (Eppendorf) were used with the amplification conditions suggested in the polymerase's manufacturer's instructions. The PCR products were purified (Gel extraction Kit, QIAGEN, # 28704), digested with the appropriate restriction enzymes to generate the sticky ends adapted for oriented cloning and cloned into the pEasyFloxII vector (for details on the cloning strategy, see Fig 28A, B, C). They were transformed into TOP10 chemically competent cells (provided with TOPO TA Cloning Kit, Invitrogen), following manufacturer's instructions. At least ten bacterial colonies were isolated from each of the three cloning events and the plasmid DNA was extracted from each. To identify those which could contain the desired fragments, the plasmid DNAs were digested with several restriction enzymes. Among the ones which turned out to be positive for expected restriction pattern, at least two for each cloning event were sent to Sequiserve for sequencing. Once the right clones were selected, the fragments were again cut and trans-cloned to generate the final vector, as shown in Fig 28D.

5.11.2 Cloning of the probe for the Southern blot analysis of ES cells positive for homologous integration of the targeting vector

The probe for the Southern blot analysis was amplified via PCR from the genomic clone used for the construction of the targeting vector. The PCR was performed with the following oligonucleotides: *Pink-for*: 5'-CAAGGGCGGAGTTAGTTGGATAG-3' and *Pink-rev*: 5'-CCAACCAAAGAGTACACATGGATG-3' and the following amplification conditions: 95°C, 5 min, 1 cycle / 95°C, 1 min-60°C, 1 min-72°C, 1 min, 30 cycles / 72°C, 10 min, 1 cycle . The PCR reaction was purified, cloned into a pCRII vector and transformed into TOP10 chemically competent cells as described before.

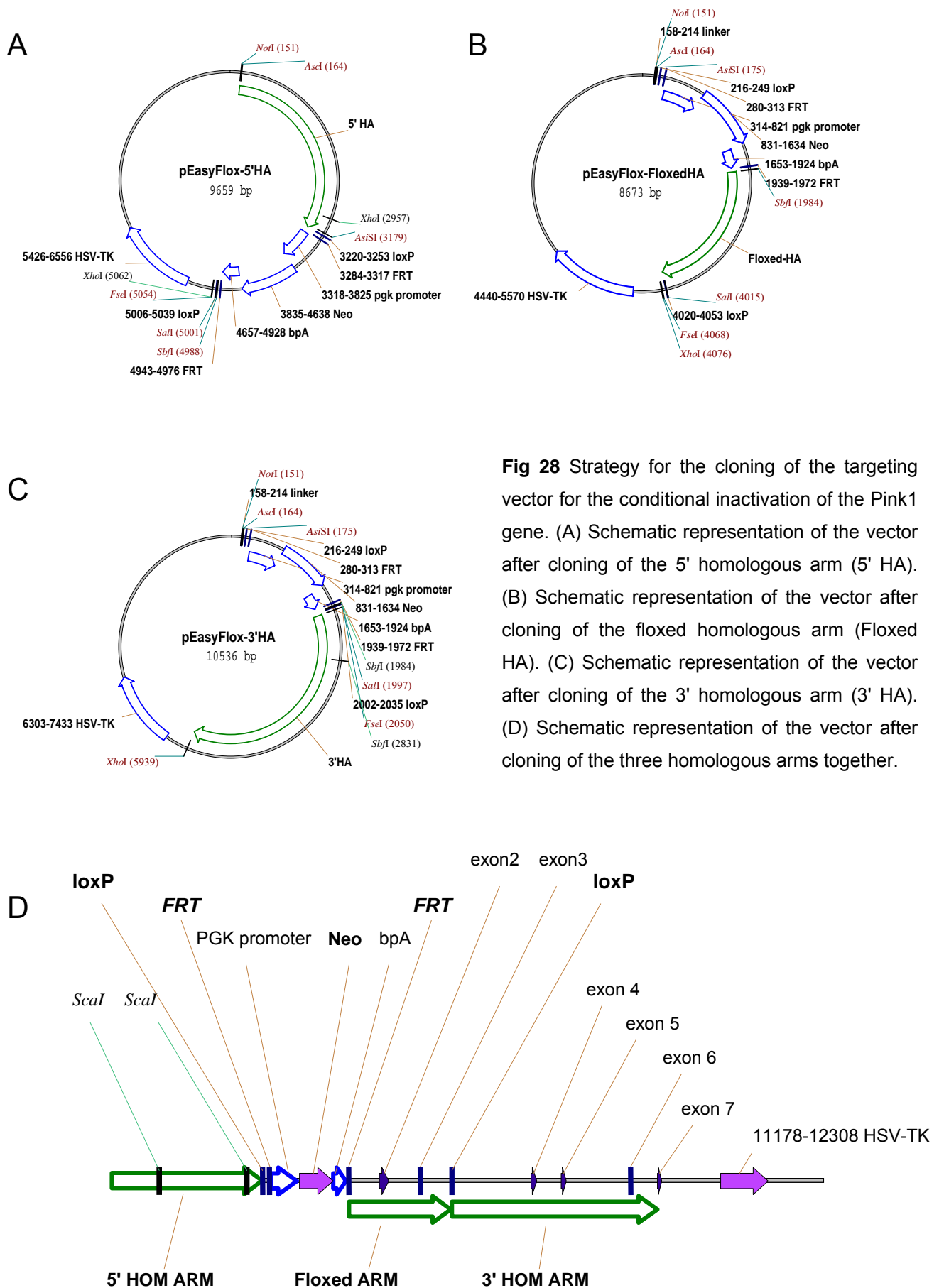


Fig 28 Strategy for the cloning of the targeting vector for the conditional inactivation of the Pink1 gene. (A) Schematic representation of the vector after cloning of the 5' homologous arm (5' HA). (B) Schematic representation of the vector after cloning of the floxed homologous arm (Floxed HA). (C) Schematic representation of the vector after cloning of the 3' homologous arm (3' HA). (D) Schematic representation of the vector after cloning of the three homologous arms together.

5.11.3 Southern blot procedure

The Southern blot was performed as described elsewhere (Southern, 1975). Briefly, 10 µg of wild-type 129Sv/Pas genomic DNA were digested with BamHI O/N at 37°C. On the second day, the digested DNA was run on an electrophoretic agarose gel 0.7% in TBE 1X (0.089 M Tris base, 0.089 M Boric acid, 0.0027 M EDTA) O/N at 35 V. After the run, the gel was photographed in a Gel Documentation System (Herolab) with a phosphorescent ruler lined up along side it, such that the ruler was lined up with the top of the wells. This was done so that it was possible to later estimate the size of the band on the film/blot. Then, the gel was treated with 0.25N HCl for 20 min to depurinate the DNA; and, after a rinse in distilled water, transferred into a solution containing 0.4N NaOH and shacked for other 20 min to denature the DNA. After the treatments, the DNA was ready for transfer on nylon membrane. The apparatus for transfer was set up, from bottom to top, as follows: a large dish was prepared, filled with 0.4N NaOH for alkaline transfer with a glass plate on top of it to rest the gel; two pieces of 3MM Whatman paper were cut to the width of the gel and length such that the ends of the 3MM paper were in contact with the bottom of the dish; the 3MM paper was wet with 0.4N NaOH; the gel was then layed on the 3MM paper and a Hybond N+ nylon membrane (GE Healthcare, # RPN303B), cut to the exact size of the gel, leaned on it; three pieces of 3MM paper, cut to the size of the gel and wet into 0.4N NaOH, were layed on the membrane; additional blotting paper was added on top of it, covered with a glass and a weight was put on top to keep the blot in place (see Fig 29).

After each step, the bubbles were smoothed out gently with a glass pipette. The blotting was left O/N and, on the third day, the membrane was recovered from the gel, let dry on a 3MM paper and kept at room temperature until processed for hybridization.

5.11.4 Preparation of the radiolabelled probe and membrane hybridization

To prepare the probe to detect the DNA fragment corresponding to the wild type band derived from the BamHI digestion on the genomic DNA, the plasmid containing the genomic DNA probe was digested with EcoRI. The digestion was run on a gel

and the desired fragment was purified as described before. The DNA probe was labeled with the Rediprime II DNA Labeling System (GE Healthcare, # RPN1633) and radioactive ^{32}P α -dCTP (Amersham Pharmacia), following manufacturer's instructions.

Southern blot

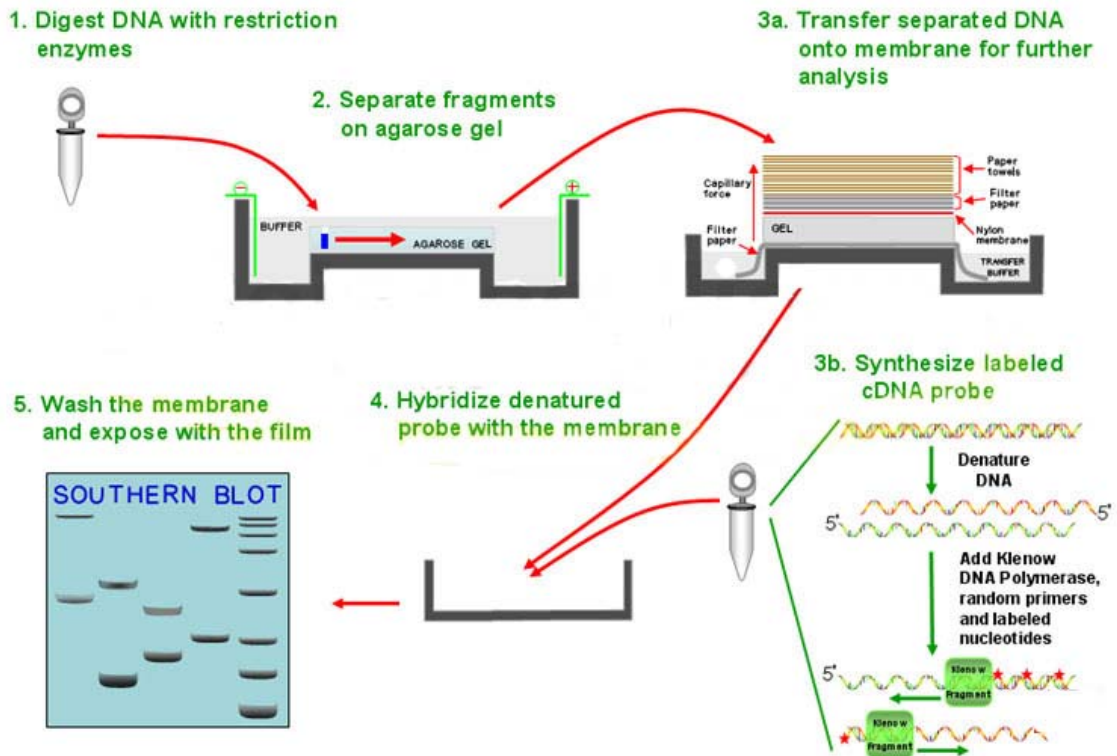


Fig 29 Drawing to show the various phases of the Southern blotting as described in the text.

6 REFERENCES

- Adolphs R, Schul R, Tranel D. 1998. Intact recognition of facial emotion in Parkinson's disease. *Neuropsychology* 12(2):253-258.
- Adolphs R, Tranel D, Damasio H, Damasio A. 1994. Impaired recognition of emotion in facial expressions following bilateral damage to the human amygdala. *Nature* 372(6507):669-672.
- Adolphs R, Tranel D, Damasio H, Damasio AR. 1995. Fear and the human amygdala. *J Neurosci* 15(9):5879-5891.
- Adolphs R, Tranel D, Hamann S, Young AW, Calder AJ, Phelps EA, Anderson A, Lee GP, Damasio AR. 1999. Recognition of facial emotion in nine individuals with bilateral amygdala damage. *Neuropsychologia* 37(10):1111-1117.
- Ahmed BY, Chakravarthy S, Eggers R, Hermens WT, Zhang JY, Niclou SP, Levelt C, Sablitzky F, Anderson PN, Lieberman AR, Verhaagen J. 2004. Efficient delivery of Cre-recombinase to neurons in vivo and stable transduction of neurons using adeno-associated and lentiviral vectors. *BMC Neurosci* 5:4.
- Almeida M, Han L, Bellido T, Manolagas SC, Kousteni S. 2005. Wnt Proteins Prevent Apoptosis of Both Uncommitted Osteoblast Progenitors and Differentiated Osteoblasts by β -Catenin-dependent and -independent Signaling Cascades Involving Src/ERK and Phosphatidylinositol 3-Kinase/AKT. *J Biol Chem* 280(50):41342-41351.
- Altman J. 1969. Autoradiographic and histological studies of postnatal neurogenesis. IV. Cell proliferation and migration in the anterior forebrain, with special reference to persisting neurogenesis in the olfactory bulb. *J Comp Neurol* 137(4):433-457.
- Alvarez-Buylla A, Lim DA. 2004. For the long run: maintaining germinal niches in the adult brain. *Neuron* 41(5):683-686.
- Alvarez-Buylla A, Seri B, Doetsch F. 2002. Identification of neural stem cells in the adult vertebrate brain. *Brain Res Bull* 57(6):751-758.
- Arendt T, Gartner U, Seeger G, Barmashenko G, Palm K, Mittmann T, Yan L, Hummeke M, Behrbohm J, Bruckner MK, Holzer M, Wahle P, Heumann R. 2004. Neuronal activation of Ras regulates synaptic connectivity. *Eur J Neurosci* 19(11):2953-2966.

- Atkins CM, Selcher JC, Petraitis JJ, Trzaskos JM, Sweatt JD. 1998. The MAPK cascade is required for mammalian associative learning. *Nat Neurosci* 1(7):602-609.
- Baekelandt V, Claeys A, Cherepanov P, De Clercq E, De Strooper B, Nuttin B, Debysse Z. 2000. DNA-Dependent protein kinase is not required for efficient lentivirus integration. *J Virol* 74(23):11278-11285.
- Bardwell AJ, Flatauer LJ, Matsukuma K, Thorner J, Bardwell L. 2001. A conserved docking site in MEKs mediates high-affinity binding to MAP kinases and cooperates with a scaffold protein to enhance signal transmission. *J Biol Chem* 276(13):10374-10386.
- Barton GM, Medzhitov R. 2002. Retroviral delivery of small interfering RNA into primary cells. *Proc Natl Acad Sci U S A* 99(23):14943-14945.
- Bauer EP, Schafe GE, LeDoux JE. 2002. NMDA receptors and L-type voltage-gated calcium channels contribute to long-term potentiation and different components of fear memory formation in the lateral amygdala. *J Neurosci* 22(12):5239-5249.
- Belanger LF, Roy S, Tremblay M, Brott B, Steff AM, Mourad W, Hugo P, Erikson R, Charron J. 2003. Mek2 is dispensable for mouse growth and development. *Mol Cell Biol* 23(14):4778-4787.
- Belluzzi O, Benedusi M, Ackman J, LoTurco JJ. 2003. Electrophysiological differentiation of new neurons in the olfactory bulb. *J Neurosci* 23(32):10411-10418.
- Belzung C, Griebel G. 2001. Measuring normal and pathological anxiety-like behaviour in mice: a review. *Behav Brain Res* 125(1-2):141-149.
- Betarbet R, Zigova T, Bakay RA, Luskin MB. 1996. Dopaminergic and GABAergic interneurons of the olfactory bulb are derived from the neonatal subventricular zone. *Int J Dev Neurosci* 14(7-8):921-930.
- Bichler Z, Manns M, Stegemann B, Heumann R. 2004. Does neuronal stabilization of granule cells in adult hippocampus regulate neurogenesis and behaviour? *FENS Forum Abstracts vol. 2, A145-1, 2004.*
- Bitsios P, Philpott A, Langley RW, Bradshaw CM, Szabadi E. 1999. Comparison of the effects of diazepam on the fear-potentiated startle reflex and the fear-inhibited light reflex in man. *J Psychopharmacol* 13(3):226-234.

- Blair HT, Schafe GE, Bauer EP, Rodrigues SM, LeDoux JE. 2001. Synaptic plasticity in the lateral amygdala: a cellular hypothesis of fear conditioning. *Learn Mem* 8(5):229-242.
- Blanchard DC, Griebel G, Blanchard RJ. 2001. Mouse defensive behaviors: pharmacological and behavioral assays for anxiety and panic. *Neurosci Biobehav Rev* 25(3):205-218.
- Blanchard R, Blanchard, DC. 1990. Anti-predator defense as models of animal fear and anxiety. In: PF Brain SP, RJ Blanchard and D Mainardi, editor. *Fear and defence*. Chur: Harwood Academic.
- Bogoyevitch MA, Court NW. 2004. Counting on mitogen-activated protein kinases--ERKs 3, 4, 5, 6, 7 and 8. *Cell Signal* 16(12):1345-1354.
- Bonhomme F, Iskandar, D, Thaler, L, Petter, F. 1985. Evolutionary relationships among rodents. In: Hartenberger WPLK-L, editor. p 671-683.
- Boulton TG, Nye SH, Robbins DJ, Ip NY, Radziejewska E, Morgenbesser SD, DePinho RA, Panayotatos N, Cobb MH, Yancopoulos GD. 1991. ERKs: a family of protein-serine/threonine kinases that are activated and tyrosine phosphorylated in response to insulin and NGF. *Cell* 65(4):663-675.
- Boursot P, Auffray, P-J, Britton-Davidian, J, Bonhomme, F. 1993. The evolution of mouse mice. *Annual Review of Ecological System* 24:119-152.
- Brott BK, Alessandrini A, Largaespada DA, Copeland NG, Jenkins NA, Crews CM, Erikson RL. 1993. MEK2 is a kinase related to MEK1 and is differentially expressed in murine tissues. *Cell Growth Differ* 4(11):921-929.
- Brown JS, Kalish HI, Farber IE. 1951. Conditioned fear as revealed by magnitude of startle response to an auditory stimulus. *J Exp Psychol* 41(5):317-328.
- Caplen NJ, Parrish S, Imani F, Fire A, Morgan RA. 2001. Specific inhibition of gene expression by small double-stranded RNAs in invertebrate and vertebrate systems. *Proc Natl Acad Sci U S A* 98(17):9742-9747.
- Carleton A, Petreanu LT, Lansford R, Alvarez-Buylla A, Lledo PM. 2003. Becoming a new neuron in the adult olfactory bulb. *Nat Neurosci* 6(5):507-518.
- Catling AD, Reuter CW, Cox ME, Parsons SJ, Weber MJ. 1994. Partial purification of a mitogen-activated protein kinase kinase activator from bovine brain. Identification as B-Raf or a B-Raf-associated activity. *J Biol Chem* 269(47):30014-30021.

- Cavanaugh JE, Ham J, Hetman M, Poser S, Yan C, Xia Z. 2001. Differential regulation of mitogen-activated protein kinases ERK1/2 and ERK5 by neurotrophins, neuronal activity, and cAMP in neurons. *J Neurosci* 21(2):434-443.
- Chen CY, Shyu AB. 1995. AU-rich elements: characterization and importance in mRNA degradation. *Trends Biochem Sci* 20(11):465-470.
- Constantine-Paton M, Cline HT, Debski E. 1990. Patterned activity, synaptic convergence, and the NMDA receptor in developing visual pathways. *Annu Rev Neurosci* 13:129-154.
- Corson LB, Yamanaka Y, Lai KM, Rossant J. 2003. Spatial and temporal patterns of ERK signaling during mouse embryogenesis. *Development* 130(19):4527-4537.
- Cowley S, Paterson H, Kemp P, Marshall CJ. 1994. Activation of MAP kinase kinase is necessary and sufficient for PC12 differentiation and for transformation of NIH 3T3 cells. *Cell* 77(6):841-852.
- Coyle JT, Duman RS. 2003. Finding the intracellular signaling pathways affected by mood disorder treatments. *Neuron* 38(2):157-160.
- Cryan JF, Holmes A. 2005. The ascent of mouse: advances in modelling human depression and anxiety. *Nat Rev Drug Discov* 4(9):775-790.
- Davidson BL, Stein CS, Heth JA, Martins I, Kotin RM, Derksen TA, Zabner J, Ghodsi A, Chiorini JA. 2000. Recombinant adeno-associated virus type 2, 4, and 5 vectors: transduction of variant cell types and regions in the mammalian central nervous system. *Proc Natl Acad Sci U S A* 97(7):3428-3432.
- Davis M. 1990. Pharmacological and anatomical analysis of fear conditioning. *NIDA Res Monogr* 97:126-162.
- Davis M. 1992. The role of the amygdala in fear-potentiated startle: implications for animal models of anxiety. *Trends Pharmacol Sci* 13(1):35-41.
- Davis M. 1994. The role of the amygdala in emotional learning. *Int Rev Neurobiol* 36:225-266.
- Davis M. 1998. Anatomic and physiologic substrates of emotion in an animal model. *J Clin Neurophysiol* 15(5):378-387.
- Devroe E, Silver PA. 2002. Retrovirus-delivered siRNA. *BMC Biotechnol* 2:15.

- Di Benedetto B, Hitz C, Holter SM, Kuhn R, Vogt Weisenhorn DM, Wurst W. 2007. Differential mRNA distribution of components of the ERK/MAPK signalling cascade in the adult mouse brain. *J Comp Neurol* 500(3):542-556.
- Dickinson RJ, Keyse SM. 2006. Diverse physiological functions for dual-specificity MAP kinase phosphatases. *J Cell Sci* 119(Pt 22):4607-4615.
- Doetsch F. 2003. The glial identity of neural stem cells. *Nat Neurosci* 6(11):1127-1134.
- DSM-IV. 1994. *Diagnostic and Statistical Manual of Mental Disorders (DSM-IV)*: Washington D.C.: American Psychiatric Association.
- Dugan LL, Kim JS, Zhang Y, Bart RD, Sun Y, Holtzman DM, Gutmann DH. 1999. Differential effects of cAMP in neurons and astrocytes. Role of B-raf. *J Biol Chem* 274(36):25842-25848.
- Elbashir SM, Harborth J, Lendeckel W, Yalcin A, Weber K, Tuschl T. 2001. Duplexes of 21-nucleotide RNAs mediate RNA interference in cultured mammalian cells. *Nature* 411(6836):494-498.
- English JD, Sweatt JD. 1997. A requirement for the mitogen-activated protein kinase cascade in hippocampal long term potentiation. *J Biol Chem* 272(31):19103-19106.
- Falls WA. 2002. Fear-Potentiated Startle in mice. *Current Protocols in Neuroscience*.
- Falls WA, Carlson S, Turner JG, Willott JF. 1997. Fear-potentiated startle in two strains of inbred mice. *Behav Neurosci* 111(4):855-861.
- Falls WA, Kogan, J.H., Silva A.J., Willott J.F., Carlson, S., Turner J.G. 2000. Fear-potentiated startle, but not prepulse inhibition of startle is impaired in CREB α phadelta $^{-/-}$ mutant mice. *Behav Neurosci* 114:998-1004.
- Favata MF, Horiuchi KY, Manos EJ, Daulerio AJ, Stradley DA, Feeser WS, Van Dyk DE, Pitts WJ, Earl RA, Hobbs F, Copeland RA, Magolda RL, Scherle PA, Trzaskos JM. 1998. Identification of a novel inhibitor of mitogen-activated protein kinase kinase. *J Biol Chem* 273(29):18623-18632.
- Furthauer M, Lin W, Ang SL, Thisse B, Thisse C. 2002. Sef is a feedback-induced antagonist of Ras/MAPK-mediated FGF signalling. *Nat Cell Biol* 4(2):170-174.
- Gage FH. 2000. Mammalian neural stem cells. *Science* 287(5457):1433-1438.
- Galli R, Gritti A, Bonfanti L, Vescovi AL. 2003. Neural stem cells: an overview. *Circ Res* 92(6):598-608.

- Ge W, Yang, XJ, Zhang, Z, Wang, HK, Shen, W, Deng, QD, Duan, S. 2006. Long-term potentiation of neuron-glia synapses mediated by Ca²⁺-permeable AMPA receptors. *Science* 312(5779):1533-1537.
- Gegelashvili G, Schousboe A. 1997. High affinity glutamate transporters: regulation of expression and activity. *Mol Pharmacol* 52(1):6-15.
- Giroux S, Tremblay M, Bernard D, Cardin-Girard JF, Aubry S, Larouche L, Rousseau S, Huot J, Landry J, Jeannotte L, Charron J. 1999. Embryonic death of Mek1-deficient mice reveals a role for this kinase in angiogenesis in the labyrinthine region of the placenta. *Curr Biol* 9(7):369-372.
- Gray J, McNaughton, N. 2000. *The Neuropsychology of Anxiety*: Oxford University Press.
- Griebel G. 1999. Is there a future for neuropeptide receptor ligands in the treatment of anxiety disorders? *Pharmacol Ther* 82(1):1-61.
- Grillon C, Ameli R, Woods SW, Merikangas K, Davis M. 1991. Fear-potentiated startle in humans: effects of anticipatory anxiety on the acoustic blink reflex. *Psychophysiology* 28(5):588-595.
- Grillon C, Davis M. 1997. Fear-potentiated startle conditioning in humans: explicit and contextual cue conditioning following paired versus unpaired training. *Psychophysiology* 34(4):451-458.
- Grillon C, Morgan CA, 3rd, Davis M, Southwick SM. 1998. Effects of experimental context and explicit threat cues on acoustic startle in Vietnam veterans with posttraumatic stress disorder. *Biol Psychiatry* 44(10):1027-1036.
- Hannon GJ. 2002. RNA interference. *Nature* 418(6894):244-251.
- Hatano N, Mori Y, Oh-hora M, Kosugi A, Fujikawa T, Nakai N, Niwa H, Miyazaki J, Hamaoka T, Ogata M. 2003. Essential role for ERK2 mitogen-activated protein kinase in placental development. *Genes Cells* 8(11):847-856.
- Heldt S, Sundin V, Willott JF, Falls WA. 2000. Posttraining lesions of the amygdala interfere with fear-potentiated startle to both visual and auditory conditioned stimuli in C57BL/6J mice. *Behav Neurosci* 114(4):749-759.
- Hommel JD, Sears RM, Georgescu D, Simmons DL, DiLeone RJ. 2003. Local gene knockdown in the brain using viral-mediated RNA interference. *Nat Med* 9(12):1539-1544.
- Hood S, Argyropoulos V, Nutt DJ. 2000. Agents in development for anxiety disorders. *CNS Drugs* 13:421-431.

- Impey S, Obrietan K, Storm DR. 1999. Making new connections: role of ERK/MAP kinase signaling in neuronal plasticity. *Neuron* 23(1):11-14.
- Impey S, Obrietan K, Wong ST, Poser S, Yano S, Wayman G, Deloulme JC, Chan G, Storm DR. 1998. Cross talk between ERK and PKA is required for Ca²⁺ stimulation of CREB-dependent transcription and ERK nuclear translocation. *Neuron* 21(4):869-883.
- Jacobs DH, Shuren J, Bowers D, Heilman KM. 1995. Emotional facial imagery, perception, and expression in Parkinson's disease. *Neurology* 45(9):1696-1702.
- Johnson GL, Lapadat R. 2002. Mitogen-activated protein kinase pathways mediated by ERK, JNK, and p38 protein kinases. *Science* 298(5600):1911-1912.
- Kan Y, Kawamura M, Hasegawa Y, Mochizuki S, Nakamura K. 2002. Recognition of emotion from facial, prosodic and written verbal stimuli in Parkinson's disease. *Cortex* 38(4):623-630.
- Kanai Y. 1997. Family of neutral and acidic amino acid transporters: molecular biology, physiology and medical implications. *Curr Opin Cell Biol* 9(4):565-572.
- Kaufman J, Charney D. 2000. Comorbidity of mood and anxiety disorders. *Depress Anxiety* 12 Suppl 1:69-76.
- Kent JM, Mathew SJ, Gorman JM. 2002. Molecular targets in the treatment of anxiety. *Biol Psychiatry* 52(10):1008-1030.
- Kim SH, Yang YC. 1996. A specific association of ERK3 with B-Raf in rat hippocampus. *Biochem Biophys Res Commun* 229(2):577-581.
- Klein T, Magerl W, Nickel U, Hopf HC, Sandkuhler J, Treede RD. 2007. Effects of the NMDA-receptor antagonist ketamine on perceptual correlates of long-term potentiation within the nociceptive system. *Neuropharmacology* 52(2):655-661.
- Kopchia KL, Altman HJ, Commissaris RL. 1992. Effects of lesions of the central nucleus of the amygdala on anxiety-like behaviors in the rat. *Pharmacol Biochem Behav* 43(2):453-461.
- Krolak-Salmon P, Henaff MA, Isnard J, Tallon-Baudry C, Guenot M, Vighetto A, Bertrand O, Mauguiere F. 2003. An attention modulated response to disgust in human ventral anterior insula. *Ann Neurol* 53(4):446-453.
- Kuhn HG, Svendsen CN. 1999. Origins, functions, and potential of adult neural stem cells. *Bioessays* 21(8):625-630.

- Kyriakis JM, Avruch J. 1996. Sounding the alarm: protein kinase cascades activated by stress and inflammation. *J Biol Chem* 271(40):24313-24316.
- LaBar KS, Gatenby JC, Gore JC, LeDoux JE, Phelps EA. 1998. Human amygdala activation during conditioned fear acquisition and extinction: a mixed-trial fMRI study. *Neuron* 20(5):937-945.
- LeDoux JE, Sakaguchi A, Iwata J, Reis DJ. 1986. Interruption of projections from the medial geniculate body to an archi-neostriatal field disrupts the classical conditioning of emotional responses to acoustic stimuli. *Neuroscience* 17(3):615-627.
- Lee Y, Lopez DE, Meloni EG, Davis M. 1996. A primary acoustic startle pathway: obligatory role of cochlear root neurons and the nucleus reticularis pontis caudalis. *J Neurosci* 16(11):3775-3789.
- Lesch KP. 2001. Molecular foundation of anxiety disorders. *J Neural Transm* 108(6):717-746.
- Linnarsson S, Willson CA, Ernfors P. 2000. Cell death in regenerating populations of neurons in BDNF mutant mice. *Brain Res Mol Brain Res* 75(1):61-69.
- Lu KT, Walker DL, Davis M. 2001. Mitogen-activated protein kinase cascade in the basolateral nucleus of amygdala is involved in extinction of fear-potentiated startle. *J Neurosci* 21(16):RC162.
- Mackay-Sim A, Chuah MI. 2000. Neurotrophic factors in the primary olfactory pathway. *Prog Neurobiol* 62(5):527-559.
- Mattila PM, Rinne JO, Helenius H, Roytta M. 1999. Neuritic degeneration in the hippocampus and amygdala in Parkinson's disease in relation to Alzheimer pathology. *Acta Neuropathol (Berl)* 98(2):157-164.
- McNish KA, Gewirtz JC, Davis M. 1997. Evidence of contextual fear after lesions of the hippocampus: a disruption of freezing but not fear-potentiated startle. *J Neurosci* 17(23):9353-9360.
- Millan MJ. 2003. The neurobiology and control of anxious states. *Prog Neurobiol* 70(2):83-244.
- Ming GL, Song H. 2005. Adult neurogenesis in the mammalian central nervous system. *Annu Rev Neurosci* 28:223-250.
- Mitchell P, Tollervey D. 2000. mRNA stability in eukaryotes. *Curr Opin Genet Dev* 10(2):193-198.

- Morice C, Nothias F, Konig S, Vernier P, Baccarini M, Vincent JD, Barnier JV. 1999. Raf-1 and B-Raf proteins have similar regional distributions but differential subcellular localization in adult rat brain. *Eur J Neurosci* 11(6):1995-2006.
- Morris JS, Frith CD, Perrett DI, Rowland D, Young AW, Calder AJ, Dolan RJ. 1996. A differential neural response in the human amygdala to fearful and happy facial expressions. *Nature* 383(6603):812-815.
- Musatov S, Chen W, Pfaff DW, Kaplitt MG, Ogawa S. 2006. RNAi-mediated silencing of estrogen receptor {alpha} in the ventromedial nucleus of hypothalamus abolishes female sexual behaviors. *Proc Natl Acad Sci U S A* 103(27):10456-10460.
- Nicholls D, Attwell D. 1990. The release and uptake of excitatory amino acids. *Trends Pharmacol Sci* 11(11):462-468.
- Nishiyama H, Knopfel T, Endo S, Itohara S. 2002. Glial protein S100B modulates long-term neuronal synaptic plasticity. *Proc Natl Acad Sci U S A* 99(6):4037-4042.
- Ouchi Y, Yoshikawa E, Okada H, Futatsubashi M, Sekine Y, Iyo M, Sakamoto M. 1999. Alterations in binding site density of dopamine transporter in the striatum, orbitofrontal cortex, and amygdala in early Parkinson's disease: compartment analysis for beta-CFT binding with positron emission tomography. *Ann Neurol* 45(5):601-610.
- Pages G, Guerin S, Grall D, Bonino F, Smith A, Anjuere F, Auberger P, Pouyssegur J. 1999. Defective thymocyte maturation in p44 MAP kinase (Erk 1) knockout mice. *Science* 286(5443):1374-1377.
- Pages G, Lenormand P, L'Allemain G, Chambard JC, Meloche S, Pouyssegur J. 1993. Mitogen-activated protein kinases p42mapk and p44mapk are required for fibroblast proliferation. *Proc Natl Acad Sci U S A* 90(18):8319-8323.
- Papin C, Denouel A, Calothy G, Eychene A. 1996. Identification of signalling proteins interacting with B-Raf in the yeast two-hybrid system. *Oncogene* 12(10):2213-2221.
- Parpura V, Haydon PG. 2000. Physiological astrocytic calcium levels stimulate glutamate release to modulate adjacent neurons. *Proc Natl Acad Sci U S A* 97(15):8629-8634.
- Patrick CJ, Berthot BD, Moore JD. 1996. Diazepam blocks fear-potentiated startle in humans. *J Abnorm Psychol* 105(1):89-96.

- Paul S, Olausson P, Venkitaramani DV, Ruchkina I, Moran TD, Tronson N, Mills E, Hakim S, Salter MW, Taylor JR, Lombroso PJ. 2007. The striatal-enriched protein tyrosine phosphatase gates long-term potentiation and fear memory in the lateral amygdala. *Biol Psychiatry* 61(9):1049-1061.
- Petrenko AB, Yamakura T, Askalany AR, Kohno T, Sakimura K, Baba H. 2006. Effects of ketamine on acute somatic nociception in wild-type and N-methyl-D-aspartate (NMDA) receptor epsilon1 subunit knockout mice. *Neuropharmacology* 50(6):741-747.
- Phelps EA, O'Connor KJ, Gatenby JC, Gore JC, Grillon C, Davis M. 2001. Activation of the left amygdala to a cognitive representation of fear. *Nat Neurosci* 4(4):437-441.
- Pratt JA. 1992. The neuroanatomical basis of anxiety. *Pharmacol Ther* 55(2):149-181.
- Rattiner LM, Davis M, French CT, Ressler KJ. 2004. Brain-derived neurotrophic factor and tyrosine kinase receptor B involvement in amygdala-dependent fear conditioning. *J Neurosci* 24(20):4796-4806.
- Refojo D, Echenique C, Muller MB, Reul JM, Deussing JM, Wurst W, Sillaber I, Paez-Pereda M, Holsboer F, Arzt E. 2005. Corticotropin-releasing hormone activates ERK1/2 MAPK in specific brain areas. *Proc Natl Acad Sci U S A* 102(17):6183-6188.
- Roberson ED, English JD, Adams JP, Selcher JC, Kondratick C, Sweatt JD. 1999. The mitogen-activated protein kinase cascade couples PKA and PKC to cAMP response element binding protein phosphorylation in area CA1 of hippocampus. *J Neurosci* 19(11):4337-4348.
- Robinson FL, Whitehurst AW, Raman M, Cobb MH. 2002. Identification of novel point mutations in ERK2 that selectively disrupt binding to MEK1. *J Biol Chem* 277(17):14844-14852.
- Rothstein JD, Dykes-Hoberg M, Pardo CA, Bristol LA, Jin L, Kuncl RW, Kanai Y, Hediger MA, Wang Y, Schielke JP, Welty DF. 1996. Knockout of glutamate transporters reveals a major role for astroglial transport in excitotoxicity and clearance of glutamate. *Neuron* 16(3):675-686.
- Rubinson DA, Dillon CP, Kwiatkowski AV, Sievers C, Yang L, Kopinja J, Rooney DL, Ihrig MM, McManus MT, Gertler FB, Scott ML, Van Parijs L. 2003. A lentivirus-

- based system to functionally silence genes in primary mammalian cells, stem cells and transgenic mice by RNA interference. *Nat Genet* 33(3):401-406.
- Sah P, Lopez De Armentia M. 2003. Excitatory synaptic transmission in the lateral and central amygdala. *Ann N Y Acad Sci* 985:67-77.
- Schafe GE, Atkins CM, Swank MW, Bauer EP, Sweatt JD, LeDoux JE. 2000. Activation of ERK/MAP kinase in the amygdala is required for memory consolidation of pavlovian fear conditioning. *J Neurosci* 20(21):8177-8187.
- Schafe GE, Nadel NV, Sullivan GM, Harris A, LeDoux JE. 1999. Memory consolidation for contextual and auditory fear conditioning is dependent on protein synthesis, PKA, and MAP kinase. *Learn Mem* 6(2):97-110.
- Schafe GE, Nader K, Blair HT, LeDoux JE. 2001. Memory consolidation of Pavlovian fear conditioning: a cellular and molecular perspective. *Trends Neurosci* 24(9):540-546.
- Seifert G, Schilling K, Steinhauser C. 2006. Astrocyte dysfunction in neurological disorders: a molecular perspective. *Nat Rev Neurosci* 7(3):194-206.
- Selcher JC, Nekrasova T, Paylor R, Landreth GE, Sweatt JD. 2001. Mice lacking the ERK1 isoform of MAP kinase are unimpaired in emotional learning. *Learn Mem* 8(1):11-19.
- Shatz CJ. 1990. Impulse activity and the patterning of connections during CNS development. *Neuron* 5(6):745-756.
- Shimogori T, VanSant J, Paik E, Grove EA. 2004. Members of the Wnt, Fz, and Frp gene families expressed in postnatal mouse cerebral cortex. *J Comp Neurol* 473(4):496-510.
- Simpson PJ, Wang E, Moon C, Matarazzo V, Cohen DR, Liebl DJ, Ronnett GV. 2003. Neurotrophin-3 signaling maintains maturational homeostasis between neuronal populations in the olfactory epithelium. *Mol Cell Neurosci* 24(4):858-874.
- Southern EM. 1975. Detection of specific sequences among DNA fragments separated by gel electrophoresis. *J Mol Biol* 98(3):503-517.
- Sprengelmeyer R, Young AW, Calder AJ, Karnat A, Lange H, Homberg V, Perrett DI, Rowland D. 1996. Loss of disgust. Perception of faces and emotions in Huntington's disease. *Brain* 119 (Pt 5):1647-1665.
- Storm SM, Cleveland JL, Rapp UR. 1990. Expression of raf family proto-oncogenes in normal mouse tissues. *Oncogene* 5(3):345-351.

- Sundin V, Heldt SA, Buck LE, Jones WW, Willott JF, Falls WA. 1998. Fear-potentiated startle and conditioned freezing to visual and auditory conditioned stimuli are blocked by lesions of the amygdala in C57 mice. Paper presented at the Society for Neuroscience meeting, Los Angeles.
- Sweatt JD. 2001. The neuronal MAP kinase cascade: a biochemical signal integration system subserving synaptic plasticity and memory. *J Neurochem* 76(1):1-10.
- Tanaka K, Watase K, Manabe T, Yamada K, Watanabe M, Takahashi K, Iwama H, Nishikawa T, Ichihara N, Kikuchi T, Okuyama S, Kawashima N, Hori S, Takimoto M, Wada K. 1997. Epilepsy and exacerbation of brain injury in mice lacking the glutamate transporter GLT-1. *Science* 276(5319):1699-1702.
- Thomas KL, Hunt SP. 1993. The regional distribution of extracellularly regulated kinase-1 and -2 messenger RNA in the adult rat central nervous system. *Neuroscience* 56(3):741-757.
- Tiscornia G, Singer O, Ikawa M, Verma IM. 2003. A general method for gene knockdown in mice by using lentiviral vectors expressing small interfering RNA. *Proc Natl Acad Sci U S A* 100(4):1844-1848.
- Todd KJ, Serrano A, Lacaille JC, Robitaille R. 2006. Glial cells in synaptic plasticity. *J Physiol Paris* 99(2-3):75-83.
- Turgeon B, Saba-El-Leil MK, Meloche S. 2000. Cloning and characterization of mouse extracellular-signal-regulated protein kinase 3 as a unique gene product of 100 kDa. *Biochem J* 346 Pt 1:169-175.
- Valente EM, Abou-Sleiman PM, Caputo V, Muqit MM, Harvey K, Gispert S, Ali Z, Del Turco D, Bentivoglio AR, Healy DG, Albanese A, Nussbaum R, Gonzalez-Maldonado R, Deller T, Salvi S, Cortelli P, Gilks WP, Latchman DS, Harvey RJ, Dallapiccola B, Auburger G, Wood NW. 2004. Hereditary early-onset Parkinson's disease caused by mutations in PINK1. *Science* 304(5674):1158-1160.
- Visser E, Schug SA. 2006. The role of ketamine in pain management. *Biomed Pharmacother* 60(7):341-348.
- Vouret-Craviari V, Van Obberghen-Schilling E, Scimeca JC, Van Obberghen E, Pouyssegur J. 1993. Differential activation of p44mapk (ERK1) by alpha-thrombin and thrombin-receptor peptide agonist. *Biochem J* 289 (Pt 1):209-214.

- Weber JD, Raben DM, Phillips PJ, Baldassare JJ. 1997. Sustained activation of extracellular-signal-regulated kinase 1 (ERK1) is required for the continued expression of cyclin D1 in G1 phase. *Biochem J* 326 (Pt 1):61-68.
- Wellbrock C, Karasarides M, Marais R. 2004. The RAF proteins take centre stage. *Nat Rev Mol Cell Biol* 5(11):875-885.
- Werry TD, Gregory KJ, Sexton PM, Christopoulos A. 2005. Characterization of serotonin 5-HT_{2C} receptor signaling to extracellular signal-regulated kinases 1 and 2. *J Neurochem* 93(6):1603-1615.
- Whishaw IQ, Metz GA, Kolb B, Pellis SM. 2001. Accelerated nervous system development contributes to behavioral efficiency in the laboratory mouse: a behavioral review and theoretical proposal. *Dev Psychobiol* 39(3):151-170.
- Willott JF, Turner JG, Carlson S, Ding D, Seegers Bross L, Falls WA. 1998. The BALB/c mouse as an animal model for progressive sensorineural hearing loss. *Hear Res* 115(1-2):162-174.
- Wood S, Toth, M. 2001. Molecular pathways of anxiety revealed by knockout mice. *Mol Neurobiol* 23(2-3):101-119.
- Xu B, Wilsbacher JL, Collisson T, Cobb MH. 1999. The N-terminal ERK-binding site of MEK1 is required for efficient feedback phosphorylation by ERK2 in vitro and ERK activation in vivo. *J Biol Chem* 274(48):34029-34035.
- Yeomans JS, Frankland PW. 1995. The acoustic startle reflex: neurons and connections. *Brain Res Brain Res Rev* 21(3):301-314.
- Zhou L, Del Villar K, Dong Z, Miller CA. 2004. Neurogenesis response to hypoxia-induced cell death: map kinase signal transduction mechanisms. *Brain Res* 1021(1):8-19.

7 ACKNOWLEDGMENTS

I would like to thank several people who, in a way or in another, contributed to reach this important step in my working life:

Prof. Dr. Wolfgang Wurst who gave me my “scientific birth” with my first paper as first author, as a literally “Doktorvater” (Doctoral “dad”). His enthusiasm and strong will were a highly encouraging example to pursue the results. Especially one of his sentences became highly remarkable: “Just inject!” – which became a kind of “running title” for my PhD thesis!

Dr. Sabine Hölter-Koch (Behavioral Team), Dr. Ralf Kühn (RNAi Team) and Dr. Daniela Vogt Weisenhorn (Neurodegeneration Team) for their precious support as my doctoral tutors during the course of the PhD. Their suggestions from their different expertises were really useful to improve the quality of the results reported in this work.

Of course, several other members of the Wurst group for different reasons: my “lab girls”, Magdalena Kallnik and Karin Weindl, who were so patient with me and full of encouraging words in some bad moments; but were also good friends to share a dinner or a brunch together! Sabit Delić, who was a perfect working partner for scientific discussions and for experiments, but also a very good listener when I had some angry moments for whatsoever reason; Alex Blak, my “dark side”; Christiane Hitz, for the collaboration to perform the extensive work for the expression analysis paper; Annerose Kurz-Drexler for the help with non-isotopic ISH and the nice friendship; Johanna Neumann, who did a 3-months lab experience (praktikum) with me, sharing part of the analysis on the time course of activation of pMAPK, but also tons of spareribs in the beergardens!

Some of the members of our neighbouring Institute of Stem Cell Research: Silvia Cappello, whose friendship was for me very precious, but also her good suggestions to perform and to look at some stainings were really helpful for some of my experiments; Pratibha Tripathi, whose smile and good heart are unforgettable for

how much they can support! And Michael Hack, for all his help and patience in showing me the set-up material for viral injections, but also for his nice friendship later on. And of course, least but not last, their boss Magdalena Götz who accepted to be part of my defense thesis committee.

A very special thank goes to my parents, Paolo and Maddalena, who always encouraged me to pursue my goals with strength and courage; and for their financial support during my studies, which allowed me to get here! And a thank goes to my sister Lisa and my cousins, Giulia, Paola and Marta, for being always by my side, whatever choices I made in life. Without forgetting the rest of my big family, always strongly supporting all my decisions, personal and professional. And Marco Beretta, whose patience and psychological support were very precious for many years.

Some special people, who entered my life only very recently, but in a very important moment of changes: Sascha Imhof, my climbing instructor but also very special good-hearted Friend; Anne, Nadin, Frank, Andi, Gudrun, Duane, Thilo, Sara and all the other climbing people, whose joyful characters and the valid alternatives proposed to recover my soul during the writing of the thesis were of invaluable meaning!

Moreover I should thank some of my “long-lasting” friends: Sara Gennari, Mauro Francavilla, Giusy Sessa, Rossana Mineri and Luca Del Giacco, who were always present along many years with nice words in good and bad times. Without forgetting Tiziana Bonaldi, who was a careful and hearted friend during my time in Munich, pushing me up in hard moments, but also sharing with me the good times.

8 ERKLÄRUNG/DECLARATION

Barbara Di Benedetto
Libellenstr. 29
80939 München

München, den

Sehr geehrte Damen und Herren,

hiermit erkläre ich, Barbara Di Benedetto, dass die eingereichte Dissertation meine erste ist. Es gab keinen früheren Versuch eine Dissertation einzureichen oder sich einer Doktorprüfung zu unterziehen.

Ferner erkläre ich, dass die vorliegende Dissertation selbstständig und ohne unerlaubte Hilfe angefertigt worden ist. Die Dissertation wird vollständig eingereicht und wurde nicht in wesentlichen Teilen einer anderen Prüfungskommission vorgelegt.

Barbara Di Benedetto